Multi-Scale Pulmonary Modelling and Clinical Applications

Nor Salwa Damanhuri

A thesis submitted for the degree of

Doctor of Philosophy

in

BioEngineering

at the

University of Canterbury,

Christchurch, New Zealand.

Date

5th November 2015

Acknowledgements

I would like to express my deepest appreciation to my supervisor, Distinguish Professor Geoffrey Chase, for always having faith in me, throughout my PhD study and the completion of this thesis. This thesis would not have been possible without your guidance, encouragement, inspiration and support. Thank you.

I would also like to express my warm and sincere thanks to Dr Yeong Shiong Chiew, and Dr Paul Docherty for the guidance, idea, advice and knowledge. Without their help and counsel, the thesis would be infinitely more difficult.

To Dr Geoff Shaw and Dr Thomas Desaive, thank you for your skill and experiences. I appreciate it enormously.

To the rest of bio-engineering team and friends, Dr. Chris, Dr Jennifer, Melanie, Guo Peng, Musabir, Hina, Daniel, Felicity, Alex, Ruby, Dr Ummu, Dr Fatanah, Dr Azurahisham, thank you for your friendship.

I wish to extend my gratitude to my sponsors; UiTM and KPM.

I am deeply thankful to my parents, Damanhuri and Hamidah, for their continuous supports, prayers and understanding. To Aida, Aini and Amir, thanks for always be there when I need your advice and supports.

Lastly, my deepest gratitude and love to my loving and patient husband, Nor Azlan Othman, for always being there for me through this challenging journey. Thank you for always believing in me and encouraging me to complete the thesis. To my precious gems, Nur Iman Mikhail and Nur Ireena Sofea, thank you for always willingly accompany me almost every day to the bio-engineering lab. I am forever in debt for your understanding and support.

Table of Contents

List of figures

List of tables

Nomenclature

α	Patient-specific Physiological Dimension
ABM	Airway Branching Model
ABMps	Patient-specific Airway Branching Model
ALI	Acute Lung Injury
ARDS	Acute Respiratory Distress Syndrome
AUC	Area under the Curve
COPD	Chronic Obstructive Pulmonary Disease
CT	Computed Tomography
DSA	Dynostatic Algorithm
E_{cw}	Cage Elastance
E_{drs}	Time-varying Elastance/ Dynamic Respiratory System Elastance
E_{demand}	Demand Elastance
EIT	Electrical Impedance Tomography
E_{lung}	Lung Elastance
E_{rs}	Respiratory System Elastance
ETT	Endotracheal Tube
FiO_2	Fraction of inspired oxygen
FRC	Functional Residual Capacity
H1N1	Swine Flu
HU	Hounsfield Units
ICU	Intensive Care Unit
IQR	Interquartile Range
K	Expiratory Time Constant Model Parameter
LIP	Lower Inflection Point
MV	Mechanical Ventilation
P_0	Offset Pressure
PaO_2	Partial pressure of arterial oxygen
P_{aw}	Airway Pressure
PCV	Pressure Controlled Ventilation
P_{cw}	Pressure in the Cage
P_{demand}	Pressure Change due to Demand
P_{dyn}	Dynostatic Pressure
P_{exp}	Pressure during Expiration
P_{insp}	Pressure during Inspiration
PEEP	Positive End Expiratory Pressure
PF ratio	PaO2/FiO2
PIP	Peak Airway Pressure
P_{lung}	Pressure in the Lung Compartment
P_{pl}	Pleural Pressure
PV	Pressure Volume
Q_{aw}	Air Flow
Q_{exp}	Expiration Flow
Q_{insp}	Inspiration Flow
RCV	Robust Coefficient of Variation
R_{exp}	Airway Resistance during Expiration

R_{insp}	Airway Resistance during Inspiration
R_{rs}	Respiratory System Elastance
RM	Recruitment Manoeuvre
SB	Spontaneous Breathing
SIMV	Synchronized Intermittent Mandatory Ventilation
TCP	Threshold Closing Pressure
TOP	Threshold Opening Pressure
UIP	Upper Inflection Point
V	Lung Volume
VCV	Volume Controlled Ventilation
VILI	Ventilator Induced Lung Injury
Vt	Tidal Volume
WOB	Work of Breathing
ZEEP	Zero End Expiratory Pressure

Abstract

Mechanical ventilation (MV) is one of the most difficult, costly and variably delivered therapies for Acute Respiratory Distress Syndrome (ARDS) and respiratory failure patients in the intensive care unit (ICU). These patients experience severe widespread breathing problems and require MV for breathing support. However, conventional MV does not provide enough real-time information to guide or individualize therapy, and suboptimal MV settings increase the risk of further lung injury and complications.

In particular, positive end expiratory pressure (PEEP) is applied during MV to aid recovery by improving gas exchange and prevent de-recruitment of lung units. However, selection of patient-specific, optimal PEEP remains widely debated, as no standard approaches exist for setting MV. Clinicians often use general approaches or experience to select PEEP, increasing the variability and risk of care, while reducing or eliminating any patient-specific aspect of care. Thus, physiological mathematical lung models of respiratory mechanics are required, if they are suitable to be used to optimise MV settings to improve critically ill patient outcomes.

The aims of this research are to investigate and develop new, extended models of lung mechanics for ARDS and respiratory failure patients. In particular, to create model-based measures of the potential impact to healthy lung units of changing MV therapy parameters. This goal requires rapid forms of parameter identification to define patient-specific model parameters from clinical data that can be used as complementary metrics in guiding and individualising MV.

The first model, an airway branching model (ABM) was developed based on classical fluid mechanics models that are commonly used. Typically, they are not feasible for real-time applications. Thus, there is a need to develop an accurate, effective, yet simpler, ABM model that can be applied at the bed-side. To address this issue, a patient-specific airway branching (ABMps) model is developed to measure the airway pressure drop at every physiological airway branch with an extended patient-specific physiological dimension that is unique for each patient and can evolve over time with new data. With this patient-specific dimension (α), the ABMps is able to provide clinical insight on patient-specific physiological conditions. Using the retrospective clinical data from the Christchurch Hospital, it was found that α ranges from 0.45-0.66 for ARDS patients, which is smaller than normal healthy people indicating severity of condition. Hence, the airway condition of a patient can be characterised and evolve over time to provide useful patient-specific clinical guidance.

Next, a model using only the expiratory data of the breathing cycle is developed and presented that is potentially useful during clinical respiratory mechanics monitoring to guide MV. In particular, the expiratory time constant parameter, (K), can provide unique information related to respiratory system elastance in MV patients. In this thesis, the extended model is tested using clinical data from ARDS patients and investigates the relationship between the expiratory time constant and model-based inspiratory respiratory system elastance. The goal is to use this relation to titrate patient-specific PEEP, which can help prevent the risk of lung over-distension and ventilation-induced injury.

The third model extends the time varying elastance model to investigate the variability of this respiratory system elastance for MV patients. In this case, in Christchurch Hospital. With the proposed metric, a deeper understanding can be achieved that provides clinicians with more

information on how respiratory elastance varies between patients, PEEP, and ventilation time. This information is patient-specific and can be updated overtime, as well as used as a marker of patient condition.

Estimating respiratory mechanics of MV patients is unreliable when patients exhibit spontaneous breathing (SB) efforts on top of any form of ventilator support. Most well-known developed models are thus only suitable for fully sedated patients. Monitoring respiratory mechanics of SB patients requires invasive clinical protocols and equipment that are clinically too intensive to carry out. In this research, it was found that the variability of lung elastance in SB patients is due to an effective negative elastance produced by the SB effort that is created by the SB effort, but cannot be modelled directly. Thus, by extending the non-invasive time-varying elastance model to capture negative elastance, it can provide more consistent monitoring for SB patients by reviewing the distribution of negative elastance. This work thus extends capabilities of these models and quantified the level of SB efforts.

Finally, due to the asynchrony, also known as reverse triggering, airway pressure can assume an unusual and unmodelled M-wave shaped airway pressure during the MV. This M-wave airway pressure is also due to the SB efforts, exhibited by patients, even when they are fully sedated. Hence, a model-based method to reconstruct the affected airway pressure curve is introduced that enables estimation of the true underlying respiratory mechanics of these patients, as well as quantifying SB efforts. Results show that this pressure wave reconstruction method was able to accurately identify the respiratory elastance, assess the level of SB effort, and quantify the incidence of SB effort without invasive protocols or interruption to care. Hence, this method is clinically useful for clinicians in determining optimal ventilator settings to improve patient care.

Overall, these tools and methods provide significant new ways to clinically manage MV patients in the ICU. Model-based methods offer the opportunity to protocolize and individualize care. Thus, the main outcomes of this work provide a step forward towards better, more consistent and patient-specific MV.

CHAPTER 1

Introduction

1.1 Acute Respiratory Distress Syndrome (ARDS)

Acute respiratory distress syndrome (ARDS) is a severe form of Acute Lung Injury (ALI), where the lung experiences various types of injuries that lead to a respiratory failure. These injuries prevent the lung's ability to exchange gas effectively, resulting in oxygen deficient blood, direct alveolar injury, pulmonary oedema and alveolar collapse (Ashbaugh et al. 1967; Bernard et al. 1994b; Kattwinkel et al. 2004; Kollef & Schuster 1995). Injuries in the lung also cause significant inflammation leading fluid to spill into the lung, resulting in a stiffer and smaller lung and reducing the overall lung volume to a so called baby lung (Gattinoni & Pesenti 2005; Ware & Matthay 2000). The sequel to all these effects is failure to deliver oxygen to other organs and tissues leading to further organ failure and increased risk of death.

The cause of ARDS can be either direct or indirect. For example, pulmonary aspiration/near drowning, pneumonia, and smoke inhalation are several types of direct lung injury that can lead to ARDS. Similarly, ARDS can also be caused indirectly through the inflammatory response and stress due to sepsis, severe trauma to other body parts circulating fluid resuscitation , or massive blood transfusion (Burleson & Maki 2005; Ware & Matthay 2000).

ARDS was first described in 1967 (Ashbaugh et al. 1967) and, since then, the definition of ARDS has evolved and varied until it was redefined in 1994 by the American-European Consensus Conference (AECC) (Bernard et al. 1994a). Based on this definition by the AECC, ARDS was characterised as the acute onset of respiratory failure, diffuse bilateral

infiltrates on chest radiograph, the absence of elevated left heart filling pressure determined either diagnostically with a pulmonary artery catheter (pulmonary artery occlusion pressure of < 18 mmHg) or clinically (absence of evidence of left arterial hypertension) (Bernard et al. 1994b; Fanelli et al. 2013). If the ratio of partial pressure of arterial oxygen to the fraction of inspired oxygen (PaO_2/FiO_2) is less than 300 mmHg, the patient is diagnosed with acute lung injury (ALI), and if the PaO_2/FiO_2 ratio is less than 200 mmHg, the patient is diagnosed with acute respiratory distress syndrome (ARDS) (Bernard et al. 1994b). However, confusion arose among clinicians regarding the AECC definition especially on the PF ratio cut off values of 300 and 200 mmHg (Costa & Amato 2013; Fanelli et al. 2013). Thus, the definition of ARDS has been revised with the aim to improve the current limitations of the AECC definition (Kattwinkel et al. 2004) .

In 2012, ARDS was redefined, into what is now known as the Berlin definition. In particular, the term of Acute Lung Injury (ALI) has been removed to eliminate confusion (Kattwinkel et al. 2004). In the Berlin definition, it recommends to use of three categories of ARDS based on degree of hypoxemia; Mild ARDS (200 mmHg < $PaO_2/FiO_2 \leq$ 300 mmHg), moderate ARDS (100 mmHg < $PaO_2/FiO_2 \leq$ 200 mmHg), and severe ARDS ($PaO_2/FiO_2 \leq$ 100 mmHg). The acute time frame is also specified to be within 1 week. The lower the PaO_2/FiO_2 ratio, the less inspired oxygen getting into the blood, and thus the worse the patient's condition.

ARDS patients admitted to the intensive care unit (ICU) require mechanical ventilation (MV) for breathing support due to the severe arterial hypoxemia and difficulty in breathing (Ashbaugh et al. 1967). During the last several decades, ARDS has had a major influence on mortality and morbidity in ICU patients worldwide. It was reported that there are approximately 200,000 cases per year of ARDS in the USA (Rubenfeld et al. 2005; The

Acute Respiratory Distress Syndrome Network 2000) and the hospital mortality rate has been reported to be between 30% and 60% (Luhr et al. 1999; Manzano et al. 2005; Phua et al. 2009; Reynolds et al. 1998; Sigurdsson et al. 2013). However, some studies have suggested that these mortality rates have been reduced due to the implementation of new protective ventilation strategies (Bernard 2005; Rubenfeld et al. 2005; Sigurdsson et al. 2013). These results elucidate the importance of having an optimal ventilator strategy to reduce the mortality rate in ARDS patients and equally reduce cost of the ICU stay at the same time.

1.2 Mechanical Ventilation

Since there is no specific treatment for ARDS patients, the only treatment that clinicians can offer is providing an environment that can aid and support ARDS patients' recovery. Mechanical ventilation (MV) is currently the most prevalent treatment for ARDS patients in Intensive Care Unit (ICU). Although there are a range of clinical therapies suggested for ARDS patients, only a few of them have been proven to be clinically effective and only with little statistical significance (Ware & Matthay 2000). The idea of MV therapy is to assist patient and minimise the work of breathing (WOB) by maximising recruitment and oxygenation. MV provides the means of breathing support by partially or fully taking over the patients breathing effort. However, if ventilation settings are not properly adjusted, these patients are exposed to the risk of further lung injury and complications (Dreyfuss & Saumon 1998; Slutsky 1999). Hence, setting MV is a delicate balance between too little support and the risk of further lung injury due to too much support.

There are two primary, commonly used modes of MV typically used by clinicians. Specifically, pressure controlled ventilation (PCV) and volume controlled ventilation (VCV).

Under PCV, the Positive End-Expiratory Pressure (PEEP) and Peak Inspiratory Pressure (PIP) are set directly by the clinicians, and tidal volume (V_t) is as indirect result under this setting. Thus, the volume change during inspiration is a passive process. In contrast, under VCV, the PEEP and the V_t are chosen by the clinician. The V_t is set using a fixed flow rate since volume is the integral of flow rate with respect to time. The flow rate can be constant or varied during inspiration, and the PIP is an indirect result of these settings. Thus, the pressure change during inspiration is a passive process, in this latter mode.

1.3 Mechanical Ventilation Parameters

There are thus two main ventilator parameters that are clinically set, which are Positive End-Expiratory Pressure (PEEP) and Tidal Volume (V_t).

1.3.1 Tidal Volume (V_t)

The tidal volume (V_t) is the volume of air delivered to the lung per breath. If it is too high, it will over-distend the lung and cause Ventilation Induced Lung Injury (VILI) (Caironi et al. 2010; Chiumello et al. 2008; Slutsky 1999). In particular, VILI occurs as a result of excessive tidal volumes and is known as volutrauma, where VILI caused by excessive pressure is known as barotraumas (Chao & Scheinhorn 1996; Dreyfuss & Saumon 1992). Setting optimal tidal volume is important. If it is too low, it will result in an inadequate amount of oxygenation and atelectasis, which is damaging to the alveoli. In normal conditions, the goal is that V_t provides maximum gas exchange for minimum breathing effort. Tidal volume relates to lung strain over the entire organ, where strain is ratio of tidal volume over functional residual capacity (V_t /FRC).

For ARDS patients, lung stress and strain may be higher compared to healthier people. Thus, large V_t provides higher strain with a higher risk of VILI for ARDS patients. Therefore, a study by ARDS network (The Acute Respiratory Distress Syndrome Network 2000) recommended using a lower V_t range to provide safe and lung protective strategies for MV patients. The study carried out by ARDS Network reported that patients ventilated with lower V_t (6ml-8ml/kg) resulted with lower mortality rate in ARDS patient cohort than those given 12 ml/kg (The Acute Respiratory Distress Syndrome Network 2000). It is thus believed that low V_t can reduce VILI by decreasing plateau and peak pressures, and/or by stabilising alveoli (DiRocco et al. 2006). While most studies have similar results, there are still many debates about the use of low or high V_t for MV (Bruhn et al. 2011; Eichacker et al. 2002).

1.3.2 Positive end expiratory pressure (PEEP)

Positive end-expiratory pressure (PEEP) is applied during MV to prevent de-recruitment at the end of expiration by keeping unstable lung units open, and to recruit the new lung units, which improve oxygenation (Amato et al. 1998; Meade et al. 2008). PEEP represents the pressure at the end of expiration to which the lung is allowed to deflate and is greater than atmospheric pressure to hold open damaged lung units. The objective of PEEP is to increase the level of oxygenation by increasing the number of recruited alveoli by lifting the lung pressure at the end of expiration so that alveoli will remain open, and thus reducing the repetitive and damaging process of opening and collapse of these lung units to allow them to heal.

Several studies (Briel et al. 2010; Mercat et al. 2008; Schirrmann et al. 2010) noted that with adequate PEEP during recruitment manoeuvres, the collapsed alveoli can be recruited to

improve oxygenation. However, if high pressure is applied, there are high risks of over-distension of the already opened and still healthy alveoli. In some studies, it was found that compliance was lowest at highest PEEP which shows that overstretching did occur at this highest PEEP (Suh et al. 2003). Thus, using the highest PEEP possible is not the best solution for optimum ventilation therapy as it may cause more harm than good and contribute to VILI (Brower et al. 2004; Sundaresan & Chase 2012).

There is currently no standard method for PEEP selection. Thus, clinicians often resort to choosing PEEP based on personal experience, intuition or generalised approach (Levy 2004). If too high, it risks injuring healthy lung units, and if PEEP is too low, it results in continuous recruitment and de-recruitment of ARDS affected alveoli and further damage. As patient condition is variable, these PEEP selection methods may under, or over-support patients, or both over time as patient condition evolves dynamically, resulting in suboptimal ventilation, further complicating patient condition and outcome (Pavone et al. 2007; Petersen 1983; Puybasset et al. 2000; Slutsky 1999; Villar et al. 2006). Thus, the optimal PEEP determination by clinicians remains an elusive goal.

1.4 Problem in MV

The major problem in MV therapy is the lack of standardised clinical protocols for adjusting MV settings for treating ARDS, as well in general. Currently, ventilator settings and protocols are strongly dependent on the experience of the clinicians, resulting in variable protocols with limited effectiveness over broad cohorts (Briel et al. 2010; Grasso et al. 2007; Hodgson et al. 2011; Meade et al. 2008). As a result, many major, general trials have failed. Incorrect ventilator settings can cause further lung injuries, such as barotrauma, volutrauma,

atelectasis and biotrauma (Chao & Scheinhorn 1996; Lipes et al. 2012; Tremblay & Slutsky 1997). Thus, to minimise these negative effects that may negatively affect or significantly deteriorate the condition of ARDS patients, different approaches to setting MV need to be developed, proven, and implemented.

While MV is the main therapy for ARDS patients, there are major concerns on the management of MV, especially around the length of time of using MV. The longer a patient remains on ventilator, the higher the chance of complications, including airway injury due to the endotracheal tube, as well as increased risk of ventilator-associated pneumonia (VAP). Several studies suggested that MV should be applied for the shortest period of time necessary to prevent impairment of lung function and other complications (Anzueto et al. 1997; Forel et al. 2012). In support, patients on MV have a mortality rate 4 times higher than non-MV patients (Dasta et al. 2005), which increases as length of MV increases. In addition, due to the length of stay in ICU, daily costs for MV patients were consistently greater compared to non-MV patients, costing an estimated $1440 USD more per patient per day which is almost doubling the daily cost of an ICU patient (Davidson et al. 2014). Hence, the need for better, patient-specific protocols is patient-centered, as well as economic.

MV therapy aims to maximise recruitment and oxygenation, while minimising the risk of VILI. Thus, the MV setting has to be as minimally invasive as possible by adjusting the optimal level of PEEP without compromising these goals. However, while the management strategy of ventilator still remains under debate (Amato et al. 1998), it is often difficult to achieve the primary goal of improving oxygenation with optimal MV settings, as well as ensuring that the lungs heal properly. The difficulty is compounded by the fact that each patient has a unique disease state and evolution.

One of the emerging methods to achieve the objective of optimal ventilator setting is through model-based methods (Sundaresan et al. 2011a; Yuta et al. 2004). Model-based methods are capable of providing unique insight to patient-specific condition and response to treatment. These methods are relatively non-invasive or non-additionally-invasive, and have shown promising outcome in guiding therapy (Chiew et al. 2011; Sundaresan et al. 2010; van Drunen et al. 2013). Thus, the motivation of this research is to develop model-based and patient-specific lung models that are able to analyse and aid clinicians in choosing the optimum MV settings based on patient-specific needs and response.

1.5 Medical Imaging

Medical imaging is an element in assessing the heterogeneity and impact of ARDS. They are thus needed to aid model development and validation.

1.5.1 Computed Tomography

Computed tomography (CT) scan has been widely employed to study ARDS patients since it allows the clinicians to assess and monitor patient's lung condition (Gattinoni et al. 2006; Lu et al. 2001). For CT scans, Hounsfield units (HU) are used to describe the x-ray attenuation which is known as radio density that caused by different tissues. Based on the attenuation of individual pixels of the scan, the alveoli can be determined to be either recruited, de-recruited or overinflated (Sundaresan & Chase 2012). In particular, the study by Viera et al. (Vieira et al. 1998) using CT scans found that the threshold of -900 HU might be used in patients with ALI/ARDS at risk of MV induced lung barotrauma due to over-distended lung. Although CT scan is a useful tool to detect over-distended alveoli, it exposes the patient to potential risks

such as transporting patients out from the ICU and expose to additional radiation dosage (Brenner & Hall 2007; Gattinoni et al. 2001; Pesenti et al. 2001; Tubiana et al. 2008). Thus, the use of CT scan to guide MV treatment remains limited.

1.5.2 Electrical Impedance Tomography

Electrical Impedance Tomography (EIT) is another medical imaging that potentially suitable for bedside lung monitoring. It was first developed for medical monitoring by Barber and Brown (Barber & Brown 1984) and used a method by generating a cross-sectional image of lungs using the spatial distribution of electrical conductivity (Denai et al. 2010). Despite its advantages as a non-invasive bedside tool that can be used for continuous monitoring of MV therapy, it has limited spatial resolution, requires complex image reconstruction algorithms, and requires skilled operators to implement. It is an emerging, but non-invasive technology.

1.6 Review of Mathematical Respiratory System Models

In the literature, the development of mathematical models has been used with great success to delineate the physiology of the mechanical respiratory system. These models range from very simple lumped parameter models (Carley & Shannon 1988; Grodins et al. 1967; Trueb et al. 1971) to highly complex finite element models (Donovan 2011; Tawhai et al. 2011; Tawhai et al. 2004). However, to date, most models are developed for educational purposes (Chase et al. 2006b; DiCarlo 2008) and only a few have been designed with a real-time, patient-specific therapeutic goals or outcomes in mind (Ben-Tal 2006). The following sections review several mathematical models that have been developed to provide physiological insight into lung conditions that have opened up new idea and knowledge in lung mechanics modelling.

1.6.1 Recruitment Model

One of the most important strategies in MV is to recruit lung units to improve oxygenation and to also keep the lung open. Animal studies using *in vivo* microscopy showed that the ARDS affected alveoli can be characterised into three different types (Schiller et al. 2003). All the three types of alveoli demonstrated different recruitment pattern and compliance. Type 1 alveoli are characterised as the most heathy and normal alveoli, as the alveoli do not collapse at the end of expiration and do not change volume significantly during tidal ventilation. In contrast, Type 2 alveoli are defined as slightly to moderately affect by lung injury. Their sizes and shapes change significantly during tidal ventilation, and may collapse at the end of expiration. Type 3 alveoli are the most affected by the lung injury where large volume changes as pressure increases and collapse at the end of expiration. In addition, alveoli that demonstrate repetitive alveolar collapse and expansion (RACE) are larger than normal alveoli at peak inspiration. Thus, this specific aspect increases the size of the alveoli or over-distension (Schiller et al. 2001).

Traditionally, the lung was assumed to expand by isotropic expansion of alveoli during recruitment (Albaiceta et al. 2007; Hickling 2002). The recruitment of alveoli was interpreted using a static or dynamic pressure volume (PV) curve. Based on the PV curve, alveolar recruitment is assumed to occur at the lower inflection point (LIP), which was then followed by balloon-like expansion of recruited alveoli. The alveoli require an initially high pressure to overcome elastic forces before it start to expand and resulting with major volume change. Over-inflation of alveoli occurs at the upper inflection point (UIP), which resulting in sudden decrease of compliance due to the over-stretching effect.

However, this traditional theory does not agree to clinical in-vivo studies that have presented different mechanism of lung expansion. Schiller et al. found (Halter et al. 2003) that normal healthy alveoli do not expand as pressure is increased, which contributes to a very little of volume changes. Thus, this result shows that balloon-like expansion is not the correct mechanism of lung volume change. Once alveoli are recruited, the volume does not change significantly for healthy units and some ARDS affected alveoli (Schiller et al. 2003).

In addition, several studies observed that recruitment and de-recruitment occurs continuously for the entire breathing cycle especially between LIP and UIP which contribute to the hysteresis observed in PV curves (Cheng et al. 1995; Jonson et al. 1999). It is also shows that as PEEP increases, volume of the lung can increase for a given pressure which delineate that there is an additional recruitment occurs above LIP (Carney et al. 1999; Jonson et al. 1999). Thus, recruitment theory is more relevant in understanding the lung mechanics of ARDS patients. Figure 1.1 illustrates the different between traditional theory and the recruitment theory.

From this recruitment theory, a recruitment mathematical model was developed by Hickling (Hickling 1998b). This recruitment model is based on recruitment and de-recruitment using threshold opening pressure (TOP) and threshold closing pressure (TCP). The model defined the relation between pressure and volume (PV) curve and recruitment status where the PV curve changes with recruitment. It has been added into several models to capture patient-specific parameters that can guide clinicians in selecting the optimal setting of the MV (Schranz et al. 2012a; Sundaresan et al. 2009). This model is able to characterise ARDS lung physiology based on this concept of recruitment and simplified lung physiology. In particular, the lung can be modelled as a collection of alveoli or lung units with discrete layers that

subjected to superimposed pressure. The compartment of the bottom experiences higher superimposed pressure than the ones above due to the weight of the lung. Superimposed pressure is an additional pressure applied to the lung units by the gravitational force of the lungs above it.

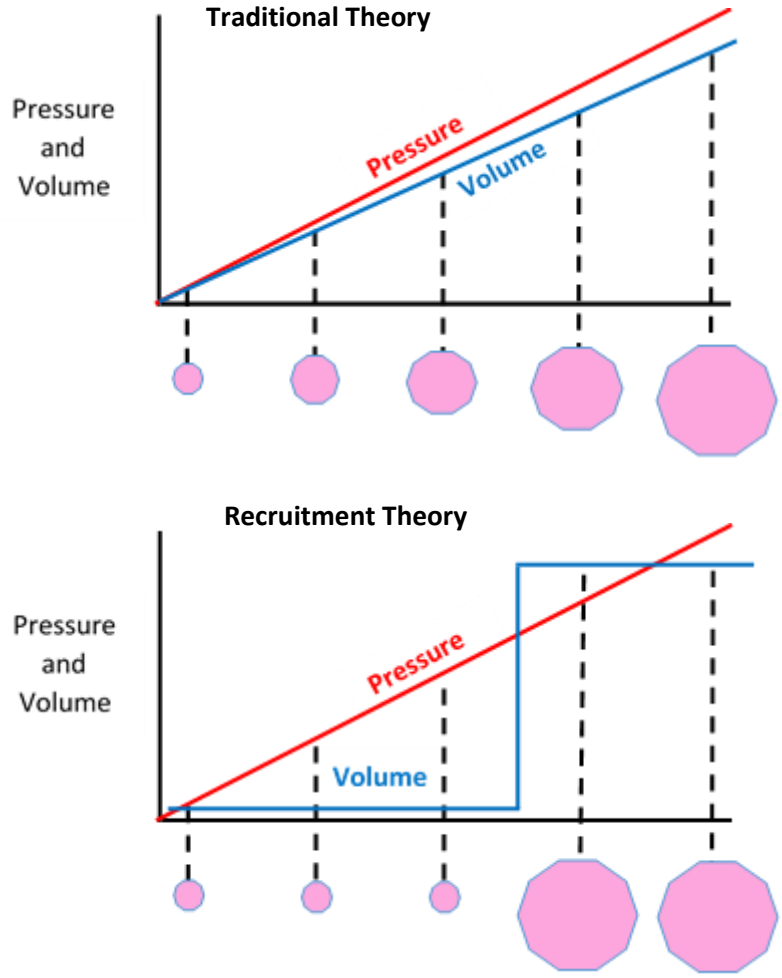

Figure 1.1: Alveolar expansion based on traditional and recruitment theory. (Top) Isotropic expansion of alveoli as isotropic balloon like based on traditional theory. (Bottom) Recruitment theory describes the alveolus is either open or closed. (Chiew 2013)

In this recruitment model, the pressure at which alveoli will start to open and inflate is known as the Threshold Opening Pressure (TOP), whereas Threshold Closing Pressure (TCP) is known as the point when the alveoli start to deflate. Since recruitment and de-recruitment

occur throughout the breathing cycle, the TOP and TCP are widely distributed along pressure, rather than the LIP and UIP as traditionally assumed (Crotti et al. 2001; Pelosi et al. 2001). In this model, quasi-static volume is calculated at each airway pressure increment. During inflation, if the applied airway pressure from MV is higher than the TOP, the unit is recruited and assumes a lung volume. Each opened unit volume is added to form the inflation PV curve. In contrast, if the TCP exceeds the applied airway pressure, the lung unit collapses and loses the unit volume, which thus creates the deflation curve. The inflation and deflation curves then create the overall lung PV curve.

Although the recruitment model by Hickling is able to capture basic characteristics of lung mechanics by simulating the relationship between pressure, volume, and the recruitment status of the lung units, this model is unable to predict the volume change resulting from a change in PEEP. Thus, with higher PEEP, it may overstretch and damage some healthy alveoli.

Similarly, Sundaresan et al. (Sundaresan et al. 2009) developed a minimal model than applied the similar recruitment concept. This model accounts for stiffer, smaller volume nature of its mechanics as well as the basic mechanism by which the recruitment of lung for gas exchange and breathing can be increased. It is able to estimate and provide unique insight to patient-specific lung condition based on calculation of the mean and standard deviation of the TOP and TCP. Despite its capability of monitoring patient-disease state, predicting recruitment for changes in PEEP, and to guide MV therapy, the minimal model designed only accounts for both two alveoli conditions, either recruited or de-recruited (Sundaresan et al. 2011a; Sundaresan et al. 2009). There is no measure of alveolar stress or strain that can lead to (local) lung damage due to excessive pressure. Thus, what will happen to the healthy alveoli

if the value of PEEP is increased to recruit collapsed alveoli? There is no clinical benefit in recruiting ARDS affected alveoli if the PEEP or pressure required damages healthy alveoli in less dependent region. Therefore, further insight into estimation of alveoli pressure may extend the model potential.

1.6.2 Model-based LIP and UIP

Another well-known method to assess the lung condition is to monitor the alveolar pressure using the static PV curve model. This model applies the concept of LIP and UIP in selecting appropriate PEEP level for MV setting (Albaiceta et al. 2008). Static PV curves have been extensively used in the treatment and management of patients with ARDS in the past (Albaiceta et al. 2003; Henzler et al. 2003; Suter et al. 1975; Venegas et al. 1998). It resembles a sigmoidal curve with no hysteresis which is unique for each patient. Thus, mathematical models such as the Venegas model (Venegas et al. 1998) which describes the shape of the sigmoidal curve can be used to identify the static PV curve (Albaiceta et al. 2007). Based on the static PV curve, clinicians typically set PEEP such that it is between the LIP and UIP. However, the LIP and UIP can take on range of values and differ between models and between patients, as well as over time. They also do not offer one unique setting (Sundaresan & Chase 2012). Hence, selecting optimal PEEP based on the static PV curve is limited in clinical application, but offers some useful insights.

1.6.3 Lumped parameter models

Lumped parameter models, such as the single compartment linear lung model (LLM), are less computationally intense. These simpler models have shown clinical potential in monitoring

patient's respiratory mechanics in real-time to guide clinical therapy (Avanzolini & Barbini 1984; Lucangelo et al. 2007). The trade-off being that these simple models are not capable of providing high resolution information compared to more complex models. This model is extensively used this research because of its identifiability and ease of use, and will be discussed in details in Chapter 5.

1.6.4 Finite Elements Models

Finite element models of the respiratory system that have been developed offer significant understanding of the underlying physiology and offer detailed resolution of complex systems (Burrowes et al. 2005; Tawhai & Bates 2011; Tawhai et al. 2004). In addition, these models allow detailed estimation on pulmonary gas flow and realistic simulation of lung behaviour as each model can represent a unique geometry for a given patient (Burrowes et al. 2011; Kitaoka et al. 2007). However, finite element model is computationally intense and requires longer time to run a simulation which limits its capability to be used for bedside monitoring.

1.6.5 Airway Branching Models

Airway branching models (ABM) are able to capture physiologically relevant information. The ABM (Horsfield et al. 1971; Weibel 1963b) with the airway dimensions and pathways of the airway system have been used to predict respiratory pressure-flow responses (Pedley et al. 1970). However, while anatomically accurate, these models require *a-priori* knowledge of the lung dimensions and can thus only be based on average lung dimensions in humans, which can limit application for patient-specific ARDS patients which have their own individual lung dimensions that change with disease state. All of these issues limit application in real-time

clinical settings. This model is also studied in this research and is presented in Chapter 3 as it offers some patient-specific potential developed in this thesis.

A summary of several other model-based methods is listed in Table 1.1. Most of the models described were impractical to identify clinically and thus cannot be used to guide therapy due to the limited time, data and resources in ICU.

Table 1.1: List of model-based methods in their respected categories

No.	Categories and Functions	References
1.	Compartment Models	(Bates 2009; Lucangelo et al. 2007; Ma & Bates 2010; Schranz et al. 2011)
2.	SLICE Methods	(Guttmann et al. 1994; Zhao et al. 2012a; Zhao et al. 2012b)
3.	Stress Index	(Grasso et al. 2007; Ranieri et al. 2000)
4.	Stress Strain Approaches	(Chiumello et al. 2008; Mead et al. 1970; Sundaresan et al. 2011c)
5.	Alveolar and Surface Tension Models	(Andreassen et al. 2010; de Ryk et al. 2007; Kitaoka et al. 2007; Morris et al. 2001; Reddy et al. 2011; Schirrmann et al. 2010)
6	Spontaneous Breathing Models	(Khirani et al. 2010; Schuessler et al. 1997; Zhao et al. 2006)
7.	Mechanical Lung Models	(Chase et al. 2006b; Kuebler et al. 2007)

1.7 Research Focus

This research focuses on multi-scale respiratory system modelling that can be used to guide patient-specific MV therapy. The main objectives of this research are to investigate and develop new extended models of lung mechanics for ARDS patients by creating model-based measures of the potential impact of changing MV therapy parameters to healthy lung units.

These models will require a rapid form of parameter identification to define patient-specific model from clinical data, in real time, to be used as a complementary metric in guiding MV. From these results, patient-specific therapies can be created and the overall approach clinically validated in pilot trials. The thesis consists of 10 chapters as follows:

- Chapter 1: Introduction
- Chapter 2 presents the dynostatic algorithm (DSA) that allows the estimation of alveoli pressure during tidal ventilation.
- Chapter 3 studies extensively on the airway branching model (ABM) and an extended model has been developed which allows the estimation of airway pressure drop at each bronchial generation with patient-specific airway dimension, α. Using this model, the airway condition of a patient can be characterised and thus, could provide clinically useful information to clinicians to guide patient-specific therapy.
- Chapter 4 introduces the importance of estimation of lung elastance in respiratory system and discuss several models that estimate lung elastance.
- Chapter 5 investigates on relation of expiratory time constant with respiratory system elastance in retrospective clinical cohorts.
- Chapter 6 explores the variability of elastance in the clinical trial.
- Chapter 7 focuses on negative elastance in spontaneously breathing patient.
- Chapter 8 presents a reconstruction airway pressure model that able to eliminate the variability of elastance in clinical data.
- Chapter 9 summarises and concludes the outcomes of this thesis.
- Chapter 10 delivers possible future work for this research.

CHAPTER 2

Dynostatic Monitoring of Clinical Data

2.1 Introduction

Estimation of the alveolar pressure is important during mechanical ventilation (MV) to assess and prevent the possibility of the over-distension condition of alveoli due to the excessive pressure delivered by the ventilator. One particular concern is that the supporting pressure to recruit collapsed lung may be too high, leading to ventilator induced lung injury (VILI) from over-distension of healthy alveoli. In particular, barotraumas is caused by excessive pressure delivered by the ventilator. Without assessment of alveolar pressure, clinical decision making is limited. To date, several studies have shown that maintaining alveolar pressure or plateau pressure below 30 cmH_2O can protect alveoli from over-distension condition and mitigate the risk of VILI (Chiumello et al. 2008; Jaswal et al. 2014; Rouby et al. 2004). However, this approach limits the ability to use greater pressure when it may be safe.

The application of such positive end expiratory pressure (PEEP) in ventilator settings has been shown to greatly improve oxygenation in ARDS patients (Amato et al. 1998; Halter et al. 2003; McCann et al. 2001; The Acute Respiratory Distress Syndrome Network 2000). However, higher levels of PEEP risk overstretching alveoli, especially for healthy, well-aerated alveoli (Ricard et al. 2003). Furthermore, it was found that compliance was the lowest at highest PEEP which indicates that overstretching and associated nonlinear mechanics do occur at higher PEEP levels (Suh et al. 2003). Thus, using the highest PEEP possible is not the best solution for an optimum ventilation therapy as it may cause more harm than good.

Thus, it is essential for clinicians to be able to estimate alveolar pressure in MV patients in real-time, preferably breath to breath.

2.2 Static Pressure Volume Curve

One of the best methods to assess alveolar pressure is the static pressure volume (PV) curve. Static PV curves are also known as static compliance curves, and are sometimes used to determine the best treatment or selecting optimal positive end expiratory pressure (PEEP) (Caramez et al. 2009; Maggiore et al. 2003; Rouby et al. 2013). Dynamically, the pressure-volume curves measured during inflation and deflation are different. This behaviour is known as hysteresis.

In ARDS patients, the static PV curve can also be considered as recruitment curves (Hickling 1998a) that describe the mechanical behaviour of the lungs and chest wall during inflation and deflation. They are calculated during stable airway conditions where there is no air flow within the respiratory airways and all viscoelastic forces are equilibrated resulting in reduced hysteresis (Henderson & Sheel 2012). The static PV curve is generally measured by three different methods: the super syringe technique, the constant flow method, and the multiple-occlusion method (Harris 2005; Stenqvist 2003). However, it is static, and thus does not necessarily capture the dynamic, higher pressures and their effects.

A static PV curve resembles a sigmoid curve with no hysteresis, and is distinctly unique for each patient. The most well-known model by Venegas et al. (Venegas et al. 1998) introduced the static PV curve as a sigmoid function that fit the overall static PV curve. It is generally characterised by an upper inflection point (UIP) and lower inflection point (LIP), as shown in

Figure 2.1. The LIP is defined as the point at which slope of the curves increases as the recruitment of alveoli increases rapidly. In contrast, the UIP is the point when alveoli begin to overstretch and resulting in a sudden decrease in compliance. However, this is a curve for the overall lung behaviour and does not capture the superimposed pressure effects of lung dependency or depth, and thus cannot capture the impact on alveoli at specific locales.

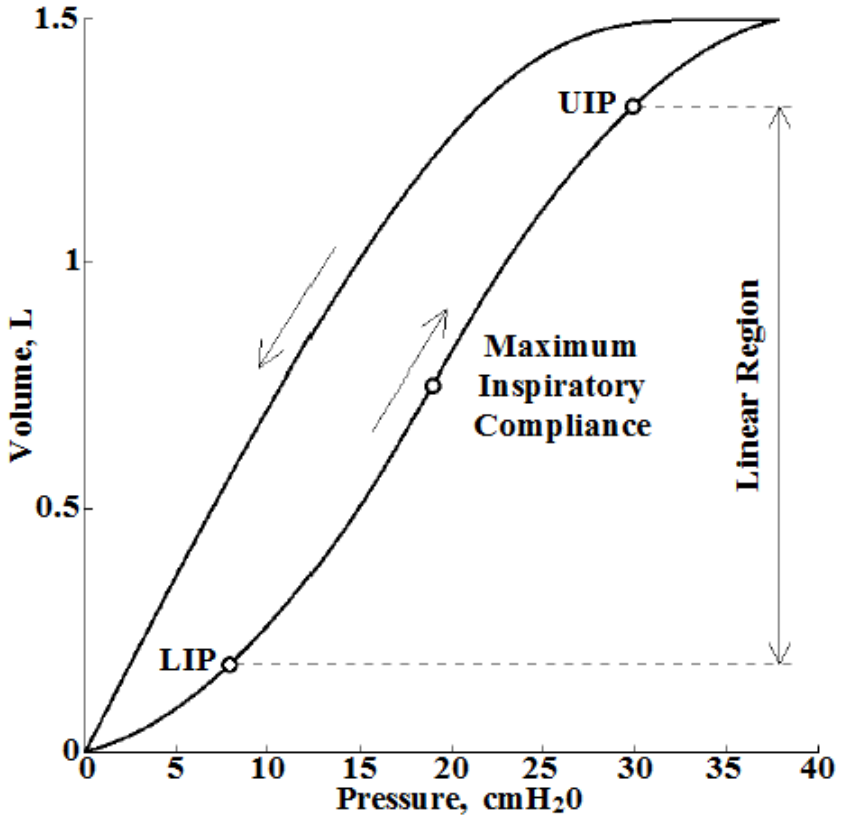

Figure 2.1: Schematic of a static PV curve showing LIP and UIP (Bersten 1998)

The LIP and UIP points provides guideline for clinicians to set PEEP (Albaiceta et al. 2008). It is suggested that PEEP should be set above LIP to avoid repetitive collapse of alveoli, and below UIP to prevent over-distension condition of alveoli (Brower et al. 2004; Ferguson et al. 2005; Jonson et al. 1999; Mercat et al. 2008; Ward et al. 2002). However, this approach still offers a large range of potential values, where a single optimal and patient-specific PEEP

value cannot be determined (Sundaresan & Chase 2012). This outcome is a result of still leaving a subjective choice to the clinician.

In addition, the location of the LIP and UIP are typically not identifiable during normal tidal ventilation (Lichtwarck-Aschoff et al. 2000). More importantly, the methods required to obtain the static PV curves are invasive (Lu & Rouby 2000; Servillo et al. 1997), time consuming, and cause interruption to MV therapy (Harris 2005; Kárason et al. 2001). These issues limit PEEP selection based on static PV loop in normal clinical situations, and it thus not practical to use in mitigating over-distension of healthy alveoli. As a result, Karason et al. (Karason et al. 2000) introduced the dynostatic algorithm (DSA) which is the most well-known method to estimate this dyno-static alveoli pressure by producing the dynostatic curve during normal breathing condition (Karason et al. 2000; Sondergaard et al. 2003b).

The DSA is a model-based method that can estimate a surrogate of alveoli pressure without the need of extensive protocol. In the DSA, the estimated alveoli pressure is based on the assumption that airway resistance is always the same during inspiration and expiration at isovolume, but not throughout inspiration or expiration (Stenqvist 2003). This assumption thus assumes the airway resistance is influenced by the airway geometry and at each airway location, the resistance at that point is the same. With this assumption, a surrogate of the alveolar pressure, dubbed as the dynostatic pressure, can be estimated during tidal ventilation. Thus, this dynostatic pressure at isovolume curve can be used as an alternative for the static PV curve.

In this chapter, two patients' cohorts with different airway pressure and flow profile were studied using the DSA. These two cohorts will provide a better understanding of the algorithm, its performance, and potential for clinical application, and limitations.

2.3 Methodology

2.3.1 Dynostatic Algorithm Model (DSA)

Proposed by Karason et al. (Karason et al. 2000), the DSA assumes the airway resistance during inspiration and expiration are the same at isovolume ($R_{insp} = R_{exp}$). It thus assumes that the airway resistance is a physiological constant, depending on the location of where it is measured and that it is not flow dependent, which is a significant simplification. Figure 2.2 shows an example of the quasi static pressure estimated using the DSA in relation to a dynamic pressure volume data during tidal ventilation.

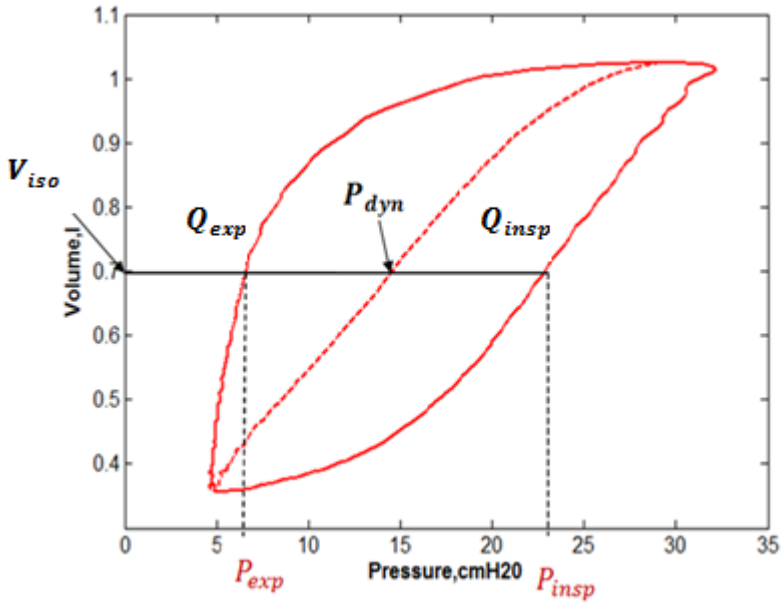

Figure 2.2: The DSA diagram and resulting quasi-static, single line pressure volume curve within the tidal ventilation.

Based on these assumptions, a surrogate of the alveolar pressure, known as dynostatic pressure (P_{dyn}), can be derived:

$$R_{insp} = \frac{P_{insp} - P_{dyn}}{Q_{insp}} = R_{exp} = \frac{P_{exp} - P_{dyn}}{Q_{exp}} \quad (2.1)$$

$$P_{dyn} = \frac{P_{insp} \times Q_{exp} - P_{exp} \times Q_{insp}}{Q_{exp} - Q_{insp}} \quad (2.2)$$

where, Q_{exp} is the expiration flow, Q_{insp} is the inspiration flow, P_{insp} is the pressure during inspiration, and P_{exp} is the pressure during expiration.

2.3.2 Patient data

A preliminary model validation was performed using datasets obtained from two retrospective ARDS cohorts consisting of 10 patient datasets from Sundaresan et al. (Sundaresan et al. 2011a) and 10 patient datasets from Bersten et al. (Bersten 1998) (Cohorts 1 and 2, respectively). Patients in Cohort 1 underwent a modified protocol-based recruitment manoeuvre, where these patients were ventilated with several different PEEP levels using a ramp flow profile (Sundaresan et al. 2011a). These patients were fully sedated and ventilated using Puritan Bennett PB840 ventilators (Covedin, Boulder, CO, USA) with volume control (tidal volume = 6-8 mL/kg), synchronized intermittent mandatory ventilation (SIMV) mode, throughout the trial.

The airway pressure and flow profile where obtained using a pneumotachometer with a data acquisition module connected to the patient's ventilation circuit Y-piece, sampling at 100Hz. Inspiratory volume was obtained through flow integration and drift correction. The end of expiratory lung volume (EELV) at each PEEP level was calculated through continuous

monitoring of the airway flow at every PEEP changes (Chiew et al. 2011). An example of airway pressure, flow rate and volume data from patient S1 is shown in Figure 2.3. The demographics and cause of ARDS for patients in Cohort 1 is presented in Table 2.1.

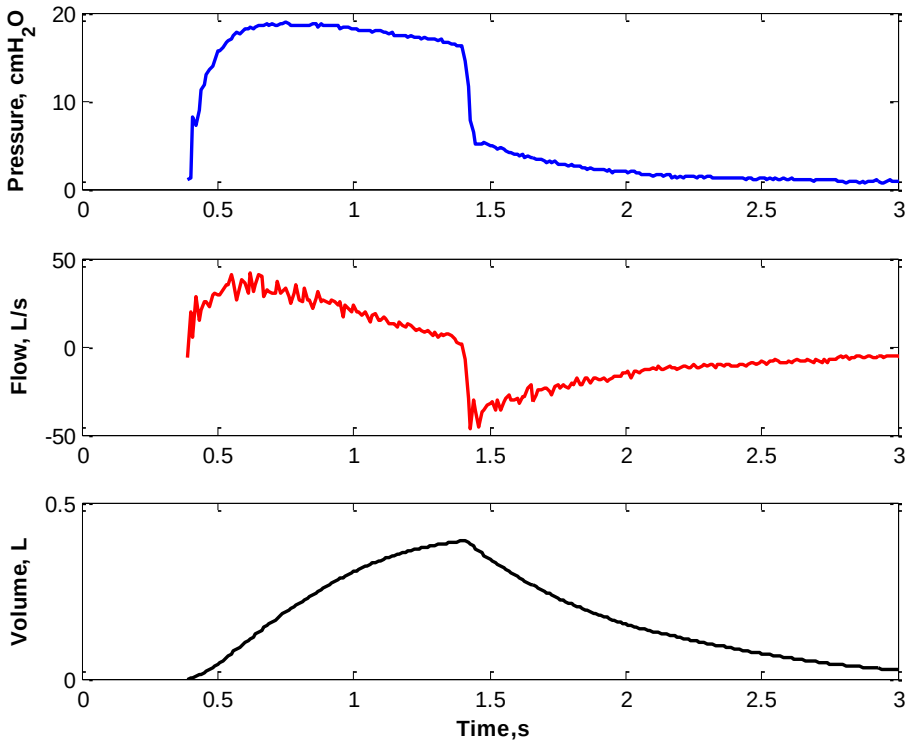

Figure 2.3: Example of the Airway pressure data (*Top*), flow rate data (*Middle*) and volume data (*Bottom*) for Patient S1 in Cohort 1.

Table 2.1: Characteristics of the patients in Cohort 1 (Sundaresan et al. 2011a)

Patient	**Sex**	**Age [years]**	**Clinical Diagnostic**
S1	Female	61	Peritonitis, COPD
S2	Male	22	Trauma
S3	Male	55	Aspiration
S4	Male	88	Pneumonia, COPD
S5	Male	59	Pneumonia, COPD
S6	Male	69	Trauma
S7	Male	56	Legionnaires
S8	Female	45	Aspiration
S9	Male	37	H1N1,COPD
S10	Male	56	Legionnaires, COPD

Patients in Cohort 2 were fully sedated and ventilated using Puritan Bennett 7200ae ventilators (Carlsbad, CA, USA) under volume control mode (tidal volume, V_t = 8-10 mL/kg) and a square-wave inspiratory flow. Airway pressure data was acquired using a (water manometer) strain gauge transducer (Bell and Howell 4-327-I; Trans America Delaval, Pasadena, CA, USA). Volumetric flow rate data was acquired using a heated, Fleisch-type pneumotachograph (HP-47034A, Hewlett-Packard, Palo Alto, CA, USA) (Bersten 1998). Trials were initially performed at baseline PEEP. Trials were then repeated at 30 min intervals following random PEEP changes between 5 and 15 cmH_2O. The final 60 s of data from each PEEP level was recorded. The end of expiratory lung volume corresponding to each PEEP level was also calculated. Each dataset included recordings of at least 3 different PEEP levels, as well as deflation to functional residual capacity (FRC) at PEEP = 0 cmH_2O. The demographics and cause of ARDS for each patient in Cohort 2 are presented in Table 2.2. Figure 2.4 shows an example of airway pressure data, flow rate data, and volume data, for patient B10.

Table 2.2: Characteristics of the patients in Cohort 2 (Bersten 1998)

Patient	**Sex**	**Age [years]**	**Clinical Diagnostic**
B1	Male	74	Ruptured abdominal aortic aneurysm
B2	Male	24	Lung contusion
B3	Female	72	Legionnaire's disease
B4	Male	48	Pancreatitis
B5	Female	68	Pulmonary embolus
B6	Male	54	Aspiration
B7	Male	73	Aspiration
B8	Male	72	Pneumonia
B9	Male	81	Aspiration
B10	Male	47	Liver transplant

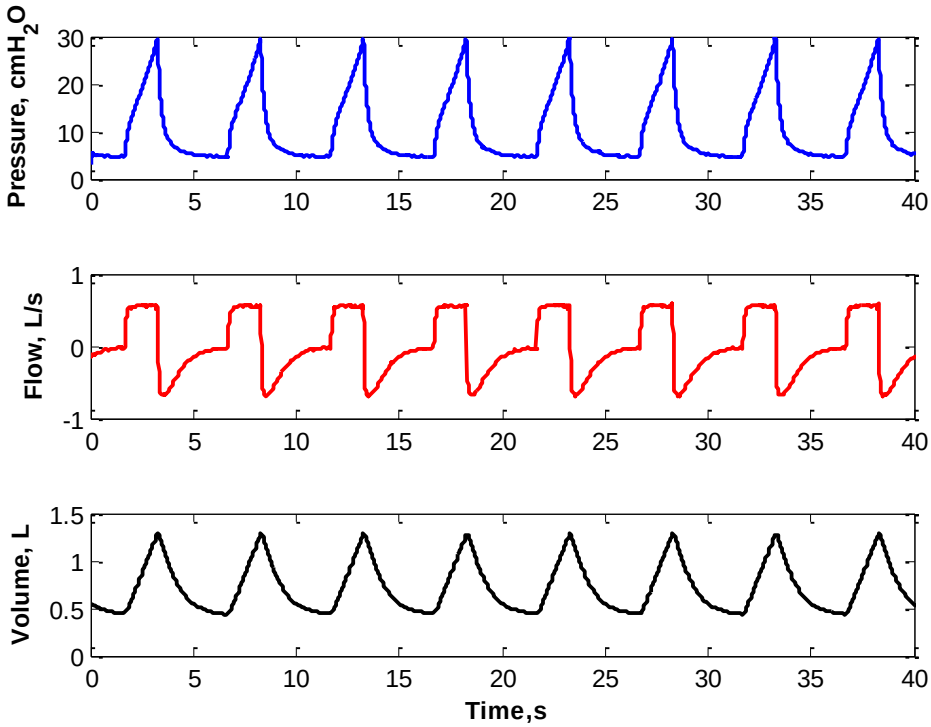

Figure 2.4: Example of Cohort 2 data from patient B10 for eight breathing cycles. *Top*: Airway pressure data. *Middle*: Flow rate data. *Bottom*: Volume data

2.3.3 Data Analysis

For each patient in this study, P_{dyn} was calculated for every breathing cycle at every PEEP using Equation 2.2. The median [Interquartile range (IQR)] of each tidal ventilation P_{dyn} were calculated for comparison. The corresponding maximum P_{dyn} at each PEEP is also calculated as a surrogate of maximum alveolar pressure during tidal ventilation.

2.4 Results

The pressure volume (PV) curves with alveoli pressure determined by the DSA for the two cohorts are presented in Figures 2.5 and 2.6. P_{dyn} results for Cohort 1 and Cohort 2 at each PEEP level are also tabulated in Tables 2.3 and 2.4, respectively.

Table 2.3: Patient-specific dynostatic pressure (P_{dyn}) for Cohort 1 at each PEEP level

Patient		P_{dyn} (cmH_2O)		
		PEEP 5	**PEEP 10**	**PEEP 15**
S1	**Median**	7.87	12.61	16.97
	[IQR]	[6.67-13.99]	[11.24-17.73]	[15.97-21.77]
	Maximum	17.43	20.72	25.92
S2	**Median**	12.29	14.71	19.42
	[IQR]	[6.65-14.39]	[12.87-18.22]	[16.93-23.54]
	Maximum	15.80	20.86	26.47
S3	**Median**	7.76	12.61	15.94
	[IQR]	[5.50-10.96]	[10.66-16.35]	[14.87-21.13]
	Maximum	13.66	18.66	24.45
S4	**Median**	9.43	13.30	18.82
	[IQR]	[8.17-11.60]	[11.81-15.34]	[16.39-21.07]
	Maximum	17.69	19.23	22.98
S5	**Median**	8.22	13.25	16.05
	[IQR]	[6.17-15.18]	[10.91-17.31]	[15.17-21.79]
	Maximum	28.69	28.06	29.87
S6	**Median**	8.36	13.61	16.93
	[IQR]	[6.22-12.96]	[10.96-17.20]	[15.13-22.19]
	Maximum	14.99	19.49	25.13
S7	**Median**	8.82	15.23	16.62
	[IQR]	[6.54-11.83]	[11.59-21.59]	[16.21-21.07]
	Maximum	19.58	28.87	40.39
S8	**Median**	9.53	13.38	15.93
	[IQR]	[6.79-12.94]	[10.95-17.38]	[14.93-20.38]
	Maximum	16.57	20.43	25.16
S9	**Median**	8.80	13.33	17.27
	[IQR]	[6.77-13.29]	[10.76-16.92]	[15.17-20.91]
	Maximum	21.12	22.38	26.79
S10	**Median**	7.72	17.06	21.20
	[IQR]	[6.18-12.10]	[12.23-21.40]	[17.63-26.58]
	Maximum	21.96	25.98	30.35

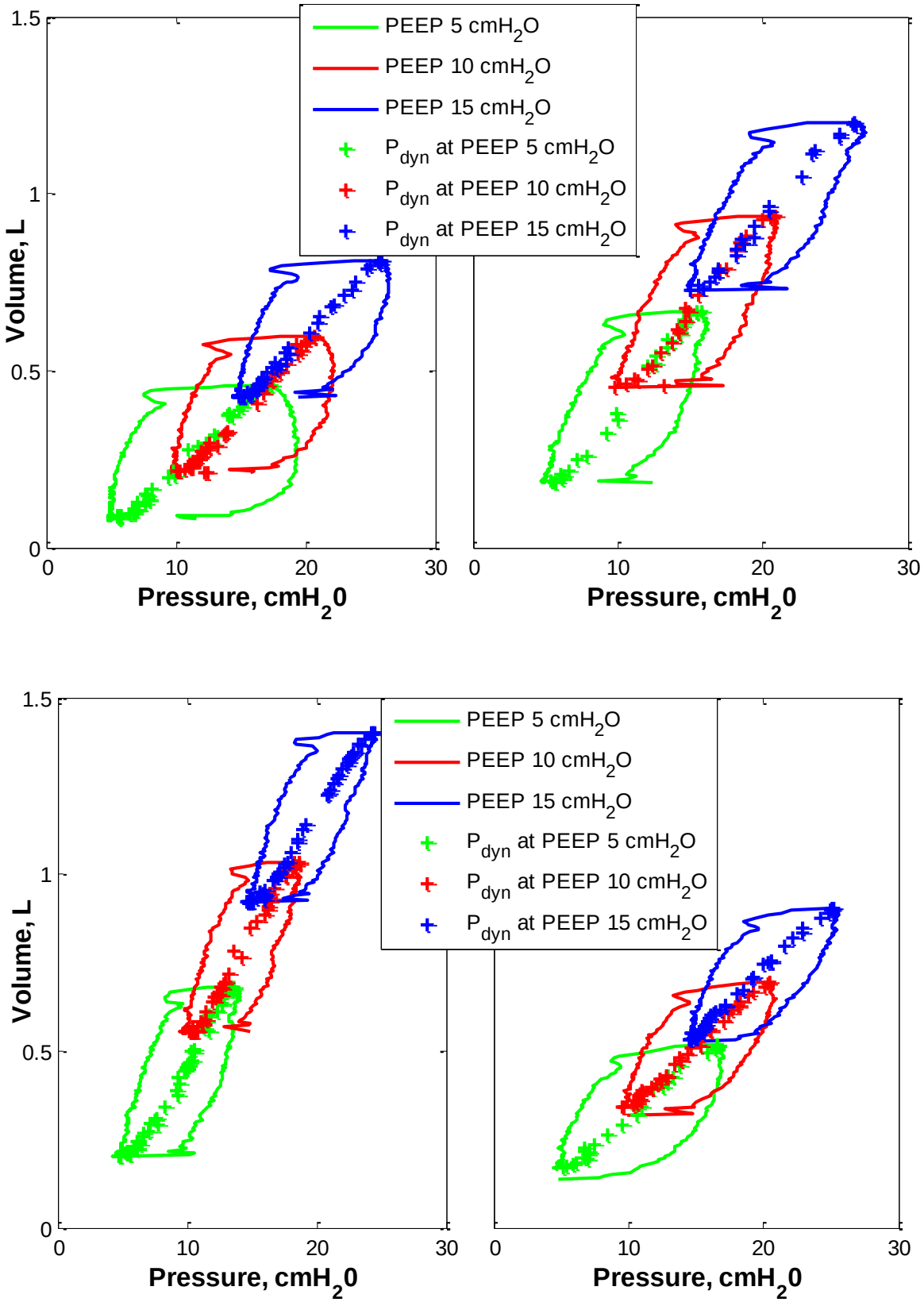

Figure 2.5: The PV curves and P_{dyn} trends from Cohort 1 at all PEEP levels for *Top Left*: Patient S1. *Top Right*: Patient S2. *Bottom Left*: Patient S3 and *Bottom Right*: Patient S8.

Table 2.4: Patient-specific dynostatic pressure (P_{dyn}) for Cohort 2 at each PEEP level

Patient		P_{dyn} (cmH$_2$O), Median [IQR] and Maximum				
		PEEP 5	**PEEP 7**	**PEEP 10**	**PEEP 12**	**PEEP 15**
B1	**Median [IQR] Maximum**	5.73 [4.99-11.40] 23.92	8.47 [7.61-11.29] 28.03	-	12.49 [11.95-15.22] 38.63	-
B2	**Median [IQR] Maximum**	4.96 [4.73-6.79] 16.89	-	10.28 [9.49-12.00] 19.27	-	-
B3	**Median [IQR] Maximum**	5.89 [5.14-10.86] 28.99	8.12 [7.42-11.35] 31.87	10.27 [9.79-13.45] 32.09	-	-
B4	**Median [IQR] Maximum**	6.01 [5.59-8.76] 23.14	10.00 [9.57-13.14] 25.82	10.90 [10.21-13.68] 24.16	-	-
B5	**Median [IQR] Maximum**	5.91 [4.47-18.14] 23.32	12.87 [6.90-21.99] 25.43	19.56 [9.64-23.22] 26.36	20.47 [15.72-23.82] 28.35	-
B6	**Median [IQR] Maximum**	4.30 [4.12-4.86] 26.01	6.77 [6.47-7.65] 28.53	9.13 [8.94-10.15] 26.44	11.16 [11.02-11.58] 26.75	-
B7	**Median [IQR] Maximum**	5.99 [5.06-8.22] 16.14	8.71 [7.42-12.30] 19.59	11.01 [10.07-13.98] 22.46	13.43 [12.51-15.56] 27.67	-
B8	**Median [IQR] Maximum**	6.14 [5.35-9.92] 19.34	9.20 [7.80-13.59] 20.60	-	14.02 [12.88-16.86] 27.88	-
B9	**Median [IQR] Maximum**	-	-	11.42 [9.86-17.02] 31.50	17.54 [15.04-22.95] 36.49	18.86 [16.97-22.46] 44.18
B10	**Median [IQR] Maximum**	5.74 [5.00-11.24] 23.92	8.47 [7.61-11.29] 28.03	11.04 [10.11-14.41] 37.19	12.48 [11.95-15.22] 38.63	-
B11	**Median [IQR] Maximum**	4.70 [4.41-5.72] 16.17	6.84 [6.55-7.63] 21.67	9.02 [8.86-10.68] 24.57	-	-
B12	**Median [IQR] Maximum**	6.13 [4.79-14.37] 26.51	-	11.21 [9.57-18.01] 30.30	-	16.93 [14.17-21.78] 34.23

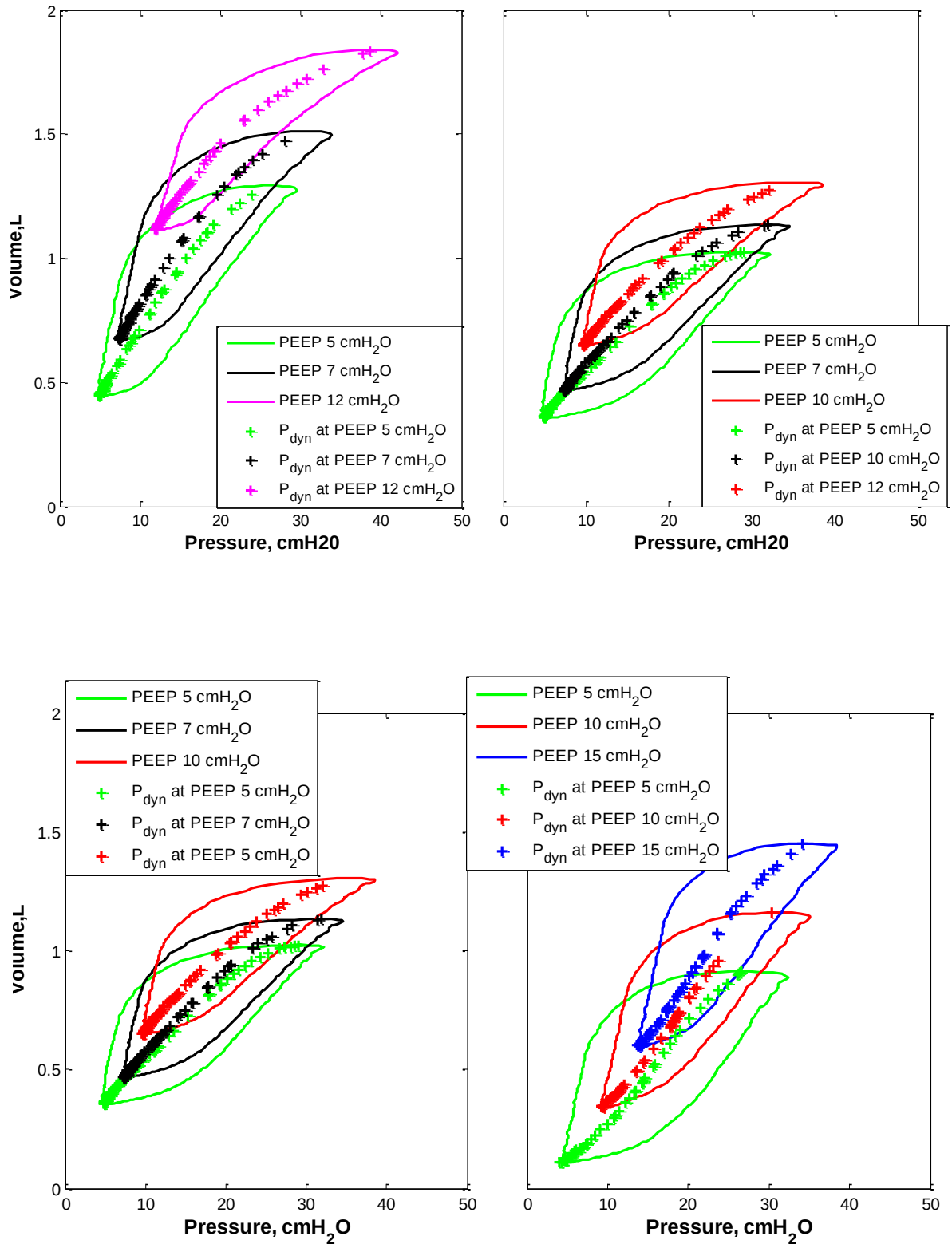

Figure 2.6: The PV curves and P_{dyn} trends from Cohort 2 at all PEEP levels for *Top Left*: Patient B1. *Top Right*: Patient B3. *Bottom Left*: Patient B3 and *Bottom Right*: Patient B12.

2.5 Discussion

The DSA model is capable of on-line monitoring of P_{dyn} without added invasive respiratory manoeuvre. This information is important, especially for assessing patient-specific ARDS lung condition and their response to MV settings. These disease states and responses to therapy are patient-specific, and can be highly variable over time as condition evolves. Thus, it is imperative to have real-time assessment.

For safety, some studies have suggested that during tidal ventilation, the alveolar pressure or plateau airway pressure should be maintained below 30 cmH_2O to prevent barotrauma (Chiumello et al. 2008; Jaswal et al. 2014; Rouby et al. 2004). Table 2.3 shows that for most patients included in Cohort 1, the maximum estimated P_{dyn} does not exceed 30 cmH_2O, except for Patients S7 and S10 at PEEP of 15 cmH_2O. These results show that Patients S1-S6, S8 and S9 may be safely ventilated at PEEP = 15 cmH_2O However, Patients S7 and S10 should be ventilated at a lower PEEP value of 10 cmH_2O to avoid the potential pressure induced injury (Chiumello et al. 2008).

In contrast to Cohort 1, it was found that the patients in Cohort 2 experienced higher overall P_{dyn} when PEEP is set above 7 cmH2O. Four of 10 patients had peak P_{dyn} over 30 cmH_2O when PEEP is 7 cmH_2O. Of note, the ventilation tidal volume in Cohort 2 was set at 8-10 ml/Kg, which is ~25% higher than the tidal volume settings in Cohort 1. This higher tidal volume setting contributed to higher peak P_{dyn} at lower PEEP settings. Thus, a possible hypothesis is that patients can be ventilated with lower tidal volume with increased frequency to maintain adequate minute ventilation, which has also been reported (Imai et al. 2001;

Meade et al. 2008). However, these results also indicate the trade-off between tidal volume and pressure, and flow pattern that make this problem more complex than a simple limit.

It can be seen in Figures 2.5 and 2.6 that P_{dyn} increases with PEEP and follows a sigmoidal curve that is similar to the static compliance curve (Venegas et al. 1998). P_{dyn} is a surrogate of the alveolar pressure. Thus, P_{dyn} trends in this study should follow the characteristics of a standard static compliance curve, as expected. In addition, combining P_{dyn} at different PEEP levels, the location of LIP and UIP can potentially be identified, which may be useful for optimal PEEP selection (Albaiceta et al. 2008). Hence, this approach could enable more quantified PEEP selection.

While the static compliance curve characteristics were apparent in both Cohorts 1 and 2, there are differences in P_{dyn} trends between Cohort 1 and Cohort 2, as shown in Figures 2.4 and 2.5. For Cohort 1, three P_{dyn} curves at different PEEP can be connected and form one sigmoidal curve similar to a static compliance curve as described by Venegas et al. (Venegas et al. 1998). Comparatively, Cohort 2 exhibit different characteristics where all three P_{dyn} curves can form 3 independent sigmoidal curves. It can be seen that the P_{dyn} trend shifted to the left when the patient is ventilated at higher PEEP. This shift observed in Cohort 2 also implies that patients respiratory system compliance increases with PEEP, and this observation can be translated into PEEP induced time-dependent alveoli recruitment (Bates & Irvin 2002). However, this trend is not always observed, suggesting patient specificity of response to MV.

Sundaresan et al. (Sundaresan et al. 2011a), Chiew et al. (Chiew et al. 2011), Crotti et al. (Crotti et al. 2001), and Pelosi et al. (Pelosi et al. 2001) have showed similar trends, noting that the ventilation pressure has reached above alveoli threshold opening pressure, leading to

recruitment. This recruitment then leads towards reducing the overall threshold opening pressure for recruited lung units, increasing compliance. Equally, there is also a protocol difference between Cohorts 1 and 2 for the duration of each PEEP level is maintained. In Cohort 1, each PEEP level is only maintained for 10 to 15 breathing cycles, compared to Cohort 2 where every PEEP level is maintained for 30 minutes. Thus, in Cohort 1, there may not be sufficient time for time dependent recruitment (Bates & Irvin 2002), whereas Cohort 2 allows time-dependent recruitment and has more than sufficient time for stabilisation, which in turn changes the observed underlying respiratory mechanics.

The DSA has shown the potential to provide useful information in guiding mechanical ventilation. However, it is not without flaws. One of the main limitation of the DSA is that the assumption of equal resistance during inspiration and expiration at isovolume may not be entirely valid in some or many cases leading to incorrect decisions (Mols et al. 2001). Poiseuille equation shows that airway resistance is also dependent on the flow profile (Damanhuri et al. 2012), and it is clear that the inspiration flow profiles are different to expiration in both Cohorts 1 and 2. Thus, one would not expect this assumption to hold, and it may be very poor depending on the flow profile used on inspiration.

Furthermore, the DSA cannot be applied for all ventilator modes, as stated in (Sondergaard et al. 2003a). Next, the DSA can only provide information on the overall lung condition, which is not specific, as the lung consists of many branches and lung units, each with their own structure, shape, and interaction with pressure and flow. Thus, a more patient-specific model is required that could give more information on the lung at the specific branches that include the airway resistance and alveolar pressure information.

2.6 Summary

The DSA is the first on-line monitoring method proposed in calculating alveolar pressure for ARDS or MV patients. It has potential to guide clinicians in selecting the best PEEP based on the measurement of the alveolar pressure without additional invasive equipment or protocols needed. However, the ability of this method to guide therapy is limited because it does not provide or include information about airway resistance. It thus cannot offer further insight into patient-specific condition (Kárason et al. 2001; Mols et al. 2006). In Chapter 3, a patient-specific airway branching model (ABMps) is presented. Prior airway branching models (ABM) have not been patient-specific or applied in real-time. This model seeks to bridge this gap and combine the DSA and ABM models to estimate the pressure drop due to airway resistance in detail. The model will provide unique insight and understanding into the topic on the airway resistance during mechanical ventilation.

CHAPTER 3

Airway Branching Model

3.1 Introduction

One widely used model that is able to capture physiologically relevant information of lung morphology is the airway branching model (ABM) (Horsfield et al. 1971; Weibel 1963a). The ABM using known airway dimensions and pathways of the airway system has been used to predict respiratory pressure-flow responses (Pedley et al. 1970). The ABM models the human lung as a bifurcating tree with 23 generations physiologically and the alveoli are present in all generations beyond approximately generation 17 where gas exchange occurs (Soong et al. 1979). It is an idealized model of observed anatomy to which fundamental fluid mechanics can be applied.

In the ABM, a pressure drop occurs after each branch is due to the resistive components of the airway wall and the head loss (Burrowes et al. 2005; Katz 2012). By estimating the pressure drop for each of these airway branches, the alveoli pressures can be estimated for a given ABM structure and model input. This outcome provides the opportunity to monitor 'regional' specific alveoli pressures that could be used to understand healthy and damaged alveoli pressure, and thus potentially to prevent over-distension of the lung that could lead to lung injury.

In practice, the ABM has been used to estimate respiratory pressure-flow responses in non-critically ill subjects (Horsfield et al. 1971; Katz et al. 2011; Pedley et al. 1970; Weibel 1963a). However, ABM models are very general. They use a set of global airway dimensions

that do not reflect patient-specific conditions and have not been validated in critically ill patients with respiratory failure. These issues limit bedside application of this model in monitoring or titrating mechanical ventilation.

As mentioned in Chapter 2, the dynostatic algorithm (DSA) is currently the most well-known method to estimate alveoli pressure by producing the dynostatic curve during typical, dynamic breathing conditions (Karason et al. 2000; Sondergaard et al. 2003b). However, the ability of this method to guide therapy is limited because it does not provide or include information about airway resistance. It thus cannot offer further insight into patient-specific or alveoli-specific condition (Karason et al. 2001; Mols et al. 2006). Therefore, the proposed patient-specific airway branching model (ABMps) seeks to bridge this gap and merge the DSA and ABM models to estimate the pressure drop using the physiological dimensions of human airways.

In particular, this study develops the ABMps to capture patient-specific airway pressure changes and unique patient-specific clinical information that is not available from the general ABM or DSA. Three models are presented: 1) the general ABM; 2) the dynostatic algorithm; and 3) the patient-specific ABMps. These models seek to add the patient and/or condition specificity that the DSA lacks, while retaining the ability to capture alveolar pressures. It thus introduces a mixture of novel elements to the overall modelling approach.

The models are compared in a retrospective analysis using clinical data from critically ill mechanical ventilation patients to validate the overall approach. Weibel's well-known model (Weibel 1963a) includes alveolar volume. However, this work is seeks to capture alveolar

pressures and thus does not include alveolar volume, which is a difference in the two analyses. This work has been published as a journal article (Damanhuri et al. 2014).

3.2 Methodology

3.2.1 General Airway Branching Model

The general ABM is a symmetrical branching tree with physiological airway branching dimensions (Damanhuri et al. 2012). Most of the general ABMs assume that the airway generations go up to 23 generations (Katz 2012; Pedley et al. 1970). In this study, the general ABM models the trachea as generation 0 and the alveoli are located at generations 17-23. Figure 3.1 shows the schematic ABM structure and the physical dimensions at every branch generation are shown in Table 2 (Pedley et al. 1970). It is assumed that the airway dimensions are kept constant during inspiration.

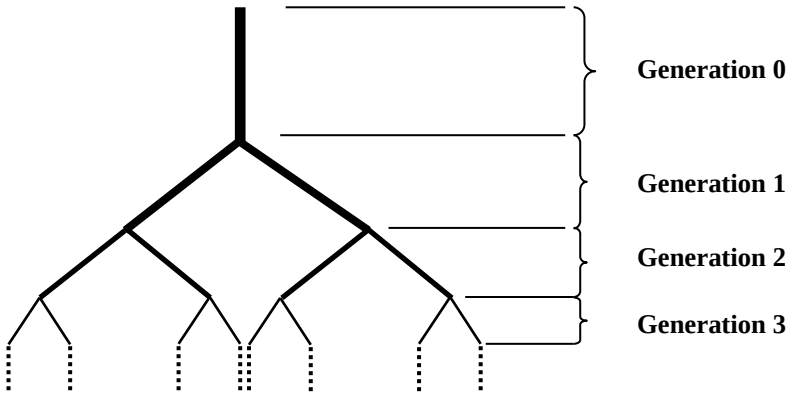

Figure 3.1: The airway tree structure in which airways are specified by generation number, beginning with trachea (Bates 2009)

This modelling approach captures head loss as part of Poiseuille model used. Poiseuille flow is defined (Bates 2009; West 2012) :

$$\Delta P_n = \frac{128\mu LQ}{\pi D^4} \qquad (3.1)$$

where μ, is the dynamic viscosity of air ($1.9x10^{-5}$ Pa·s /$1.9x\ 10^{-7}$cmH_2O·s), L is the length of the particular airway branch, D is the diameter of the particular airway branch and Q is the flow rate of airway branch.

Table 3.1: Physical measurements of bronchial paths (Pedley et al. 1970).

Branch Generations	Diameter (mm)	Length (mm)	Reynolds number
-1 (ETT)	9	330	390
0 (Tracheal)	18	120	775
1	12.20	48	573
2	8.30	19	427
3	5.60	8	307
4	4.50	13	198
5 -16	3.50 – 0.60	10.70 – 1.70	123 – 0.60
17 – 22	0.57 – 0.43	1.50 – 0.63	0.56 – 0.41
23	0.40	0.50	0.02

Head loss is defined as a pressure drop along the branching system that consists of major and minor losses (Katz et al. 2011). The major loss is defined as the pressure drop in the straight sections of the airway branching system (Katz et al. 2011) :

$$\Delta P_{major} = f\frac{LV^2}{2D} \qquad (3.2)$$

The model thus assumes that laminar flow exists in the branches since the diameter for all branches is less than 30 mm with Reynolds number less than 2000 (Burrowes et al. 2005;

Horsfield & Woldenberg 1989; Katz 2012). Thus, the laminar flow friction factor (*f*) is defined:

$$f = \frac{64}{Re} \tag{3.3}$$

where *Re* is the Reynolds number based on the branch diameter:

$$Re = \frac{\rho V D}{\mu} \tag{3.4}$$

where V is the velocity of the flow of the airway branch. The velocity of the flow can be defined in terms of flow rate:

$$V = \frac{4Q}{\pi D^2} \tag{3.5}$$

Hence, substituting Equations 3.3, 3.4 and 3.5 into Equation 3.2, the major head loss can be derived:

$$P_{major} = \frac{128 \mu L Q}{\pi D^4} \tag{3.6}$$

Equations 3.1 and 3.6 show that pressure drop due to Poiseuille flow and the major loss are the same, as expected.

In this specific model, estimates from (Damanhuri et al. 2012) incorporate minor loss information due to the bifurcation of each branch starting from generation 1, as shown in Figure 3.2. Every time the branch bifurcates to the next generation, there is a change in the velocity distribution. Thus, this airway resistance and minor loss will contribute to the pressure drop over the bronchial paths.

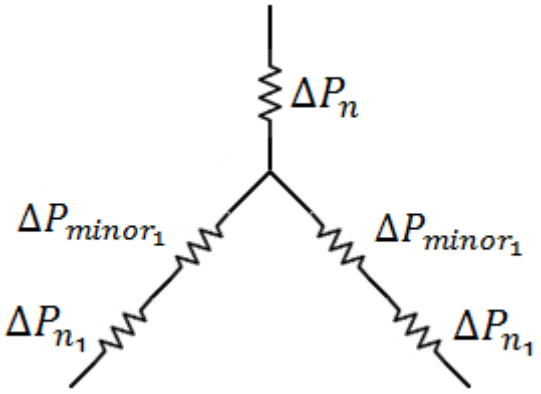

Figure 3.2: The Poiseuille pressure drop, ΔP_n, and minor loss pressure drop, ΔP_{minor} at each of the branching respiratory system for ABMps.

In addition to the resistance component of the bronchial part, there is an additional resistance in the endotracheal tube (ETT). All of the patients in this study had ETT with the same dimensions. The length of the ETT was 330 mm and the diameter was 9 mm (Straus et al. 1998; Sundaresan 2010). The resistance induced by the ETT is added to the overall model results. In all cases, the ETT dimensions can be assumed to be known with no loss of generality.

The ETT is at generation -1, the trachea at generation 0, and then continuing to the remaining generations up to generation 23. With the added ETT in the ABM model, the total pressure drop due to the resistance component, minor loss and the artificial conducting airway can be modelled:

$$\Delta P_{ABM} = \Delta P_n + \Delta P_{minor} \tag{3.7}$$

where

$$\Delta P_n = \frac{128\mu}{\pi} \sum_{n=-1}^{23} \frac{L_n Q_n}{2^n {D_n}^4} \tag{3.8}$$

$$\Delta P_{minor} = \frac{8K_L\rho}{\pi^2}\sum_{n=-1}^{23}\frac{{Q_n}^2}{{D_n}^4} \quad (3.9)$$

where K_L is the minor loss coefficient (= 2) (Munson et al. 1990), ρ is the density (1.25 kg/m^3), n represents the airway branch generation, L_n is the length of the particular airway branch, and D_n is the diameter of the particular airway branch. The flow rate of airway branch (Q_n) is assumed to be half of the previous generation flow rate based on an even split between the two branches.

This combined model is unique for this clinical application (Damanhuri et al. 2012). However, it is entirely general based on the data in Table 3.1 and fixed structure.

3.2.2 Dynostatic Algorithm Model (DSA)

In this study, another method of pressure drop estimation is performed by using the dynostatic algorithm (Sondergaard et al. 2003a; Sondergaard et al. 2003b). This dynostatic model as proposed by Karason et al. (Karason et al. 2000) has been explained in detail in Chapter 2. Thus, the pressure drop (ΔP_{DSA}) during inspiration is estimated:

$$\Delta P_{DSA} = P_{insp} - P_{dyn} \quad (3.10)$$

where P_{insp} is the pressure during inspiration and P_{dyn} is the dynostatic pressure.

3.2.3 Patient-Specific Airway branching model (ABMps)

This general ABM presented is extended to account for patient-specific physiological conditions observed in measured pressure and volume data. The ABMps airway pressure drop is defined:

$$\Delta P_{ABM_{PS}} = \Delta P_{n_{PS}} + \Delta P_{minor_{PS}} \tag{3.11}$$

A patient-specific multiplier (α) can be used to uniformly alter the bronchial diameter defined in Table 2 to better match the observed data. Incorporating this factor into Equations 3.8 and 3.9, yields Equations 3.12 and 3.13, respectively.

$$\Delta P_{n_{PS}} = \frac{128\mu}{\pi} \sum_{n=0}^{24} \frac{L_n Q_n}{2^n \alpha^4 {D_n}^4} \tag{3.12}$$

$$\Delta P_{minor_{PS}} = \frac{8K_L\rho}{\pi^2} \sum_{n=0}^{24} \frac{{Q_n}^2}{\alpha^4 {D_n}^4} \tag{3.13}$$

where α is defined as patient-specific relative of airway diameter and is limited to α = [0.45, 1.50]. If α = 1.0, the patient will follow the general airway dimensions proposed by (Horsfield et al. 1971). If α is < 1.0, the patient-specific airway is relatively smaller than the Horsfield model (Horsfield et al. 1971), perhaps indicating that airway constriction. Finally, if α >1.0, the patient has an effectively larger airway. Larger and smaller airways in this context imply differences in resistance in the observed data. Hence, they may also capture relative over-distension with pressure, as well as patient-specific state.

To estimate a patient-specific α, $\Delta P_{ABM_{PS}}$ is assumed to be the same as ΔP_{DSA}, where ΔP_{DSA} is the most currently well-accepted method to estimate alveoli pressures. Hence, substituting Equations 3.12 and 3.13 into Equation 3.11, a patient-specific α can be derived:

$$\alpha = \sqrt[4]{\frac{128\mu}{\pi \Delta P_{DSA}} \sum_{n=0}^{24} \frac{L_n Q_n}{2^n {D_n}^4} + \frac{8K_L \rho}{\pi^2 \Delta P_{DSA}} \sum_{n=0}^{24} \frac{{Q_n}^2}{{D_n}^4}} \tag{3.14}$$

Patient-specific α values are identified through a minimal difference algorithm. Figure 3.3 shows the flow chart in determining patient-specific α.

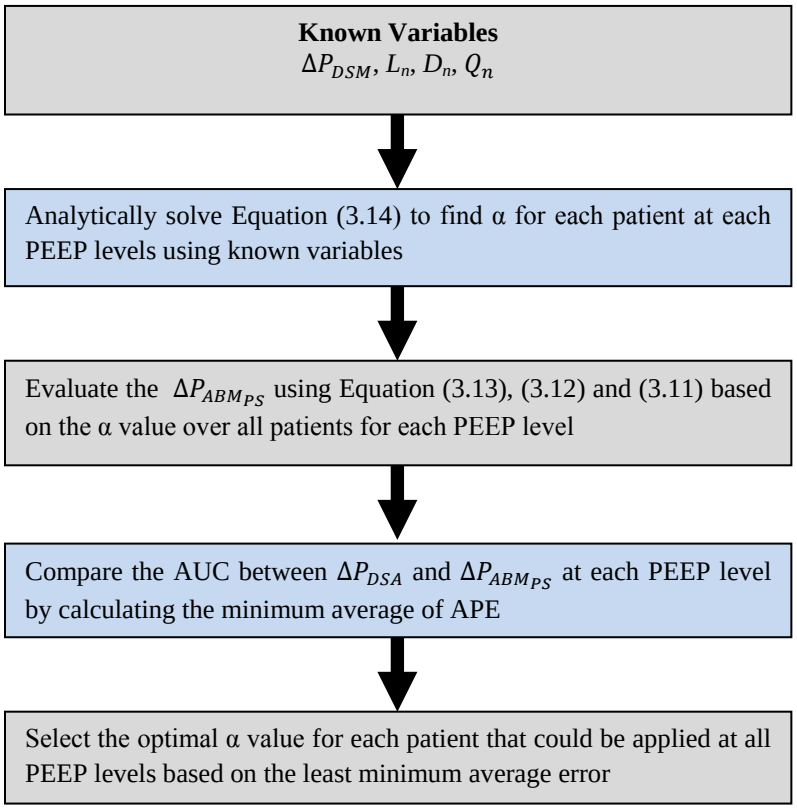

Figure 3.3: A flowchart on selecting the optimal α for each patient in ABMps model.

The value for α for each patient and PEEP value was calculated using measurements of ΔP_{DSA}, and Q_n and values of L_n, and D_n, from Table 2 in Equation 3.13. Thus, a different α value is obtained for each PEEP level and for each patient. The area under the curve (AUC) is

the area under the pressure drop curve for all the three models. The AUC of pressure drop with respect to time for a single inspiration cycle shown in Figure 6 provides a good single value measure of the pressure drop when identifying the patient-specific α. The AUC of $\Delta P_{ABM_{PS}}$ is compared with AUC of ΔP_{DSA} for all patients at each PEEP level by calculating the minimum average of the absolute percentage error (APE). This comparison ensures the model is not over fit to the data but that patient-specific aspects are used to capture and represent the fundamental trend.

3.2.4 Patient Data

To compare the three models, retrospective data from 10 acute respiratory distress syndrome (ARDS) patients in the Christchurch Hospital Intensive Care Unit (ICU) was used, with the data acquisition process detailed in Chapter 2 (Sundaresan et al. 2011a). The details for each patient are shown in Table 3.2.

Table 3.2: Summary of patient auto-PEEP settings (Sundaresan et al. 2011b).

Patient	Sex	Age [years]	Clinical Diagnostic	Auto-PEEP [cmH_2O]
S1	Female	61	Peritonitis, COPD	10
S2	Male	22	Trauma	12
S3	Male	55	Aspiration	10
S4	Male	88	Pneumonia, COPD	10
S5	Male	59	Pneumonia, COPD	12
S6	Male	69	Trauma	11
S7	Male	56	Legionnaires	7.5
S8	Female	45	Aspiration	12
S9	Male	37	H1N1,COPD	12
S10	Male	56	Legionnaires, COPD	3

3.2.5 Data Analysis

To assess model performance, the pressure drop or, more specifically, the area under the pressure drop curve (AUC) for inspiration breathing cycle was estimated and compared for all three models. AUC was used instead of the sum square error due to its unique ability to capture the pressure drop trend shape, as well as its maximum magnitude. Significance tests were carried out using paired Wilcoxon rank-sum test.

3.3 Results

The estimated airway resistance for each branch generation is presented in Figure 3.4 for each patient. The AUC for all 10 ARDS patients and all 3 models are shown in Table 3.3. It is clear that the general ABM has a very large difference compared to the DSA ($p<0.05$). Table 3.4 shows the patient-specific α that relates to the patient specificity and disease state. The α values for COPD patients were significantly lower than the other patients in the cohort (rank-sum $p<0.0001$, Kolmogorov-Smirnov $p=0.001$), indicating a more resistive airway, as expected from critically ill ARDS and respiratory failure patients with stiffer and damaged lung units.

Figure 3.5 shows the trend of α values for all patients over PEEP = 5 cmH_2O, 10 cmH_2O and 15 cmH_2O. Figure 3.6 compares the pressure drop curve for one breathing cycle for patient S1, as an example, for all three models at PEEP = 5 cmH_2O, 10 cmH_2O and 15 cmH_2O, with patient-specific $\alpha = 0.57$. Figure 3.7 shows the pressure and volume curve for all the three models for the same patient and α value in Figure 3.6.

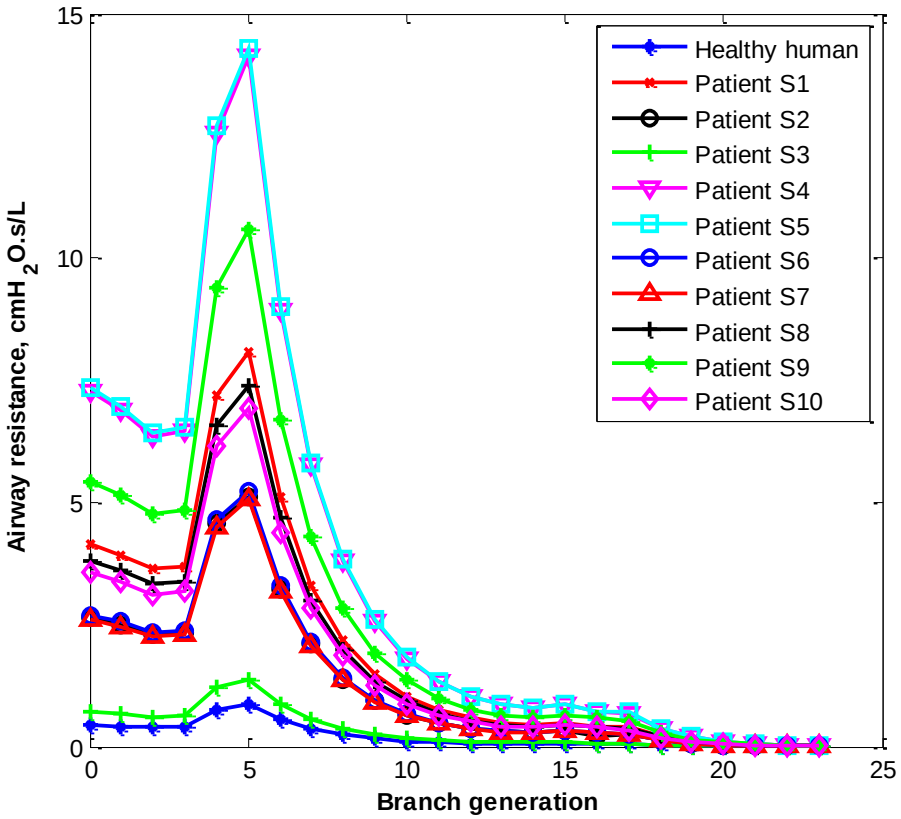

Figure 3.4: Airway resistance for each branch for every patient of the ABMps model.

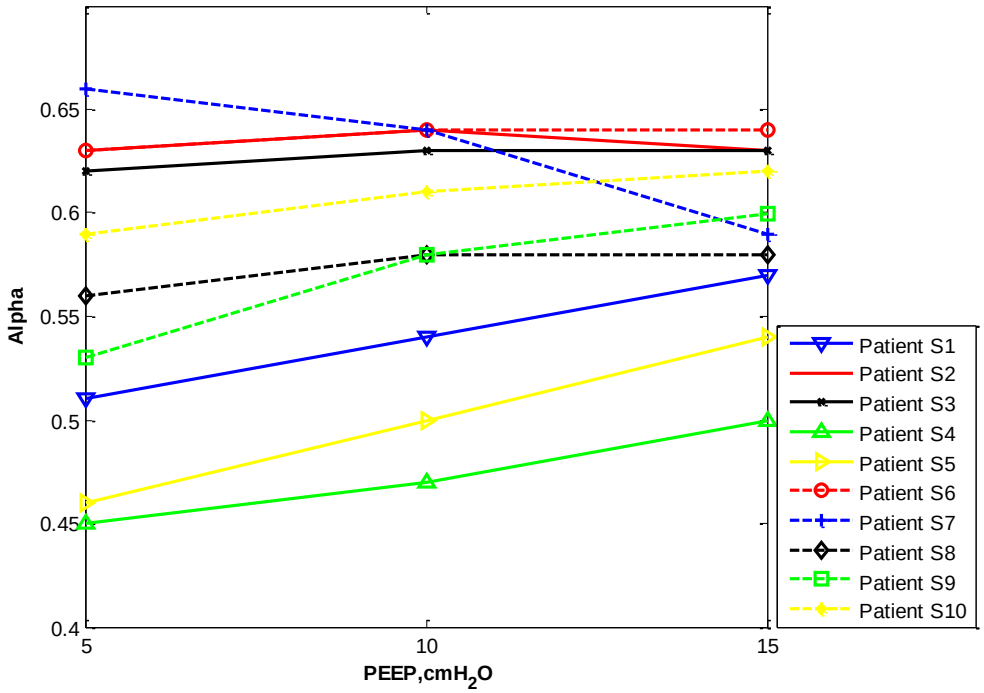

Figure 3.5: Comparison of all α values for all patients vs PEEP for ABMps.

Table 3.3: AUC of airway pressure drops for Sundaresan's patients (Sundaresan et al. 2011a), with PEEP = 5, 10 and 15 cmH_2O for general ABM, ABM-specific and DSA.

Patient	Auto-PEEP (cmH_2O)	PEEP (cmH_2O)	Optimal α	ABMpsAUC ($cmH_2O.s$)			General ABM AUC ($cmH_2O.s$)	DSA AUC ($cmH_2O.s$)	Error = AUC(ABMps-DSA) (%)
				PEEP 5 cmH_2O	PEEP 10 cmH_2O	PEEP 15 cmH_2O			
		5	0.51	5.35	5.10	5.18	0.37	5.35	0.14
S1	10	10	0.54	4.22	4.02	4.09	0.35	4.02	0.09
		15	0.57	3.44	3.28	3.33	0.36	3.33	0.06
		5	0.63	3.11	3.03	2.79	0.50	3.11	0.13
S2	12	10	0.64	2.99	2.91	2.68	0.49	2.91	0.10
		15	0.63	3.18	3.10	2.86	0.45	2.86	0.19
		5	0.62	2.89	2.84	2.62	0.42	2.89	0.11
S3	10	10	0.63	2.63	2.58	2.38	0.41	2.58	0.08
		15	0.63	2.73	2.68	2.47	0.38	2.47	0.15
		5	0.45	10.0	9.66	10.30	0.40	10.00	0.21
S4	10	10	0.47	8.20	8.05	8.36	0.40	8.05	0.16
		15	0.50	6.59	6.52	6.77	0.41	6.77	0.15
		5	0.46	8.82	8.45	7.92	0.41	8.82	0.42
S5	12	10	0.50	6.76	6.48	6.07	0.39	6.48	0.23
		15	0.54	4.79	4.59	4.30	0.37	4.30	0.26
		5	0.63	3.03	2.92	2.92	0.46	3.03	0.07
S6	11	10	0.64	2.82	2.72	2.72	0.44	2.72	0.04
		15	0.64	2.80	2.70	2.70	0.44	2.70	0.03
		5	0.66	1.80	1.84	1.83	0.34	1.80	0.03
S7	7.5	10	0.64	1.98	2.03	2.02	0.35	2.03	0.02
		15	0.59	2.81	2.88	2.86	0.34	2.86	0.03
		5	0.56	3.76	3.69	3.71	0.37	3.76	0.04
S8	12	10	0.58	3.27	3.20	3.22	0.36	3.20	0.03
		15	0.58	3.09	3.15	3.11	0.36	3.11	0.02
		5	0.53	5.96	6.02	6.01	0.48	5.96	0.04
S9	12	10	0.58	4.42	4.46	4.45	0.49	4.46	0.02
		15	0.60	3.74	3.78	3.77	0.49	3.77	0.01
		5	0.59	3.76	3.62	3.70	0.47	3.76	0.07
S10	3	10	0.61	3.32	3.20	3.27	0.45	3.20	0.06
		15	0.62	3.15	3.04	3.10	0.46	3.10	0.04
Mean [IQR]			0.58 [0.54-0.63]				0.41 [0.37-0.46]	4.12 [3.20-4.42]	0.07 [0.03-0.15]

Table 3.4: Patient-specific α vs disease state.

Number of Patients	Clinical Diagnostic	Range of α
5	COPD	0.45 – 0.62
2	Aspiration	0.56 – 0.63
2	Trauma	0.63 – 0.64
1	Legionnaires	0.59 – 0.66

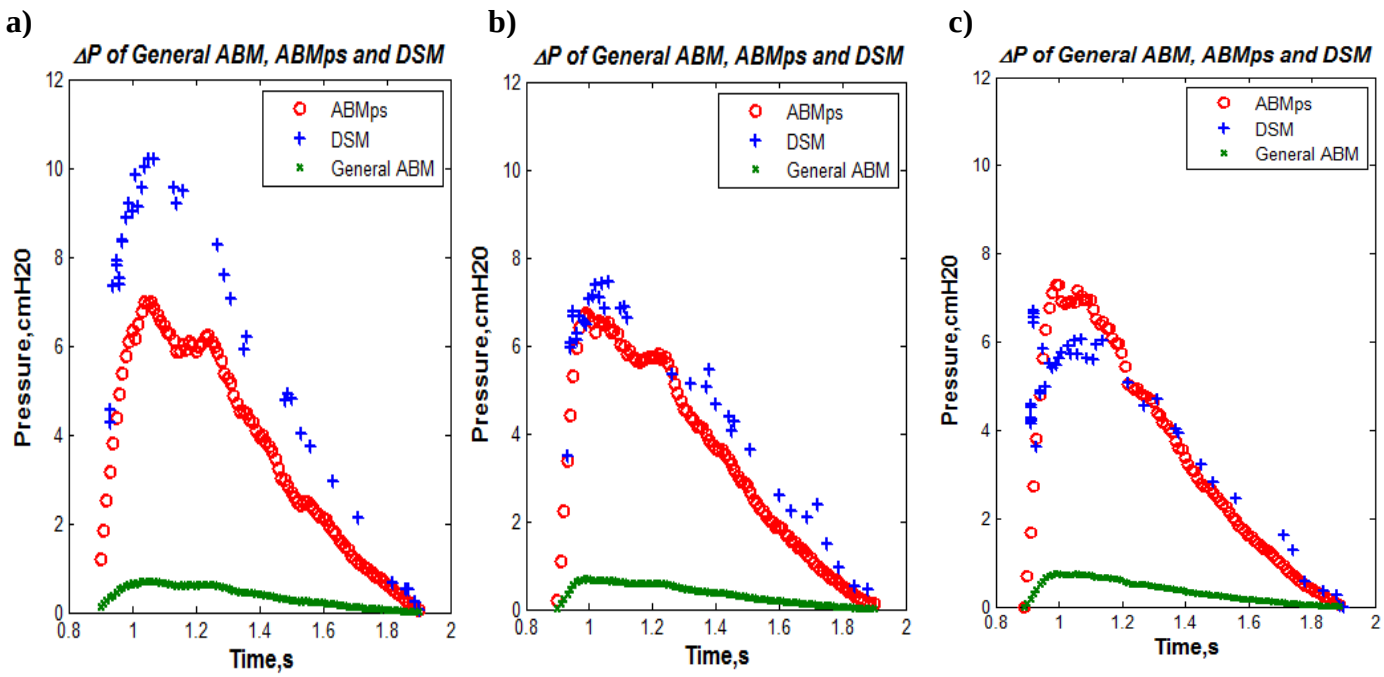

Figure 3.6: Comparison of airway pressure drop for one breathing cycle for patient S1 with COPD for general ABM, ABMps, and DSA with α = 0.57. Plot of general ABM, ABMps, and DSA at (a) PEEP = 5cmH_2O (b) PEEP = 10cmH_2O, and (c) PEEP = 15cmH_2O.

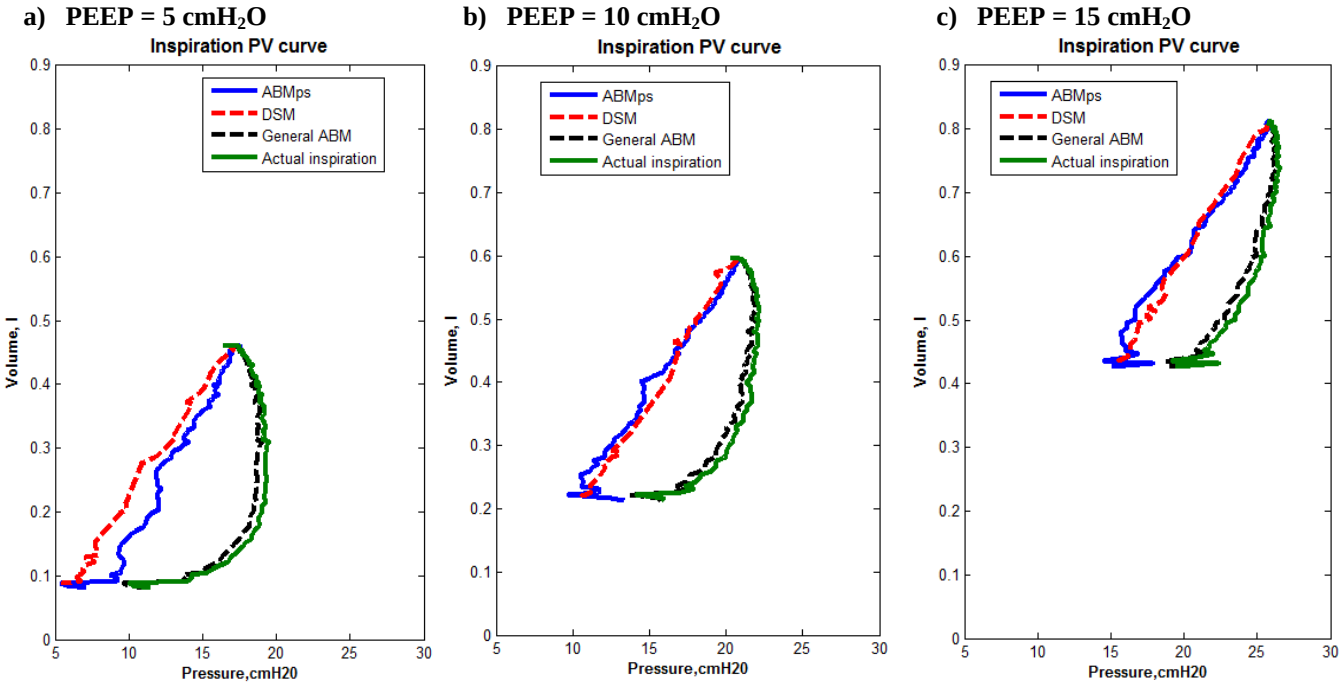

Figure 3.7: Comparison of pressure volume curve for patient S1 with COPD for general ABM, ABMps, DSA, and actual inspiration with α = 0.57.

3.4 Discussion

It can be observed in Figure 3.4 that the airway resistance is higher at the trachea (generation 0) and 5^{th} generation branch for all patients. Initially, the resistance starts to drop from generation 0, which is the trachea, up to generation 4. The resistance starts to rise at generation 5 as the length of the bronchial tube is higher at this generation compared to the previous branches (Pedley et al. 1970). Airway obstructions increase the airway resistance, as seen in Figure 3.3, where for COPD patients, S1, S4, S5, S9 and S10, the airway resistances were higher compared to the healthy human and other patients. With the increased airway resistance in COPD patients, these results clearly show that a higher resistance results in the higher airway pressure drop observed, and thus the consequent reduced volume. This estimation of airway resistance by the ABMps cannot be done by using the DSA model and highlights a useful feature of this approach.

With the patient-specific α value, the airway resistance can be estimated, which leads to estimating the pressure drop. Furthermore, the airway resistance for each patient is different and shows that airway resistance is higher for COPD patients as expected until their auto-PEEP pressure is exceeded opening new lung volume. Thus, this ABMps can be used to detect the disease state independently or automatically, which could not be done by the DSA.

The estimated airway pressure drop using the patient-specific ABMps with α value was significantly different from the pressure drop estimated using the general ABM ($p<0.05$). Table 3.3 shows that AUC pressure drop in the general ABM typically exhibited very large differences for all patients at all PEEP levels compared to the DSA with $p<0.05$. In contrast, a good comparison is observed between the AUC of pressure drops in ABMps and DSA in

Tables 3.3 and Figure 3.6. This result clearly shows that the general ABM does not capture the observed mechanics of critically ill mechanical ventilation patients despite it being a mix of classical mechanics and measured behaviour (Damanhuri et al. 2012). However, if it is extended with patient-specific α, it is a far better representation of the patient-specific airway dimension. In addition, these patient-specific aspects dominate the differences from the general ABM modelling approach to matching the patient-specific DSA results. This last result matches the inter-patient variability noted in MV patients as a whole, and shows the need for a patient-specific approach to estimated model-based alveolar pressures in this cohort.

Figure 3.6 illustrates an example of estimated pressure drops for Patient S1 between general ABM, ABMps and DSA models. With $\alpha = 0.57$ at PEEP = 15 cmH_2O, the AUC of pressure drop for Patient S1 in ABMps and DSA yields the same result of 3.33 $cmH_2O.s$, where the general ABM yields a far lower 0.36 $cmH_2O.s$. This difference indicates that the ABMps was able to predict the same airway pressure drop as the DSA by incorporating the α term that was unique for each specific patient's branching system. Equally, the general ABM, as defined in Table 3.2, is not capable of accurately capturing the observed mechanics in mechanical ventilation patients with significant respiratory dysfunction and failure. This difference, and small $\alpha < 1.0$ value are due to the respiratory failure status of these patients limiting lung volume and creating a stiffer, smaller, and thus more resistive lung.

From Tables 3.3 and 3.4, it is also noted that all α values for all patients are less than 1.0. Therefore, all pulmonary paths have a smaller diameter than the expected diameters from Table 3.2. This finding reflects the clinical condition of these patients. In particular, patients with restrictive airway conditions, such as Chronic Obstructive Pulmonary Disease (COPD),

have constricted airways and respiratory failure by definition. Thus, α is smaller comparatively (α =0.45-0.62) than would be assumed for a healthy individual, per Table 3.2. Smaller α values also occurred in aspiration patients (α =0.56-0.63) where the restrictive airway condition of the lung is developed due to the entrance of foreign materials into the bronchial generations. Thus, with the use of α, the ABMps is not only able to capture similar alveolar pressure as DSA but is it also able to track patient disease state over time as shown in Table 3.4 and Figure 3.5. The greater airway resistance modelled with $\alpha < 1.0$ results in higher pressure drops at the alveoli, as expected, and is thus a better match with the DSA. In addition, ARDS patients are often associated with regional airway collapse (Halter et al. 2007) at higher branch generations, which will also greatly alter the airway resistance (Pedley et al. 1970) and supports the overall interpretation presented for these patient-specific results.

Equally, the inspiration pressure volume curve for the general ABM and the ABMps can be modelled and compared with the DSA curve and the actual dynamic inspiration pressure volume curve, as shown in Figure 3.7. The general ABM does not capture alveoli pressure like the DSA in critically ill patients. The general ABM would look a lot like the inspiration curve in Figure 3.7 and shifted slightly to lower pressure. This outcome occurs because the ΔP drops are 10 times smaller than the ΔP drops in the ABMps in Table 3.3. Thus, the general ABM was not effective at capturing the estimated alveoli pressure volume curve in this cohort.

Both the ABMps and DSA take into account the airway resistance that occurs in the lung and leads to the airway pressure drop. Furthermore, the ABMps is designed with minor loss and patient-specific airway dimensions based on the α value, that is unique for each patient. Hence, in Figure 3.6 the pressure volume curve for the ABMps is very similar to the DSA as

PEEP increases from 5 cmH_2O to 15 cmH_2O with the patient-specific $\alpha = 0.57$. Although the ABMps had smaller error in comparison to the DSA at lower PEEP, this inspiration pressure volume curve could still be applied as a guidance tool for clinicians to provide a better solution for mechanically ventilated patients.

Although the ABMps estimates pressure drops at every physiological airway branch, there are limitations to its predictive capability. This ABMps assumes that the bifurcations run throughout the entire generations from the 1st generation up to the 23rd generation based on physiological measurements and assumption by referring to the Weibel et al. model, which has been used widely in deterministic studies (Katz 2012; Pedley et al. 1970; Weibel 1963a). However, this assumption may not be applied in real scenarios if one or more of the bronchial paths are blocked as in COPD.

Nevertheless, the ABMps with the patient specific α value is capable to show that every patient has $\alpha < 1.0$, which reflects that patient's pulmonary paths have a reduced equivalent diameter that results in a different resistance as compared to the healthy human physiological measurements. This reduced equivalent diameter thus is a surrogate that captures the (variable) clinical condition of each patient and potential smaller volume. For example, COPD patients have a blockage of bronchial portions of the lungs that reduce volume. In contrast, respiratory failure or ARDS patients may experience a similar total loss of lung volume due to collapsed alveoli distributed throughout the lung. However, in both cases, adjustment to MV settings may be needed to try to recruit this lost volume, and, equally, in both cases, additional pressure is the typical mechanism used for this recruitment.

In this research, the ETT dimensions were the same across all patients. However, while ETT dimensions may vary between patients, the ABMps remains capable of estimating this pressure drop so that an accurate estimation of the pressure drop in the deep bronchial paths can be used for predicting the alveolar pressure drop. The ETT dimensions are typically known, and were consistent in this research, thus maintaining the ability to estimate this alveolar pressure drop, which is important if it is to be used to avoid and prevent further lung injury due to the provision of excessive pressure. Simply, there is no loss of generality from the consistent and typical adult ETT dimensions used here.

Although an average value of minor loss coefficient is used in this model, the ABMps was able to capture the pressure drop in the airway branching system. In addition, at the very low flows at the later generations, the contributions to pressure drop of these minor loss coefficient constants are almost negligible (Katz et al. 2011). Thus, the use of this average value of minor loss coefficient and an ETT specific loss capture much of the loss seen. Equally, while a distribution of loss coefficients based on anatomical studies could be used, it cannot be validated given the limited measurements of pressure and flow available in pulmonary medicine. Thus, given these points, an average value is used because it captures the overall losses and pressure drops, even if intermediate pressures may not be fully accurate, and thus provides a good estimate of alveolar pressure, which is the main goal of this model.

With the use of α, the ABMps was able to capture similar alveolar pressure as the DSA with further insight of patient-specific airway dimensions during mechanical ventilation. However, due to limited patient data, the application of α as a surrogate of patient-specific condition was not fully validated, although the concept was demonstrated. In particular, as a patient

recovers from ARDS, the regional collapsed alveoli may be recruited, resulting in a change in patient airway condition that would be seen in a change in the effective value of α. Thus, the clinical utility of patient-specific α in tracking patient disease state warrants further investigation over larger cohorts given this initial set of results.

3.5 Summary

In this chapter, the study assesses the efficacy of a physically derived ABM to capture clinical data. The ABM significantly underestimates the total pressure drop from trachea to the alveoli. Thus, with a patient-specific airway branching model, it is able to assess the pressure drop of the airway more accurately using clinically available airway pressure and flow measurements. Using this model, the airway condition of a patient can be characterised and thus, could provide clinically useful information to clinicians to guide patient-specific therapy. This results show that even though the ABMps model is derived via classical simple Poiseuille flow and minor loss equations, the extension to a patient-specific airway dimension, α, produced consistent trends and compared well to the DSA model as the current standard for estimating alveolar pressures. This α value can be easily calculated at the bedside in a similar fashion to offer additional insight beyond the DSA with respect to potential to recruit volume (increase in α after a change in treatment) and to monitor patient condition. Overall, these results provide a general model framework that can be customised to each patient at the bedside to help guide care. The results justify further prospective trials to assess the clinical utility of patient-specific value of α in assessing patient condition.

CHAPTER 4

Application of Lung Elastance in Mechanical Ventilation

4.1 The concept of lung elastance

One of the important metrics that can be used in managing mechanical ventilation (MV) is monitoring the lung elastance of ARDS patients. Elastance changes with patient condition since injured lung tissue, combined with a build-up of fluid, affects the resulting elasticity of the lungs (Gattinoni & Pesenti 2005). Elastance is a measure of the tendency of the lung to recoil to its original form and is the reciprocal of compliance. In particular, ARDS affected lungs have relatively higher elastance and significantly more hysteresis compared to healthy lungs, and has been used in other studies to assess the level of lung injury (Suarez-Sipmann et al. 2007; The ARDS Definition Task Force 2012).

Other studies have shown that a more optimal MV setting occurs when the lung is inflated at the minimum inspiratory elastance (Carvalho et al. 2007; Chiew et al. 2011; Lambermont et al. 2008; Suarez-Sipmann et al. 2007). Specifically, lung volume is achieved with minimal added pressure, which implies maximum oxygenation for a minimum change in lung pressure or stress. Thus, models that capture patient-specific lung elastance (1/compliance) and recruitment can provide insight into otherwise un-measurable metrics of lung condition, thereby aiding clinical decision making (Chase et al. 2006a; Chiew et al. 2011; Sundaresan et al. 2011a; Sundaresan et al. 2009).

In addition, considering how elastance changes within the breath and throughout patient care, provides a new clinical perspective. Thus, it provides a non-invasive method that could provide real-time monitoring of lung condition based on measurement of lung elastance. Since this approach adds no additional sensors or cost, and provides a useful measure, it could be used to guide clinicians in PEEP titration to obtain optimal MV settings.

In this chapter, two model-based methods are introduced to estimate lung elastance in ARDS patients.

4.2 Elastance estimation using single compartment lung model

Lumped parameter respiratory system models offer a simple and relatively inexpensive method of assessing lung mechanics and/or gas exchange, and thus, for capturing essential respiratory dynamics. Lumped parameter models can be computationally implemented directly at the bedside and are thus clinically viable. One of the most commonly used lumped parameter models is the single compartment lung model (Mead & Whittenberger 1953). The single compartment lung model, as shown in Figure 4.1, is modelled as a combination of an elastic and resistive component that uses readily measurable airway pressure (P_{aw}), lung volume (V), and air flow (Q_{aw}) to estimate the overall respiratory elastance (E_{rs}) and overall respiratory resistance (R_{rs}) (Bates 2009) .

Using standard mechanics, the respiratory system model can be defined:

$$P_{aw}(t) = R_{rs}Q_{aw}(t) + E_{rs}V(t) + P_0 \qquad (4.1)$$

where P_0 is the offset pressure. P_0 is usually zero at atmospheric pressure but it will change when PEEP is applied and can also account for Auto-PEEP (Bates 2009). The airway pressure (P_{aw}) comprises the sum of the pressure drop due to the resistance component of the endotracheal tube (ETT) and patient's branching airway (Damanhuri et al. 2014), the pressure required to overcome the elastic tendencies of the lung tissues, and the offset pressure. Patient-specific respiratory elastance (E_{rs}) reflects the lung stiffness and can be identified from measured data. Thus, a lower E_{rs} indicates a more compliant lung.

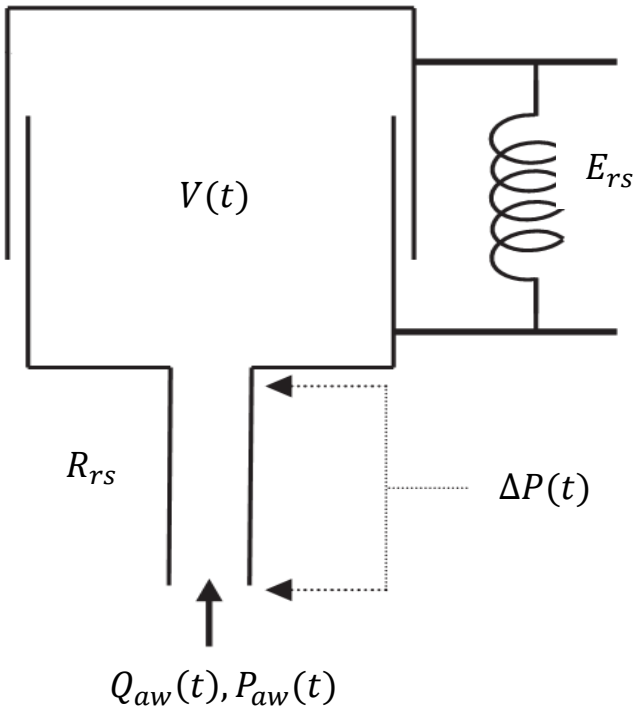

Figure 4.1: The single compartment schematic diagram of the lung mechanic system.

The physiological relevance of the identified model parameters depends on the simplifying assumptions of the model. In this model, the integral-based method (Hann et al. 2005) is used to identify the parameters E_{rs} and R_{rs} that best fit Equation 4.1 using the measured inspiratory pressure (P_{aw}) and air flow (Q_{aw}) from each breathing cycle. Integral-based

parameter identification is similar to multiple linear regression, where using integrals significantly increases robustness to noise (Chiew et al. 2011; Hann et al. 2005).

$$\int P_{aw}(t) = R_{rs} \int Q_{aw}(t) + E_{rs} \int V(t) + \int P_0 \qquad (4.2)$$

Chiew et. al (Chiew et al. 2011) based their model development on a concept of minimal elastance during recruitment of the lung. During each breathing cycle, as pressure rises for a given PEEP level, E_{rs} is decreasing as new lung volume is recruited faster than pressure can build up in the lung. This response indicates recruitability of the lung. If there is little or no recruitment, E_{rs} rises with pressure, which indicates that the inspiratory pressure was unable to recruit new lung volume, leading to increased stress and risk of ventilator induced lung injury (VILI). Thus, the already recruited lung is stretched and possibly damaged. Hence, by monitoring patient-specific and breath-specific respiratory elastance during changes in PEEP level can provide insight into patient condition, help guide MV setting of PEEP, and prevent lung injury.

4.3 Time varying elastance model

Time varying elastance (E_{drs}), as proposed by Chiew et. al (Chiew et al. 2011), is an extension of respiratory system elastance (E_{rs}) with the aim of providing a higher resolution metric for use in guiding optimal PEEP selection. It is an in-breath-specific respiratory elastance over an inspiratory time period that can potentially provide further unique insight into patient-specific lung condition and response to MV settings (Carvalho et al. 2006; Chiew et al. 2011; Kárason et al. 2001). Furthermore, the minimum value of E_{drs} during PEEP titration can aid, as with E_{rs}, in identifying an optimal patient-specific PEEP to help the

patient reduce the work of breathing (WOB) and maximise recruitment of the lung without further lung injury (Marini et al. 1985; Otis et al. 1950).

By calculating the value of E_{drs} over each breath, it is possible to identify the change of respiratory elastance within a breathing cycle as a function of PEEP and pressure over that breath. A decreasing value of E_{drs} over a breath indicates recruitment over pressure build up, while an increasing value of E_{drs} suggests poor recruitment (Chiew et al. 2011). By identifying the time-variant of E_{drs} over each breath, it allows the clinicians to see the changes in lung dynamically with each breathing cycle as pressure increases and thus provides a more detailed view of patient lung condition. This type of information cannot be provided by the calculation of a single value of E_{rs} averaged over a breath. Thus, the estimation of E_{drs} provides more information and higher resolution in patient monitoring.

To investigate the variability of respiratory elastance, the modified single compartment lung model is used. This model incorporates E_{drs} to capture patients-specific and breath-specific respiratory mechanics, including those with spontaneous breathing (SB) effort. This model also proposes negative and positive components for the respiratory elastance (Chiew et al. 2015), when considering SB efforts, where the positive component within a short time period during inspiration is assumed to be effectively constant over the breath. In contrast, the negative component is variable depending on how strongly the patient initiates the breathing cycle, representing a significant patient-and breath- specific, unknown that is typically an unmeasurable quantity without significant, added and invasive sensors.

The single compartment lung model in Equation 4.1 includes all resistive and elastic components of the respiratory system for a fully sedated patient (Bates 2009). To account for

patients with spontaneous breathing respiratory mechanics, the term, respiratory elastance (E_{rs}), is replaced with a time-varying elastance (E_{drs}) that is comprised of 3 subcomponents including: the cage elastance (E_{cw}), the demand elastance (E_{demand}) and the lung elastance (E_{lung}). These terms are then defined:

$$E_{drs}(t) = E_{cw}(t) + E_{demand}(t) + E_{lung}(t) \quad (4.2)$$

$$P_{aw}(t) = (E_{cw}(t) + E_{demand}(t) + E_{lung}(t))V(t) + R_{rs}Q(t) \quad (4.3)$$

$$P_{aw}(t) = P_{cw}(t) + P_{demand}(t) + P_{lung}(t))V(t) + P_{rs} \quad (4.4)$$

where E_{lung} is a measure of the elastic properties of the lung or the collection of alveoli. E_{lung} decreases if overall alveoli recruitment outweighs the pressure build-up. E_{lung} will increase if the overall alveoli are stretched with lesser or no further recruitment (Chiew et al. 2011). Thus, E_{lung} is the representation of true lung mechanics that captures the patient-specific response to MV in each breathing cycle and thus also provides an indication of the patient disease state (Chiew et al. 2015). The elastic properties of the chest wall (E_{cw}) in Equations 4.3-4.5 consist of the stiffness contribution mode by the rib cage and intercostal muscles. This elastance subcomponent can be assumed not to vary with disease-state and is thus considered a patient-specific constant (Chiumello et al. 2008). Finally, E_{demand} represents the unmeasured patient-specific inspiratory demand, which varies depending on patient-specific and breath-specific effort. This elastance is negative (E_{demand} <0) as it represents the reduced apparent elastance seen in measured P_{aw} and Q_{aw} that is due to the patient-specific and breath-specific inspiratory effort creating a pressure reduction in the measured P_{aw} delivered by the ventilator that is used or needed to open the lung. Table 4.1 provides a further nomenclature.

Table 4.1: List of abbreviation

	Units	Definition
P_{aw}	cmH_2O	Airway pressure
P_{pl}	cmH_2O	Pleural pressure (oesophageal pressure)
P_{cw}	cmH_2O	Chest wall pressure
P_{demand}	cmH_2O	Demand pressure
P_{lung}	cmH_2O	Lung pressure during MV
P_{rs}	cmH_2O	Pressure drop due to respiratory system resistance
E_{rs}	cmH_2O/l	Respiratory system elastance
E_{cw}	cmH_2O/l	Cage elastance
E_{demand}	cmH_2O/l	Demand elastance
E_{lung}	cmH_2O/l	Lung elastance
R_{rs}	cmH_2O/l	Respiratory system resistance
R_{lung}	$cmH_2O.s/l$	Lung resistance
R_{cw}	$cmH_2O.s/l$	Chest wall resistance

A schematic representation of this extended compartment model is shown in Figure 4.2.

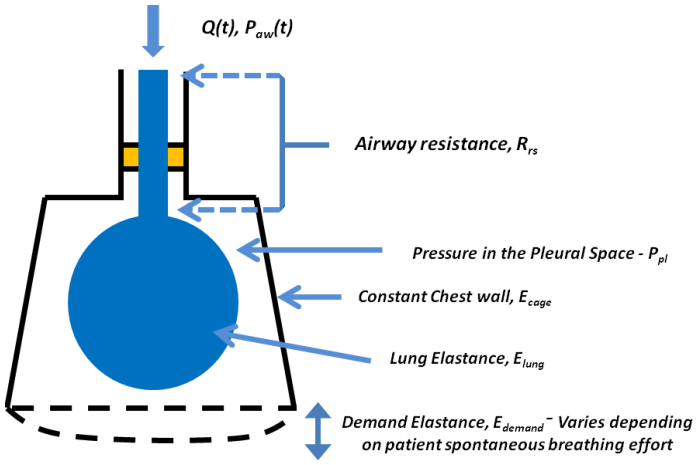

Figure 4.2: The measured airway pressure consists of 4 pressure components: 1) Pressure drop due to airway resistance (P_{rs}), 2) pressure in the lung compartments (P_{lung}), 3) and 4) pressure change in the pleural space (P_{cw} + P_{demand}).

P_{cw} and P_{demand} are the pressure components generated from E_{cw} and E_{demand}. Combining these pressure components will thus give information on the pleural pressure (P_{pl}), which is the pressure change in the pleural space (chest wall). P_{lung} is the pressure in the lung during MV and P_{rs} is the pressure drop due to the conducting airway. Again, all these terms are also shown in Table 4.1.

In a fully sedated patient, E_{drs} values were always positive ($E_{drs} > 0$) and had similar elastance to ARDS patients (Carvalho et al. 2008; Chiew et al. 2011; Suarez-Sipmann et al. 2007) as there was no external energy input from SB efforts. However, if the patient exhibits spontaneous inspiratory effort, this value will reduce E_{drs} (t) to become negative due to E_{demand} ($E_{demand} < 0$). The negative value of E_{demand} will decrease the overall values of E_{drs} and result in variability in the overall respiratory elastance. As patient demand aids breathing effort, the effective overall airway pressure is thus reduced from sedated state (Damanhuri et al. 2015). In any given breathing cycle, the time-varying E_{drs} of Equation 4.3 captures all three elastance components together, and thus a general conceptual and modelling approach is created in this analysis.

It is important to note that E_{drs}, is an overall, effective elastance. It is assessed as the change in pressure for a given tidal volume of flow. Thus, lower effective elastance implies less risk of lung damage (Carvalho et al. 2007; Chiew et al. 2011). This non-invasive model-based monitoring and analysis method is hypothesized to be able to capture new insight into the dynamic respiratory mechanics, particularly for SB patients during fully controlled or partially assisted MV modes. This model is validated to investigate further on the negative elastance in SB patients using clinical data, and is presented in Chapter 7.

4.4 Summary

Lung elastance is an important parameter used to quantify the condition and response to therapy of a patient suffering from respiratory failure. With the estimation of the lung elastance (E_{rs}), the effect of PEEP on lung elastance has a potential for guiding MV therapy. The time varying elastance model provides more robust method to determine the dynamic lung condition in fully sedated and SB patients. The estimation of E_{drs} allows a more true measurement of dynamic lung elastance over the inspiration cycle that cannot be provided by a single average value of E_{rs}.

CHAPTER 5

Expiratory Time Constant Model Using Clinical Data

5.1 Introduction

Respiratory system models can provide real-time information on patient condition and response to treatment based on mechanical ventilation (MV) airway pressure (P_{aw}) and flow (Q_{aw}) data (Chiew et al. 2011; van Drunen et al. 2014). However, most respiratory mechanics models require specific data profiles and specialised, often invasive and/or interruption of care, protocols for model identification (Oostveen et al. 2003; Schranz et al. 2012a; Schranz et al. 2011; Stahl et al. 2006). These models also focused only on data collected during inspiration, and data during expiration are essentially neglected. Recent research conducted by Al Rawas et al. (2013) and van Drunen et al. (2013) on expiratory data had found high correlation between the inverse expiratory time constant and respiratory system elastance in both human and experimental animal trials. These finding have led to a potential to use of the expiratory data during clinical respiratory mechanics monitoring to guide MV.

In particular, the study by van Drunen et al. (van Drunen et al. 2013) has shown that the inverse of expiratory time constant parameter (K) provides potential ability to track changes in disease state throughout therapy (van Drunen et al. 2013). In this animal study, trends in K were comparable to respiratory elastance trends obtained using the invasive end-of inspiratory pause method (E_{static}) that interrupts care, as well as respiratory elastance derived from the single compartment lung model (E_{rsIB}). These outcomes are shown in Figure 5.1.

The top of Figure 5.1 shows the result from a phase 2 condition, which is defined as a progression from a healthy state to an induced ARDS state at a constant PEEP, where the bottom figure shows the results of phase 3, which is an induced ARDS state staircase recruitment manoeuvre (RM). In both phases, E_{rsIB}, E_{static}, and K followed similar trends. Hence, these results show that the expiratory time constant model was able to identify trends and fundamental changes in respiratory mechanics, as determined by the invasive end-inspiratory pause method and the single compartment linear lung model.

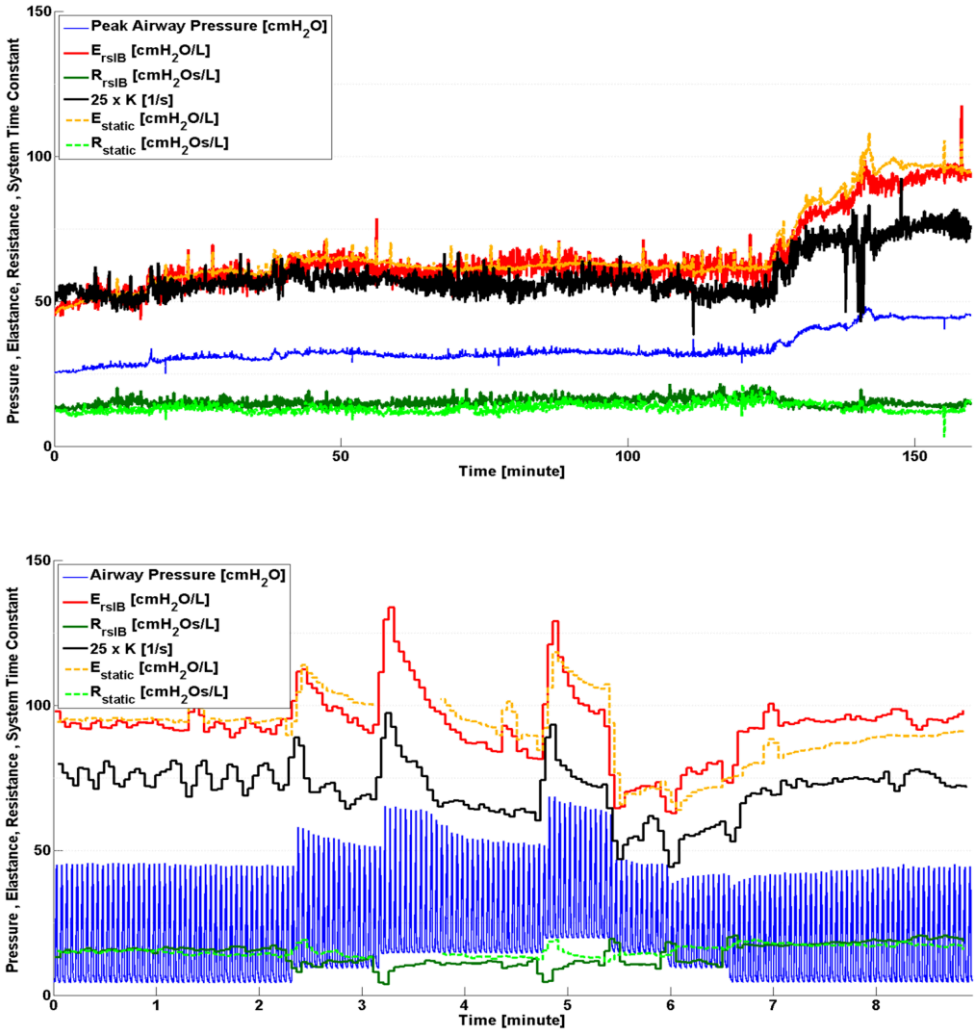

Figure 5.1: *Top* Respiratory system mechanics monitoring during phase 2, disease progression for animal data 1. *Bottom* Respiratory system mechanics monitoring during phase 3, disease state recruitment manoeuvre for animal data 1. Note that values of K have been scaled for clarity and serve only as an indication for trend comparison.

This chapter extends the investigation on the relation of expiratory time constant with respiratory system elastance using retrospective clinical cohorts (Bersten 1998; Sundaresan et al. 2011a). These data are comprised of step-wise recruitment manoeuvres (RM) with PEEP changes to provide a variation of respiratory system elastance response to different PEEP levels (Chiew et al. 2011). These respiratory system elastance variations thus provide a unique platform to investigate the relation of expiratory time constant with respiratory system elastance. Importantly, information on respiratory system elastance response to PEEP has shown clinical potential for guiding PEEP titration (Carvalho et al. 2007; Carvalho et al. 2008; Carvalho et al. 2013; Lambermont et al. 2008; Suarez-Sipmann et al. 2007; Suter et al. 1978; Zhao et al. 2010a). Thus, a good correlation between these metrics will imply that the expiratory time constant can also be used to titrate PEEP under similar assumptions (van Drunen et al. 2013) using easily measured, non-invasive data, and without interrupting care.

5.2 Methodology

5.2.1 Expiratory Time Constant Model

The expiration process is defined as a passive process, where the lung and chest wall are elastic and have a tendency to return to their equilibrium positions after being actively inflated during inspiration. The single compartment lung model, as mentioned earlier in Chapter 4, is only focused on the inspiration cycle because inspiration and expiration are two different physiological processes that must be considered separately when determining lung properties (Möller et al. 2010). The equation of respiratory system is repeated here for clarity as:

$$P_{aw}(t) = R_{rs}Q_{aw}(t) + E_{rs}V(t) + P_0 \qquad (5.1)$$

Thus, the expiratory time constant model is derived from the single compartment lung model, but focuses on expiration data. van Drunen et al. (2013) proposed a method of calculating the inverse of time constant parameter (*K*) during the expiration cycle time.

It is important to note that expiration is a passive process that unloads the inspired tidal volume over a resistance at a constant ventilator applied end expiratory pressure (P_{aw}= PEEP) with P_0 = PEEP (Möller et al. 2010). Thus, Equation 5.1 in expiration becomes:

$$PEEP = R_{rs}Q_{aw}(t) + E_{rs}\int V(t)dt + PEEP \tag{5.2}$$

Differentiating Equation 5.2 yields:

$$0 = R_{rs}\frac{dQ_{aw}(t)}{dt} + E_{rs}Q_{aw}(t) \tag{5.3}$$

By dividing Equation 5.3 with R_{rs}, a simple differential equation is yielded:

$$0 = \frac{dQ(t)}{dt} + \frac{E_{rs}}{R_{rs}}Q_{aw}(t) \tag{5.4}$$

Hence, the expiratory time constant model derived from the single compartment lung model is defined:

$$Q_{aw}(t) = Q_0 e^{t/\tau} = Q_0 e^{-Kt} \tag{5.5}$$

where Q_0 is the value of maximum expiratory flow and $\tau = 1/K = R_{rs}/E_{rs}$ is the time constant for this model during expiratory time (Al-Rawas et al. 2013).

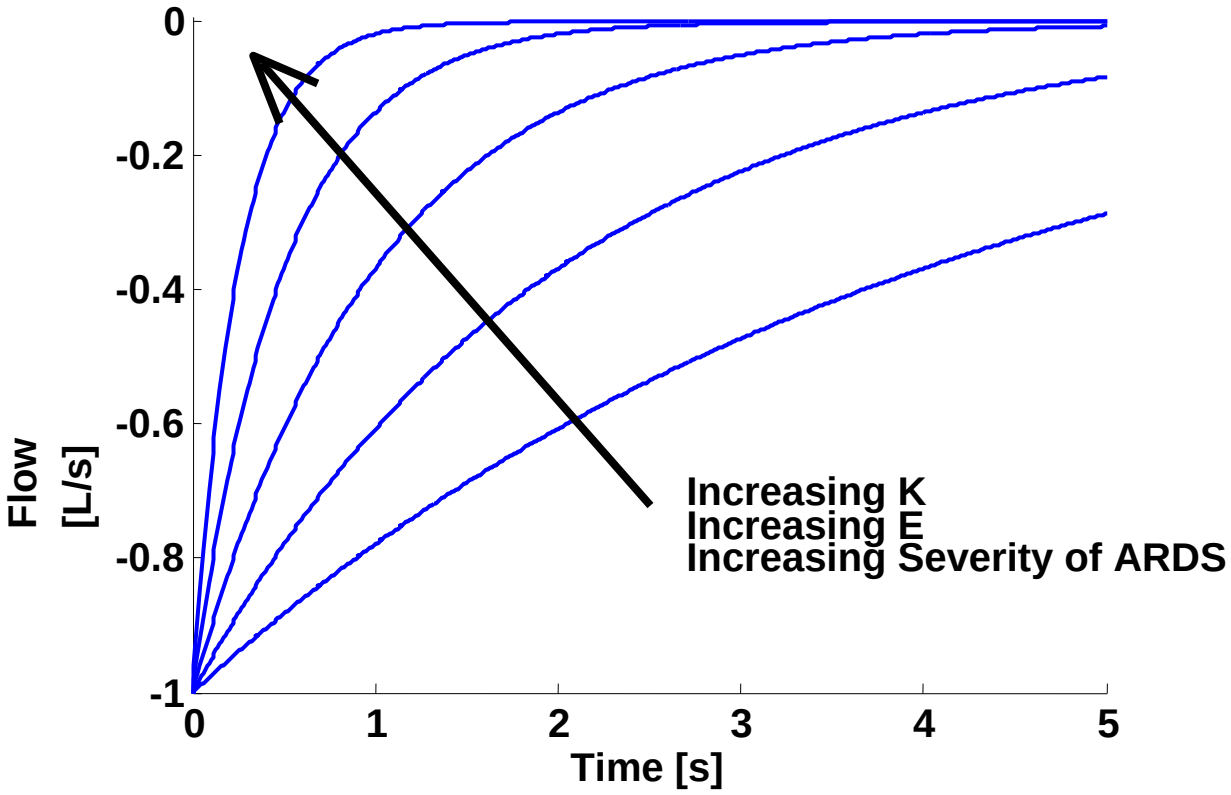

Figure 5.2: Example of how expiratory flow profiles over time may be used to determine changes in a patients' disease state, assuming Rrs is constant.

If R_{rs} is assumed constant (Chiew et al. 2011), the parameter *K* is directly proportional to E_{rs} where an increasing *K* implies a stiffer lung as ARDS progresses, as illustrated in Figure 5.2**.**

5.2.2 Patient Data

This model is assessed using two retrospective clinical ARDS cohorts, consisting of 10 patient-datasets from Sundaresan et al. (Sundaresan et al. 2011a) and 12 patients-datasets from Bersten et al. (Bersten 1998), denoted Cohorts 1 and 2, respectively. The associated protocols have been described in detail in Chapter 2.

5.2.3 Analysis

The expiratory time-constant model parameter, *K*, is calculated continuously for every breathing cycle at each PEEP level for both cohorts (Bersten 1998; Sundaresan et al. 2011a) based on flow rate and airway pressure data respectively. Validation is performed by comparing trends of the estimated *K* values during expiration cycle to trends of E_{rs}/R_{rs} and E_{rs} during inspiration cycle that derived from the single compartment lung model. Results of *K*, R_{rs}, E_{rs}/R_{rs}, and E_{rs} are recorded in Median and Inter-Quartile Range (IQR). Furthermore, performance was assessed by calculating the Pearson correlation coefficient (R^2) where trend comparisons between the estimated *K* for expiration, and both E_{rs}/R_{rs} and E_{lung} for inspiration were made. Good correlation results will indicate similarity as often assumed. In contrast, poor correlation results will show the need to treat them separately.

5.3 Results

Correlation between *K* and inspiration derived E_{rs} are compared and shown in Figure 5.3 for both Cohorts 1 and 2. The Pearson correlation for *K*- E_{rs} for Cohort 1 is $R^2 = 0.568$, Cohort 2 is $R^2 = 0.184$ and the overall value is $R^2 = 0.435$. Figure 5.4 illustrates the correlation between *K* and inspiration derived E_{rs}/R_{rs} for both Cohorts 1 and 2 with a correlation results *K*- E_{lung}/R_{lung} is $R^2 = 0.340$ for Cohort 1 and $R^2 = 0.002$ for Cohort 2 and $R^2 = 0.078$ all together. The Median and Inter-Quartile Range (IQR) of E_{rs}, R_{rs}, E_{rs}/R_{rs} and, *K* for each data set from both cohorts are tabulated in Tables 5.1 (Cohort 1) and 5.2 (Cohort 2), respectively.

Figure 5.5 and 5.6 present the changes of E_{rs} comparing to expiratory time constant *K* with PEEP increase for both Cohort 1 and Cohort 2. Figure 5.7 compares the trend of R_{rs} between

a Chronic Obstructive Pulmonary Disease (COPD) patient and a non COPD patient for all PEEP levels from Cohort 1. Figure 5.8 shows the trend comparison of expiration time constant, *K*, inspiration E_{rs} and inspiration E_{rs}/R_{rs} between Patient S1 from Cohort 1 and Patient B10 in Cohort 2 for all PEEP levels at every breathing cycle. The model-fitting for airway flow and pressure between measured and calculated values for dataset S3 are depicted in Figure 5.8.

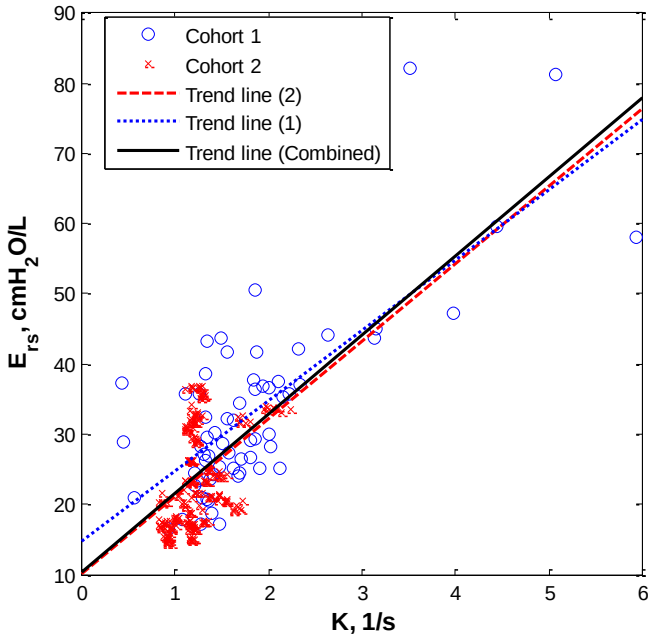

Figure 5.3: Correlation plots of *K* vs E_{rs} for both all data sets with R^2 = 0.568 for Cohort 1 and R^2 = 0.184 for Cohort 2 and R^2 = 0.435 for both Cohorts at all PEEP levels.

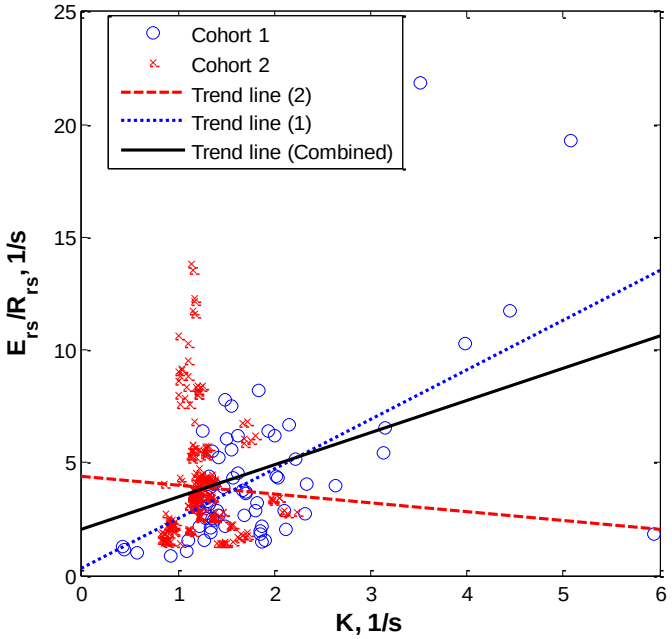

Figure 5.4: Correlation plots of K vs E_{rs}/R_{rs} for both all data sets with R^2 = 0.340 for Cohort 1 and R^2 = 0.002 for Cohort 2 and R^2 = 0.078 for both Cohorts at all PEEP levels.

Table 5.1: Median and IQR of E_{rs}, R_{rs}, E_{rs}/R_{rs}, and, K of each dataset from Cohort 1 (Sundaresan et al. 2011a).

	Median [IQR]			
Dataset	E_{rs}**(cmH$_2$O/L)**	R_{rs}**(cmH$_2$O.s/L)**	E_{rs}/R_{rs}**(1/s)**	K**(1/s)**
S1	32.54 [27.51-37.24]	10.65 [9.59-15.87]	2.53 [1.74-3.76]	1.33 [1.30-1.34]
S2	23.13 [21.31-26.17]	7.66 [7.55-8.25]	3.03 [2.50-3.46]	1.31 [1.29-1.34]
S3	20.70 [18.05- 26.81]	6.70 [6.17-7.45]	2.86 [2.33-4.37]	1.34 [1.27-1.41]
S4	25.04 [19.38-27.04]	19.68 [16.10-23.07]	1.15 [1.04-1.42]	0.93 [0.51-1.50]
S5	44.54 [42.32-49.21]	16.11 [11.54-23.98]	2.52 [2.03-3.72]	2.37 [1.93-3.01]
S6	24.84 [24.49-30.22]	5.65 [5.26-6.40]	4.32 [3.80-5.77]	1.62 [1.44-1.68]
S7	59.70 [47.16-81.18]	4.59 [4.22-5.09]	11.74 [10.27-19.25]	3.98 [3.52-4.44]
S8	29.11 [27.51-32.20]	7.24 [6.66-9.25]	3.65 [3.03-4.37]	1.81 [1.76-2.01]
S9	27.97 [25.07-30.09]	6.45 [6.21-10.86]	3.83 [2.44-4.62]	1.57 [1.49-1.72]
S10	37.18 [36.36-41.86]	5.75 [5.57-8.06]	6.42 [4.61-7.11]	2.15 [1.75-2.27]
Median [IQR]	**29.40 [24.63-37.47]**	**7.78 [6.02-12.72]**	**3.50 [2.18-5.37]**	**1.57 [1.33-1.99]**

Table 5.2: Median and IQR of E_{rs}, R_{rs}, E_{rs}/R_{rs}, and K of each dataset from Cohort 2 (Bersten 1998).

	Median [IQR]			
Dataset	E_{rs}(cmH$_2$O/L)	R_{rs}(cmH$_2$O.s/L)	E_{rs}/R_{rs}(1/s)	K(1/s)
B1	26.23 [23.47-36.62]	7.67 [7.61-7.82]	3.06 [2.99-3.43]	1.18 [1.14-1.21]
B2	15.32 [15.034-16.28]	7.09 [6.27-7.59]	2.18 [2.15-2.34]	0.94 [0.91-0.95]
B3	32.76 [30.99-36.63]	12.69 [8.83-15.43]	2.59 [2.02-4.18]	1.22 [1.13-1.26]
B4	18.27 [17.478-19.29]	7.48 [4.04-11.02]	3.04 [1.75-4.32]	1.49 [1.31-1.67]
B5	21.12 [20.54-21.36]	7.09 [5.24-8.33]	2.86 [2.47-4.09]	1.39 [1.27-1.49]
B6	33.46 [32.39-33.70]	9.95 [5.33-11.82]	3.39 [2.85-5.94]	1.98 [1.77-2.10]
B7	17.18 [16.26-18.67]	3.71 [2.23-4.70]	5.32 [3.41-8.68]	1.16 [1.07-1.19]
B8	17.40 [16.98-20.14]	11.02 [10.88-11.30]	1.55 [1.50-1.84]	0.86 [0.85-0.89]
B9	32.23 [29.53-35.21]	6.69 [6.49-8.35]	4.39 [3.93-5.39]	1.24 [1.19-1.28]
B10	28.90 [25.43-32.91]	5.68 [3.78-7.61]	5.78 [3.34-8.71]	1.20 [1.17-1.25]
B11	17.40 [17.18-18.75]	3.04 [1.60-3.15]	5.64 [5.49-11.70]	1.16 [1.14-1.17]
B12	24.03 [23.29-24.77]	9.70 [6.80-16.57]	2.55 [1.46-3.40]	1.36 [1.35-1.45]
Median [IQR]	**23.10 [17.59-31.48]**	**7.43 [4.88-9.40]**	**3.42 [2.48-4.40]**	**1.20 [1.13-1.34]**

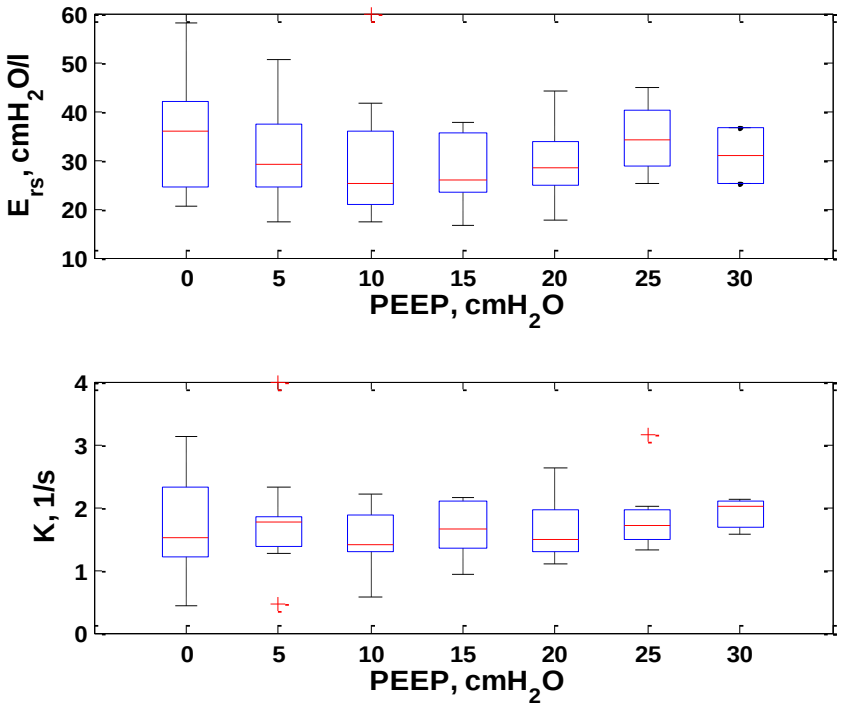

Figure 5.5: E_{rs}-PEEP and K-PEEP plot for Cohort 1. *Top* E_{rs} range for 10 patients in Cohort 1 with PEEP increase. *Bottom* K range for 10 patients from Cohort 1 with PEEP increase.

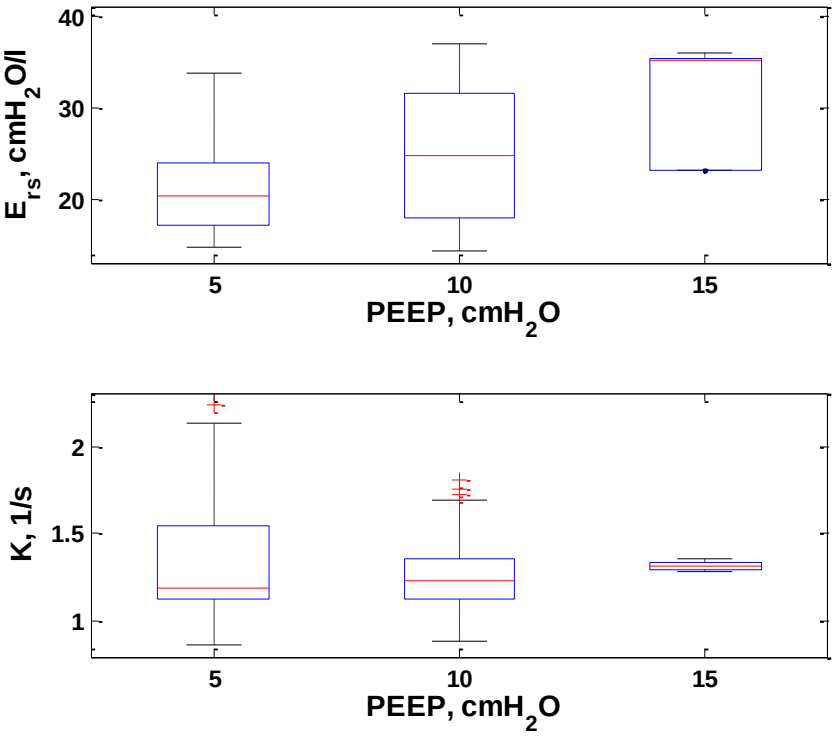

Figure 5.6: E_{rs}-PEEP and K-PEEP plot for Cohort 2. *Top* E_{rs} range for 12 patients in Cohort 2 with PEEP increase. *Bottom* K range for 12 patients from Cohort 2 with PEEP increase.

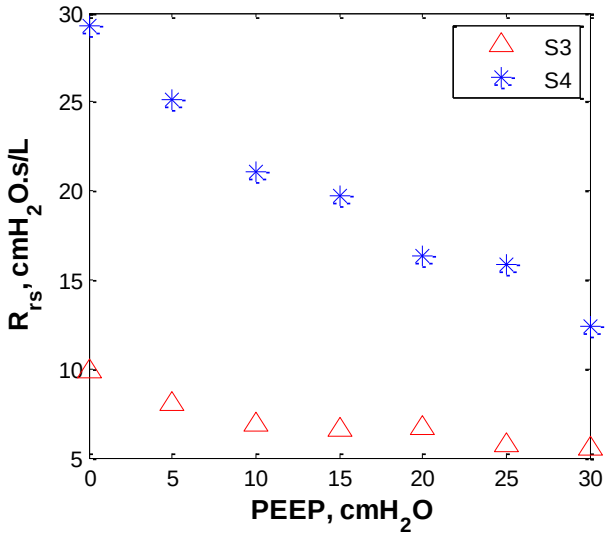

Figure 5.7: Comparison of R_{rs} between dataset S3 which is a non COPD patient with dataset S4 which is a COPD patient for all PEEP levels.

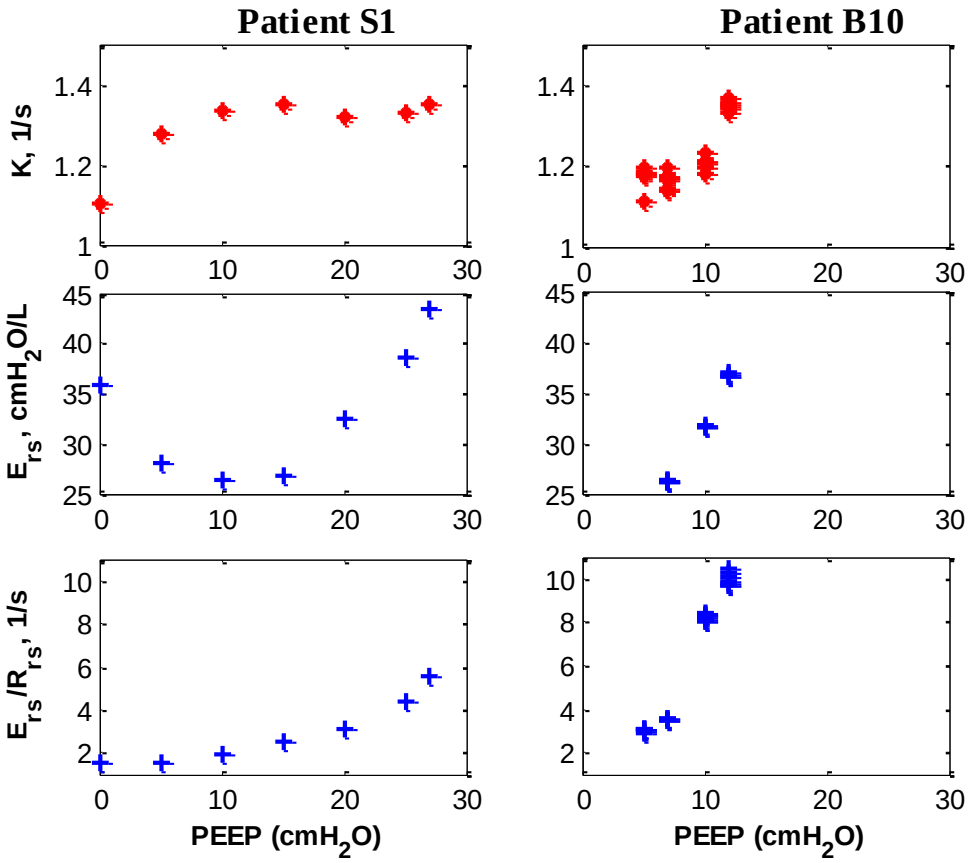

Figure 5.8: *Left* Trend comparison of expiration time constant, K, inspiration E_{rs}/R_{rs} and inspiration E_{rs}/R_{rs} for one breathing cycle for patient S1 from Cohort 1 for all PEEP levels. *Right* Trend comparison of expiration time constant, *K*, inspiration E_{rs}/R_{rs} and inspiration E_{rs}/R_{rs} for seven breathing cycle for patient B10 from Cohort 2 for all PEEP levels.

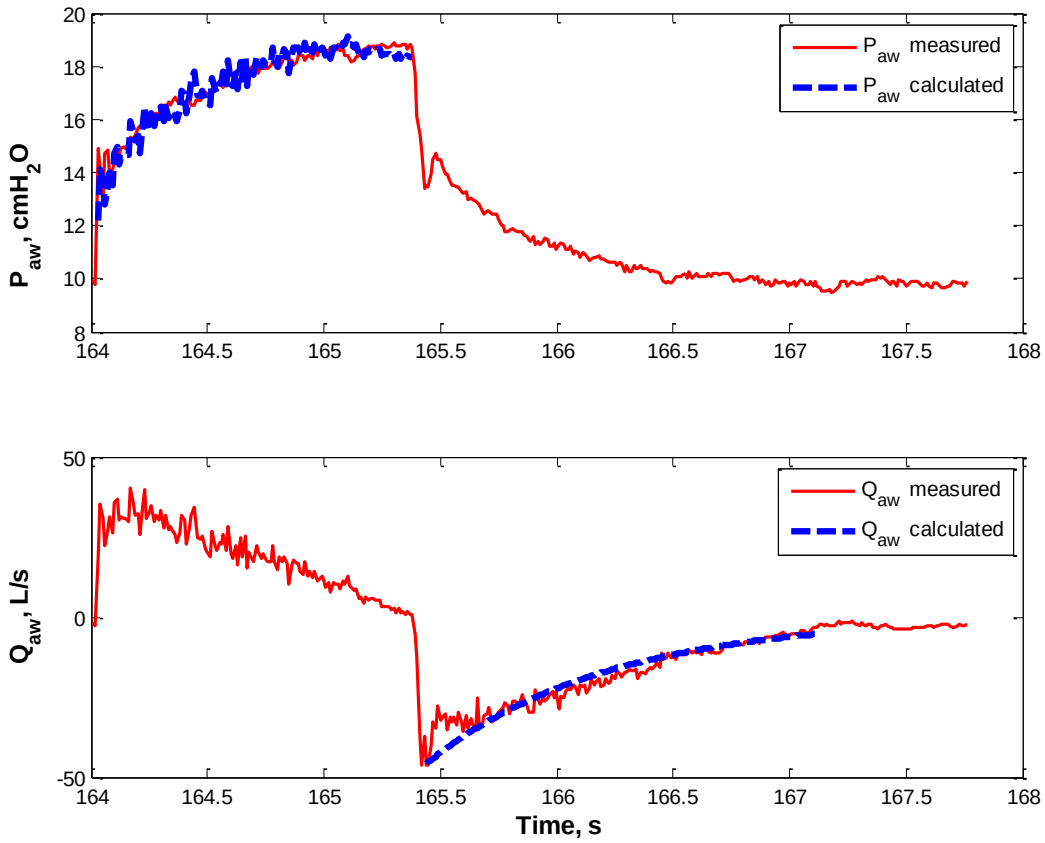

Figure 5.9: (*Top*) Model-fitting between measured airway pressure and calculated airway pressure based on the lung elastance model for Patient S3 at PEEP = 10 cmH_2O one breathing cycle. (*Bottom)* Model-fitting between measured airway flow and calculated airway flow for Patient S3 at PEEP = 10 cmH_2O for one breathing cycle.

5.4 Discussion

The expiratory time constant *K* has shown a moderate correlation with E_{rs} with R^2= 0.568 in Cohort 1 and weak correlation with R^2= 0.184 in Cohort 2, as shown in Figure 5.3. Comparatively, the correlation of *K* with the inspiration E_{rs}/R_{rs} also shows a weak correlation of R^2= 0.340 for Cohort 1 and a poor R^2= 0.002 for Cohort 2, as depicted in Figure 5.4. These results contradict to the findings by Al Rawas et al. (2013) and the animal study by van Drunen et. al (2013) that showed *K* has good correlation with respiratory elastance estimated using inspiratory data. This result indicates that although *K* is defined as E_{rs}/R_{rs}, it does not deliver the same result as those same values in inspiration because expiration and inspiration

must be considered separately when determining lung mechanics properties (Möller et al. 2010). In particular, the difference in mechanics may be due to comparing the actively driven volume increase of inspiration with passive volume reduction in expiration.

For the result shown in Figure 5.8, the calculated airway pressure using the inspiration single compartment lung model has resulted in a good fit with the measured airway pressure from the ventilator for data set S3 from Cohort 1, where the Median and IQR of the absolute percentage fitting error are 1.74 [0.79 - 2.79]%. However, a moderate fitting error is found in the calculated airway flow versus measured airway flow in this patient data set with Median and IQR of 8.60 [10.23-27.33]%. This error is due to noise that occurs early in the expiration flow cycle, as shown in Figure 5.8, thus resulting in poor model fitting at the beginning of expiration. However, a much better model fit occurred for the remaining expiration cycle. Thus, this result implies that by using the single compartment lung model, it follows the same trend as the measured data, but the K and E_{rs}/R_{rs} values are different.

Results for E_{rs} can be seen in Figures 5.5 and 5.6, showing the parameter changes in response to PEEP change. Decreasing E_{rs} which suggests overall lung recruitment with PEEP, whereas with increasing E_{rs}, it shows that the lung becomes stiffer, thus no further recruitment happened in the lung, suggesting lung over-distension (Carvalho et al. 2007; Carvalho et al. 2006; Suarez-Sipmann et al. 2007). It can be seen that from the beginning of the RM, at ZEEP, E_{rs} is relatively high for all patients from Cohort 1. As PEEP rises, it is observed that E_{rs} drops but increases again at PEEP = 25 cmH_2O. This behaviour shows that recruitment occurs at lower to middle value of PEEP and that the lung is over-stretching when the PEEP increases to higher values. In contrast, it can be observed in Figure 5.6, that E_{rs} increases as PEEP increases for Cohort 2. Hence, these results show that there is a possibility of over-

stretching of healthy lung units in this cohort even the lung is ventilated at a lower PEEP levels and airway pressures due to the heterogeneity of ARDS across all patients (Stenqvist 2003).

These results show that monitoring patient-specific E_{rs} during PEEP changes has the potential to be used in optimum PEEP titration for the ARDS patients (Chiew et al. 2012; Chiew et al. 2011). It also shows that Cohort 2 may not be recruitable or already ventilated at too higher PEEP. Thus, if K had high positive correlation with E_{rs}, as it did for Cohort 1, it could potentially be used to titrate PEEP, especially during partial ventilation support.

Overall results in this study contradict the findings in the animal study by van Drunen et al. (2013). The study by van Drunen et al. (2013) showed that K has a similar trend with E_{rs} in experimental ARDS animal trials (van Drunen et al. 2013). However, this study using human data showed otherwise. In particular, van Drunen et al. (2013) had higher tidal volumes (V_t) of 10-12 mL/kg during MV. Higher V_t during ventilation allows more air to enter into the lung, thus allowing the respiratory system elastic properties to potentially be better identified. Equally, higher V_t will thus provide better flow data resolution during the expiration cycle. Compared to the animal study by van Drunen et al. (van Drunen et al. 2013), both human patient cohorts in this study have comparatively lower tidal volumes, limiting the data available during expiration. Note that these lower V_t values are well validated as a safe threshold (Brochard et al. 1998; Parsons et al. 2005; The Acute Respiratory Distress Syndrome Network 2000). Thus, for use in humans, controlled expiration would be required to get the best resolution and value of K that better reflects and correlates with E_{rs} (Möller et al. 2010).

The discrepancy estimated parameter *K* is comparatively lower than in the studies conducted by Al Rawas et al. (Al-Rawas et al. 2013) and van Drunen et al. (van Drunen et al. 2013). One of the possibilities is that, the low variation, or ranges of parameter *K*, was not able to provide a platform for comparison between these two parameters of *K* and E_{rs}. It can be seen that *K* has not shown significant changes as PEEP increases, as observed in Figures 5.5 and 5.6 for both cohorts, especially for Cohort 2. In particular, Cohort 1 consists of 5 to 7 different PEEP levels per patient, whereas Cohort 2 only consists of 3 relatively closely PEEP levels. Thus, there may be not enough PEEP variation in Cohort 2 in particular. In addition, single compartment model estimated respiratory elastance is a lumped parameter model and there may be several hidden variables and components that might be needed to better define respiratory system elastance (Bates 2009).

In this study, a higher airway resistance in the lung can be seen in patients who suffer from Chronic Obstructive Pulmonary Disease (COPD), which is shown in Table 5.1. It can be seen from Table 5.1 that COPD patients from Cohort 1 (datasets S1, S4, S5, S9, S10) have higher resistance in the lung (R_{rs}) compared to other non-COPD patients (using a Wilcoxon rank sum test, $p<0.005$). The Median and Inter-Quartile Range [IQR] of R_{rs} for COPD is 11.00 [6.68-17.22] $cmH_2O.s/L$, while for non-COPD is 6.80 [5.66-7.86] $cmH_2O.s/L$. This higher resistance in COPD patients is due to the effectively smaller airway diameter resulting from this condition that lead to a higher airway resistance when portions of airways are fully or partially collapsed in COPD (Damanhuri et al. 2014). This effect can be seen in COPD patient (S4) in Figure 5.7, where higher R_{rs} exists due to the obstructed airways at lower pressures and PEEP, as compared to the non-COPD patient (S3). These differences are also expected clinically.

Since $K = E_{rs}/R_{rs}$, an increasing airway resistance would result in a low value of K. Significant variations in R_{rs} may thus lead to poor direct correlation between K and E_{rs} (van Drunen et al. 2013). Equally, these patients were found to have decreased K, as expected clinically, where a patient with COPD requires more time for expiration, which will lead to an increased expiratory time constant (~ $1/K$) (Lourens et al. 2000).

Cohort 1 and Cohort 2 are also clinically fundamentally different because of the difference in flow profiles used in MV. For some cases, K were relatively unchanged with PEEP, as shown in Figure 5.8 compared to the value of E_{rs} or E_{rs}/R_{rs} for dataset S1 and dataset B10. Similarly, the Median and Inter-Quartile Range [IQR] of K for Cohort 1 is 1.57 [1.33-1.99] 1/s, while Cohort 2 is a much tighter, more constant with 1.20 [1.13-1.34] 1/s across all PEEP levels. These results may be due to the fact that the same expiration flow pattern exists in both cohorts thus resulting in relatively constant values of K. In addition, it can also be seen from Figure 5.8 for S1 and dataset B10, that the trend of K does not follow either E_{rs} or E_{rs}/R_{rs} for both cohorts. This lack of correlation using the clinical data may also be a subject-specific response due to the increasing severity of ARDS collapsing airways within the lungs, thereby increasing the resistance of the conducting airways (R_{rs}) as mentioned previously in (Gattinoni & Pesenti 2005).

Furthermore, this different result may also be due to the different protocols applied in these two studies (Al-Rawas et al. 2013; van Drunen et al. 2013). A better relationship and correlation between K and PEEP might be obtained by designing a clinical protocol where V_t is varied between low and high values at constant PEEP. Equally, controlled expiration cycle might be considered. In addition, variations in R_{rs} may lead to a lower correlation between K and E_{rs} (van Drunen et al. 2013). Based on the results, as tabulated in Tables 5.1 and 5.2, it

was found that airway resistance varies across all patients. Thus, a larger study cohort would be needed to further validate this expiratory time constant model.

Although *K* has shown a poor correlation for Cohort 2, it still delivered a good indication for COPD patients in Cohort 1 due to the higher airway resistance in the lung. Thus, potential application for *K* remains in diagnosing and provide further insight into lung condition in COPD patients. Furthermore, with specific ventilation profiles and a specific clinical protocol, *K* can be extended to determine real-time lung parameters using only expiration data.

In particular, this application can be important in spontaneously breathing (SB) patients, where these patients have individual breathing effort that alters the lung mechanics on inspiration, but are similar in expiration (Grinnan & Truwit 2005). There are some techniques to measure the lung mechanics of SB patient such as the oesophageal balloon-catheter technique (Bates 2009). However, this technique is not suitable for clinical practice as it requires the balloon to be inserted into the patient and used in care, making it uncomfortable, invasive and interruptive of care for the patient (Khirani et al. 2010). Thus, the application of expiratory time constant in SB patients also warrants further investigation.

5.5 Summary

In summary, this research has shown that variations in lung resistance may lead to a lower direct correlation between inverse respiratory time constant, *K* and respiratory system elastance, E_{rs}. The reason can be due to discrepancy of *K* and difference in clinical protocol that limits tidal volume safety threshold that can affect parameter identification process.

Thus, the ability of using K as a severity indicator or patients' response to MV remains limited. Future investigation into this method is required before any implementation of the model parameter K should be considered, especially for SB patients where expiratory consistency can negate the effect of variable, patient-specific inspiratory efforts

CHAPTER 6

Variability of Elastance in Pilot Clinical Data of ARDS Patients

6.1 Introduction

Experimental animal studies (Chiew 2013; Chiew et al. 2015; van Drunen et al. 2014) have shown that breath-to-breath model-based respiratory mechanics estimation can provide unique clinical information and insight into the condition. In particular, van Drunen et al. (van Drunen et al. 2014) and Chiew et al. (Chiew 2013) monitored the progressive changes in respiratory mechanics during oleic acid induced ARDS experimental models. They found that the respiratory elastance changes, as expected, from lower to higher values when the lungs become more injured and stiffer with induced ARDS again, as expected (Carvalho et al. 2007; Carvalho et al. 2006). These were the first results to observe these changes continuously, in real-time. Thus, monitoring the changes and variation of respiratory mechanics can be useful in the clinical situation, such that clinicians can intervene for treatment before the condition escalates.

During mechanical ventilation, patients may exhibit spontaneous breathing even effort during fully controlled ventilation modes, when the patient is heavily sedated. Hence, ventilators are now incorporated with more advanced detection systems and protocols in an attempt to provide better patient ventilator interaction. However, these systems do not significantly reduce asynchronous patient-ventilator interactions.

One of the ventilation modes commonly used in the Christchurch hospital is the synchronised intermittent mandatory ventilation mode (SIMV). This ventilation mode provides mandatory

breathing cycles to the patients, and it also provides a means for patient ventilator synchronisation by allowing patient triggering of the breath. It is thus a hybrid system mixing fully controlled and patient driven breathing support. With patient triggering and/ or spontaneous breathing effort, respiratory mechanics in these patients become more variable, particularly because the patient-specific inspiratory effort is not typically measured or known. This variability can then mask the respiratory mechanics based on the known ventilator inputs, so that the actual respiratory elastance trend cannot be identified accurately. Thus, this variability may affect management of MV guided by respiratory mechanics. Hence, understanding the underlying variability in respiratory mechanics will enable clinicians to understand when observed variability is within or outside expected natural variation, and thus in selecting optimal MV setting.

This study thus aims to quantify the variability in model-based respiratory mechanics (elastance and resistance). A time-varying elastance model is used to estimate the respiratory mechanics of patients included in a prior prospective pilot clinical trial. The variability of dynamic elastance (E_{drs}) across all PEEP in MV patients was analysed. The goal is to provide a fundamental understanding of the patient-ventilator natural variability, leading to a definition of what level of variability is natural and what level constitutes a significant level of change in respiratory mechanics due to other factors.

6.2 Methodology

6.2.1 Patient Data and Analysis

A clinical trial, Clinical Utilisation of Respiratory Elastance (CURE), is being carried out in the intensive care unit (ICU) of Christchurch, New Zealand. All patients are ventilated using

a Puritan Bennet PB840 ventilator (Covidien, Boulder, CO, USA) The airway pressure and flow curves for each patient were recorded and analysed using a time-varying elastance model proven on sedated, MV patients (Chiew et al. 2011).

In this trial, several recruitment manoeuvres (RM) are performed by the attending clinician throughout the duration of MV. Prior to the study, written informed consent was obtained, and the trial and the use of the data were approved by the New Zealand South Regional Ethics Committee. The trial number is ACTRN12613001006730. Table 6.1 shows the patient details for those included in this study.

Table 6.1: Characteristics of the patients

Patient No.	Gender	Age	Clinical Diagnostic
1	Female	53	Faecal peritonitis
2	Male	71	Cardiac surgery and contracted hospital acquired pneumonia
3	Male	60	Pneumonia
4	Male	36	Pneumonia
5	Male	61	Pneumonia

6.2.2 Inclusion and Exclusion Criteria

The inclusion and exclusion criteria for CURE trial patients are defined:

Inclusion Criteria

1. Patient on Mechanical Ventilation.

2. Patient requiring invasive ventilation (Intubation or tracheotomy).
3. Patients diagnosed with all degrees of ARDS severity (Partial Pressure of arterial blood gas oxygen per Fraction of Inspired Oxygen (PF Ratio) < 300 mmHg as per Berlin Definition (The ARDS Definition Task Force 2012), by intensive care clinicians.
4. Arterial line in situ.

Exclusion Criteria

1. Patients who are likely to be discontinued from MV within 24 hours.
2. Patients with age less than 16.
3. Patients who have moderate or severe traumatic brain injury, and/or a measured intracranial pressure ≥ 20 cm H_2O,
4. Any medical condition associated with a clinical suspicion of raised intracranial pressure.
5. Patients who have a high or spinal cord injury with loss of motor function.
6. Patients who have significant weakness from any neurological disease.
7. Patients who have acute severe pancreatitis and are expected to be ventilated for more than 10 days.
8. Patients who have a pneumothorax.
9. Patients who have asthma as the primary presenting condition.
10. Patients who are moribund and/or not expected to survive for more than 72 hours.
11. Patients whose care may be compromised if given increased sedation and/or muscle relaxants for the purpose of assessing lung recruitment.
12. Lack of clinical equipoise by intensive care unit (ICU) medical staff managing the patient.

Termination criteria

1. Mean arterial pressure (MAP) less than 60 mmHg for more than 5 minutes.
2. Desaturation less than 88% for more than 5 minutes.
3. Lack of clinical equipoise by the clinician E.g. When a patient has a low blood pressure and thought to be intolerant of PEEP changes.

These criteria ensure a focus on the ARDS and respiratory failure patients most likely to benefit from patient-specific optimise MV therapy.

6.2.3 Data Acquisition

The CURE trial uses a software system (CURE Soft) developed using the JAVA platform (Szlavecz et al. 2014). CURE Soft applies the information of patient's measured airway pressure and flow data to estimate respiratory mechanics parameters using an extended single compartment model that captures time-varying respiratory elastance model. This estimated, patient-specific model-based data is used to provide information on patient lung condition, disease progression and response to MV treatment (Chiew et al. 2011).

6.2.4 Time Varying Elastance Model

To investigate on the variability of elastance in ARDS patients, the time-varying elastance model is applied, which has been described in detail in Chapter 4. It is repeated here for clarity as:

$$P_{aw}(t) = R_{rs} \times Q(t) + E_{drs} \times V(t) \qquad (6.1)$$

$$E_{drs}(t) = E_{cage} + E_{demand} + E_{lung} \quad (6.2)$$

6.2.5 Data Analysis

In this study, the area under the curve of E_{drs} (AUC E_{drs}) for every breathing cycle is estimated and analysed in each MV patient. A total of 97,944 breathing cycles in 3 ventilation days were studied in this data set. The variability of AUC E_{drs} for each patient was quantified. For each patient, the median and interquartile range (IQR) of AUC E_{drs} were calculated. The median and IQR captures the centre and width of variability for a given patient. Robust coefficient of variation (RCV = median absolute deviation/median) of AUC E_{drs} was also calculated. A lower RCV indicates lower variability where as higher RCV indicates higher variability (Wysocki et al. 2006).

In addition, the distribution and variability of AUC E_{drs} is also presented in cumulative distribution functions (CDF), which are useful as they show the entire distribution that is often summarised as median and IQR, providing further and complete insight into the distribution.

6.3 Results

6.3.1 Variability by ventilation days and PEEP

Tables 6.2 and 6.3 show the summary of patients' AUC E_{drs} distribution by ventilation day and by PEEP level. Due to the extensive number of data points per patient, only the first 3

days of the data were analysed for each patient. Figures 6.1 and 6.2 show the corresponding box-whiskers plot for each patient by day and by PEEP level.

Table 6.2: The IQR of AUC E_{drs} and RCV for all five patients by ventilation days.

Patient No.	No. of breaths analysed	AUC E_{drs} Median [IQR] ($cmH_2O.s/l$) and RCV			Total AUC E_{drs} Median [IQR] ($cmH_2O.s/l$) and RCV
		Day 1	Day 2	Day 3	
1	5417	27.45 [19.97-30.79] 0.23	7.41 [2.38-16.36] 1.04	20.80 [16.68-23.74] 0.20	18.25 [9.98-23.57] 0.44
2	5857	8.39 [3.49-15.69] 0.62	5.14 [4.23-6.33] 0.35	3.96 [3.49-4.55] 0.29	4.66 [3.71-6.81 0.26
3	6582	14.76 [14.02-15.48] 0.21	3.52 [2.74-13.43] 1.41	18.70 [16.83-19.76] 0.11	15.04 [11.17-17.88] 0.35
4	7310	17.94 [15.81-18.86] 0.14	17.46 [16.83-18.03] 0.05	20.42 [20.12-20.72] 0.02	18.40 [17.22-20.34] 0.10
5	7482	20.50 [18.06-22.36] 0.13	17.67 [16.16-19.68] 0.20	20.15 [19.66-20.79] 0.04	19.72 [17.45-21.15] 0.14

Table 6.3: IQR of AUC E_{drs} and RCV for all five patients for all PEEP levels.

Patient No.	PEEP Levels (cmH_2O) AUC E_{drs} Median [IQR] ($cmH_2O.s/l$) and RCV				
1	***PEEP 12*** 14.85 [10.25 - 16.83] 0.26	***PEEP 16*** 10.27 [3.47– 19.94] 0.85	***PEEP 19*** 28.89 [16.16-33.41] 0.32	***PEEP 21*** 28.63 [35.86-37.85] 0.15	***PEEP 23*** 41.43 [40.78-41.96] 0.06
2	***PEEP 11*** 11.97 [6.21-18.13] 0.43	***PEEP 13*** 15.84 [15.99-19.23] 0.10	***PEEP 15*** 4.35 [3.56-6.91] 0.76	***PEEP 19*** 21.34 [20.65-22.77] 0.44	***PEEP 21*** 23.67 [23.34-25.54] 0.06
3	***PEEP 10*** 3.55 [3.00-4.20] 0.42	***PEEP 12*** 2.77 [2.32-3.35] 0.49	***PEEP 15*** 14.34 [13.28-21.67] 0.50	***PEEP 17*** 15.93 [6.56-24.53] 0.57	***PEEP 19*** 8.30 [2.62-16.78] 1.02
4	***PEEP 19*** 21.53 [18.93 – 22.55] 0.13	***PEEP 21*** 17.74 [16.16-18.44] 0.10	***PEEP 23*** 18.25 [17.29-19.28] 0.09	***PEEP 26*** 17.60 [16.93-18.16] 0.04	***PEEP 31*** 23.30 [22.83-24.64] 0.05
5	***PEEP 13*** 17.73 [16.46-18.95] 0.14	***PEEP 15*** 17.35 [14.95-20.89] 0.22	***PEEP 17*** 20.17 [19.69-20.80] 0.04	***PEEP 21*** 22.23 [20.73-23.00] 0.08	***PEEP 22*** 20.46 [18.41-22.18] 0.12

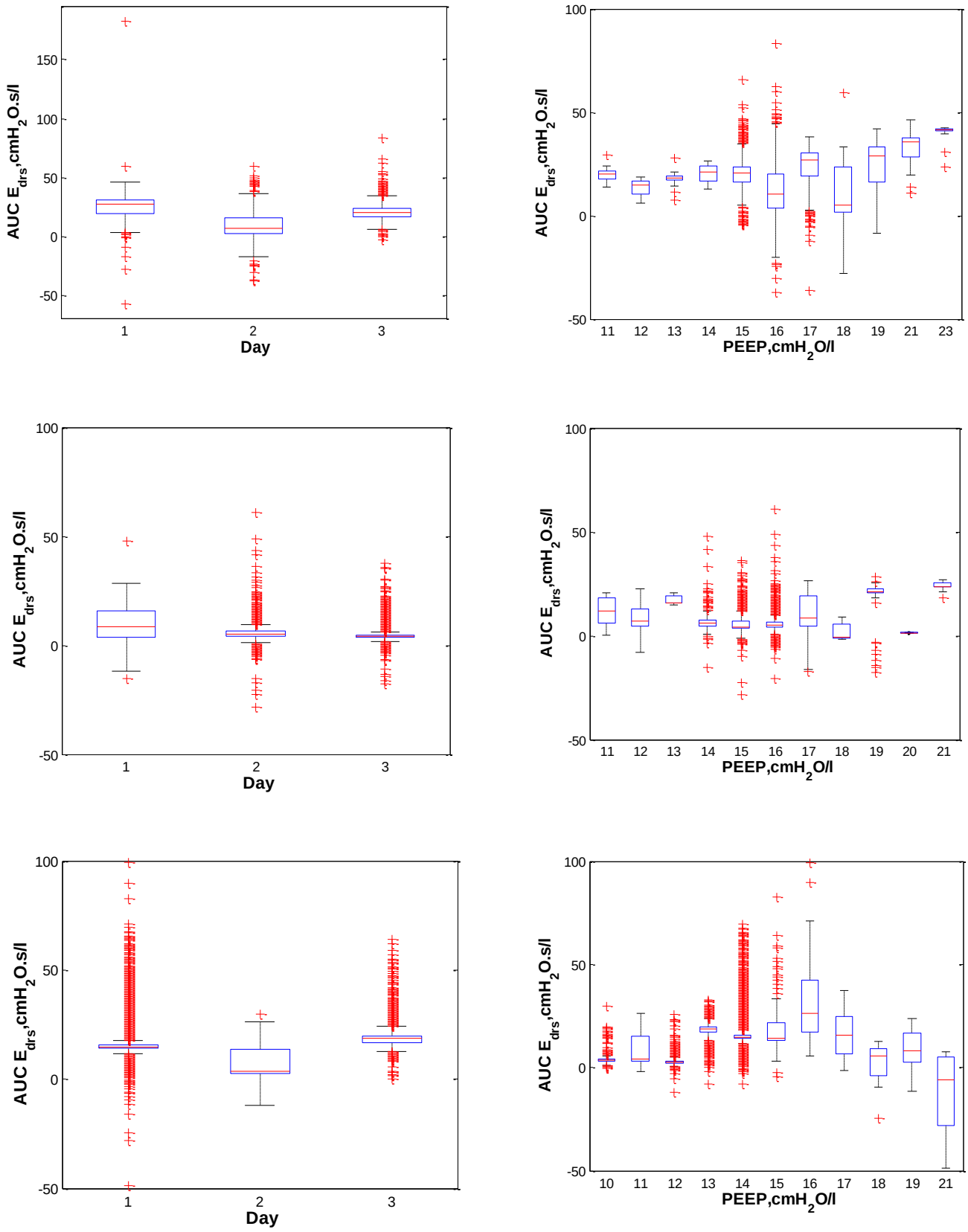

Figure 6.1: The distribution of AUC E_{drs} by ventilation days (*Left*) and by PEEP level (*Right*) for (*Top*) Patient 1. (*Middle*) Patient 2 (*Bottom*) Patient 3.

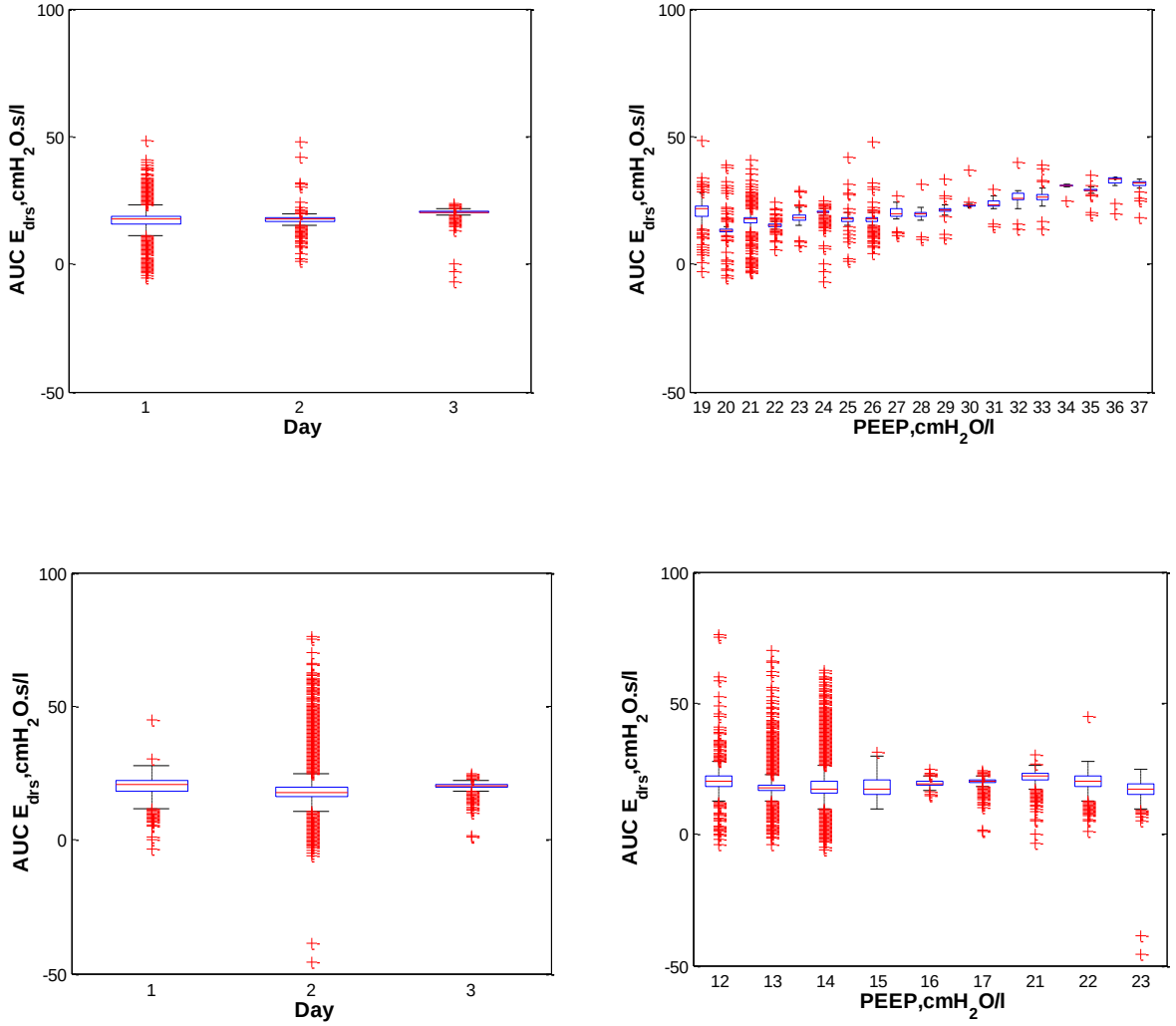

Figure 6.2: The distribution of AUC E_{drs} by ventilation days (*Left*) and by PEEP level (*Right*) for (*Top*) Patient 4 and (*Bottom*) Patient 5.

Figures 6.3 and 6.4 show the airway pressure and AUC E_{drs} for Patients 1 and 3, where asynchrony events occurred during MV that resulted in a sudden change of AUC E_{drs}. In contrast, Figure 6.5 depicts an airway pressure and AUC E_{drs} for Patient 2 that shows a smooth and transient AUC E_{drs} with no trace of asynchrony events, which were not evident for patient and time period.

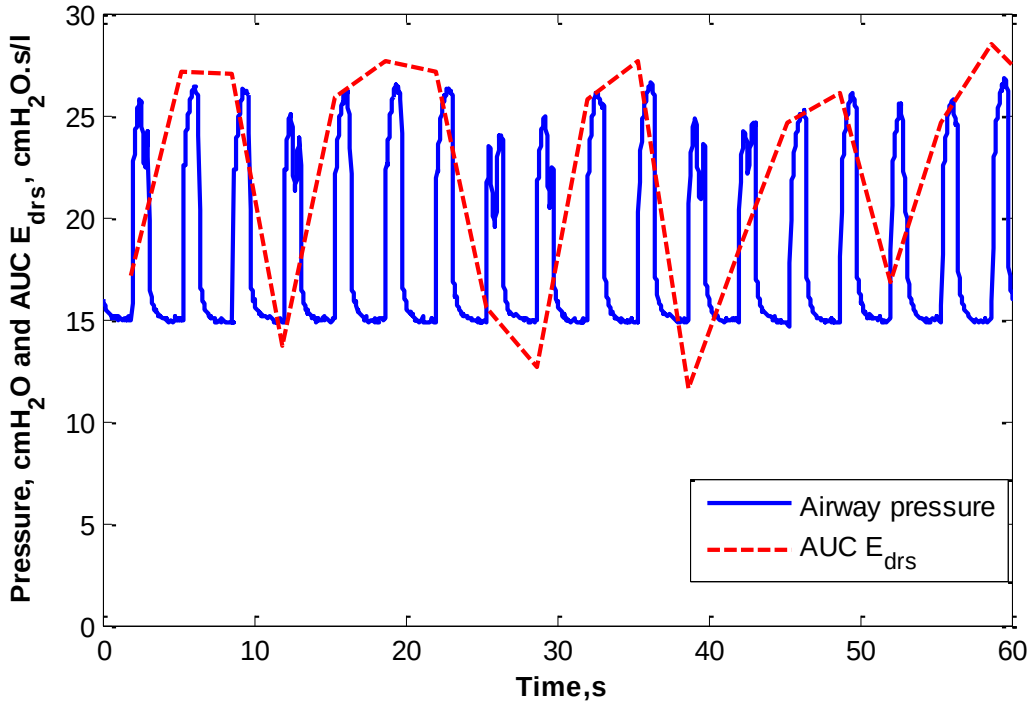

Figure 6.3: Airway pressure and AUC E_{drs} plots for Patient 1 containing asynchrony events which resulting with a sudden change of AUC E_{drs} indicating an asynchrony event has occurred

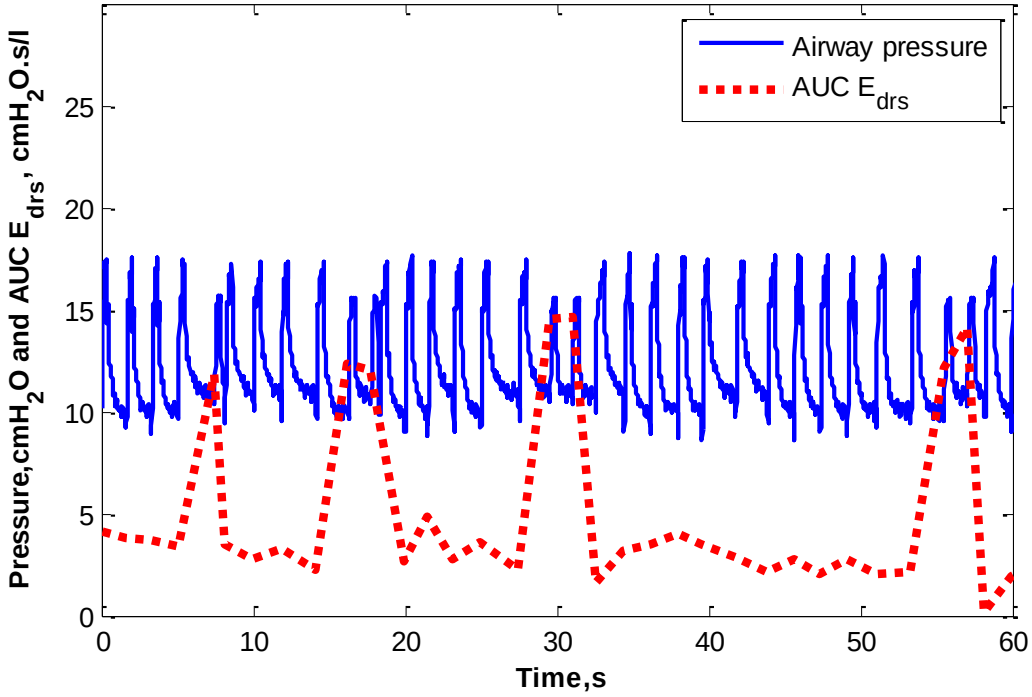

Figure 6.4: Airway pressure and AUC E_{drs} plots for Patient 3 containing asynchrony events which resulting with a sudden change of AUC E_{drs} indicating an asynchrony event has occurred.

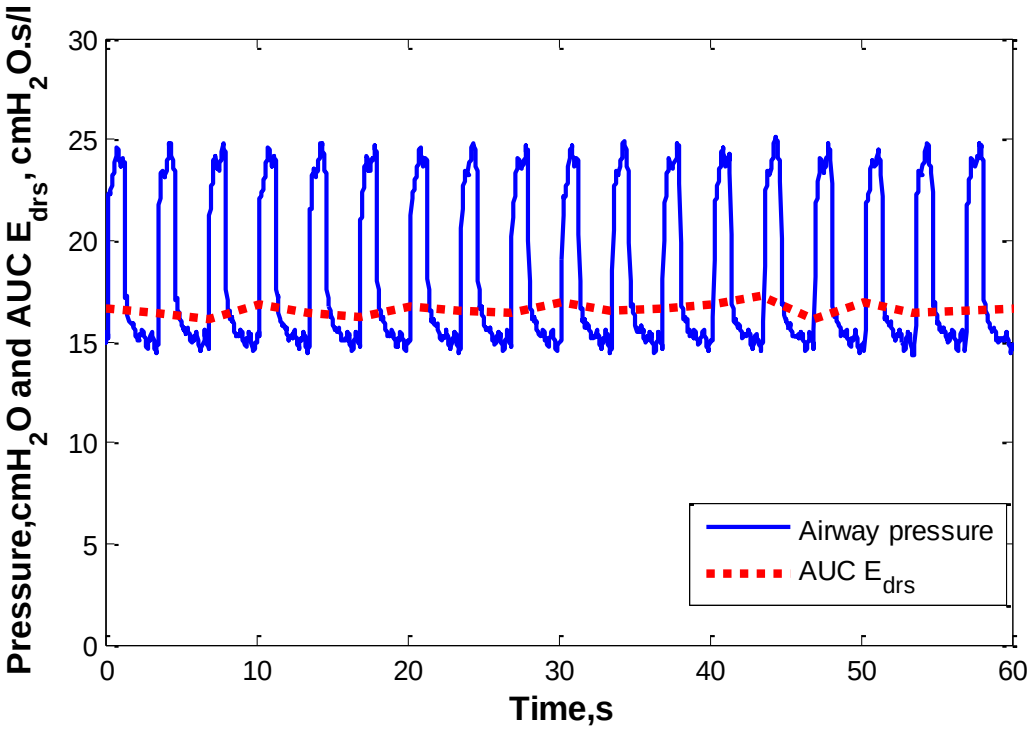

Figure 6.5: Airway pressure and AUC E_{drs} plots for Patient 2 which shows a constant airway pressure, resulting in a smooth and transient AUC E_{drs}.

6.3.3 Cumulative distribution functions (CDF) of AUC E_{drs} by patients

Figure 6.6 presents the cumulative distribution functions (CDF) of AUC E_{drs} across all PEEP levels for each patient. The CDFs of Patient 1 and 4 are shown in Figure 6.7, along with dashed lines indicating the 95% confidence intervals of AUC E_{drs} in each patient.

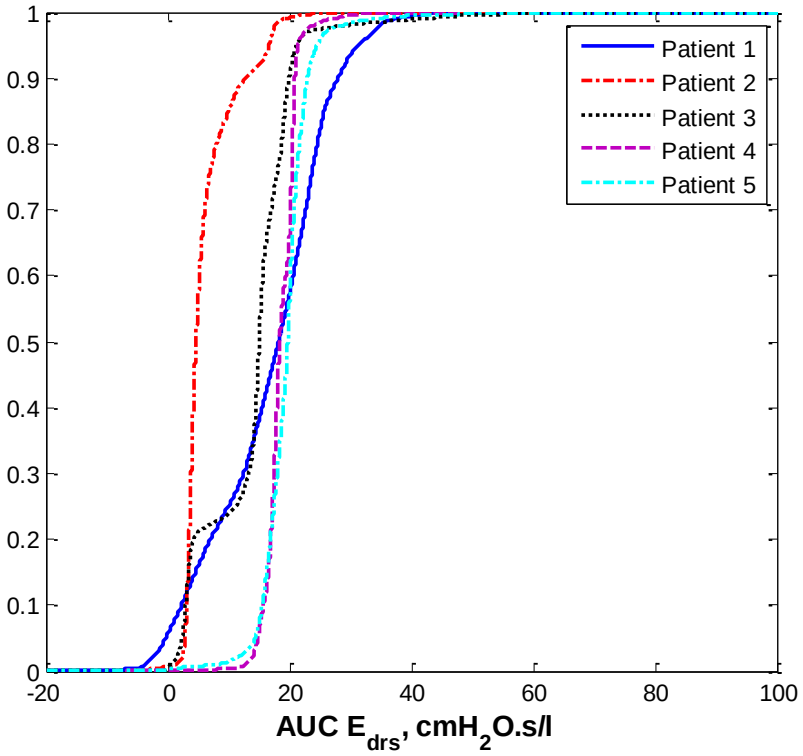

Figure 6.6: Cumulative distribution function (CDF) plot of AUC E_{drs} for all five patients at all PEEP levels.

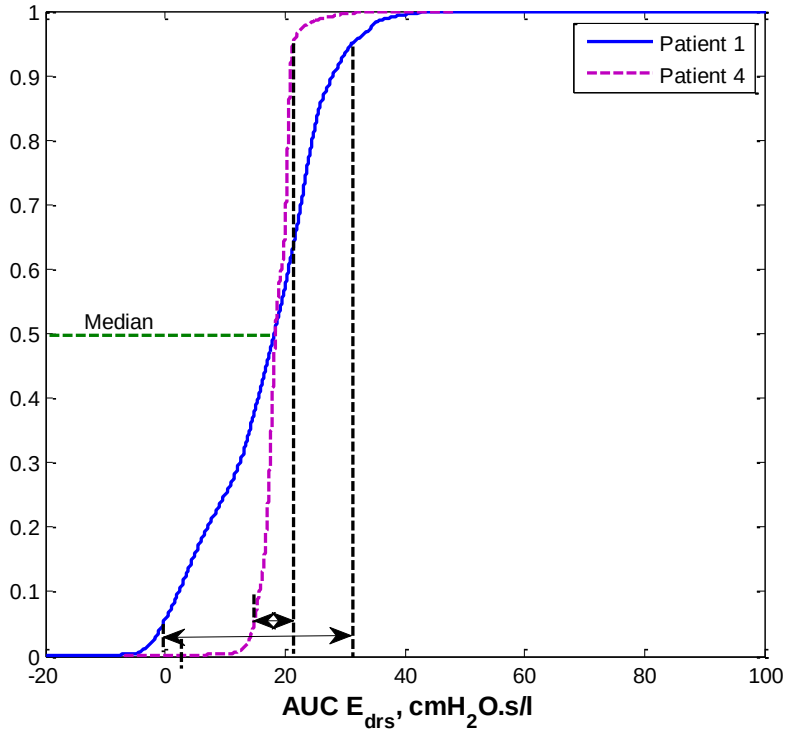

Figure 6.7: Cumulative distribution function (CDF) plot of AUC E_{drs} for Patient 1 and Patient 4 at all PEEP levels. The dashed line show the 95% confidence interval (5th and 95th percentile) of AUC E_{drs}.

6.3.4 Breath to breath variability

Breath to breath variability of AUC E_{drs} in Patients 1-3 are presented in a Poincare´ plot in Figures 6.8, 6.9 and 6.10, respectively. The Poincare´ plots show the distribution of AUC E_{drs} for all the three days. A linear line in each figure distinguishes the location of between AUC $E_{drs\ i}$ and AUC $E_{drs\ i+1}$ relative to a 1:1 line defining their equality with no breath-breath variability. The width around the 1:1 line indicates breath-breath variability.

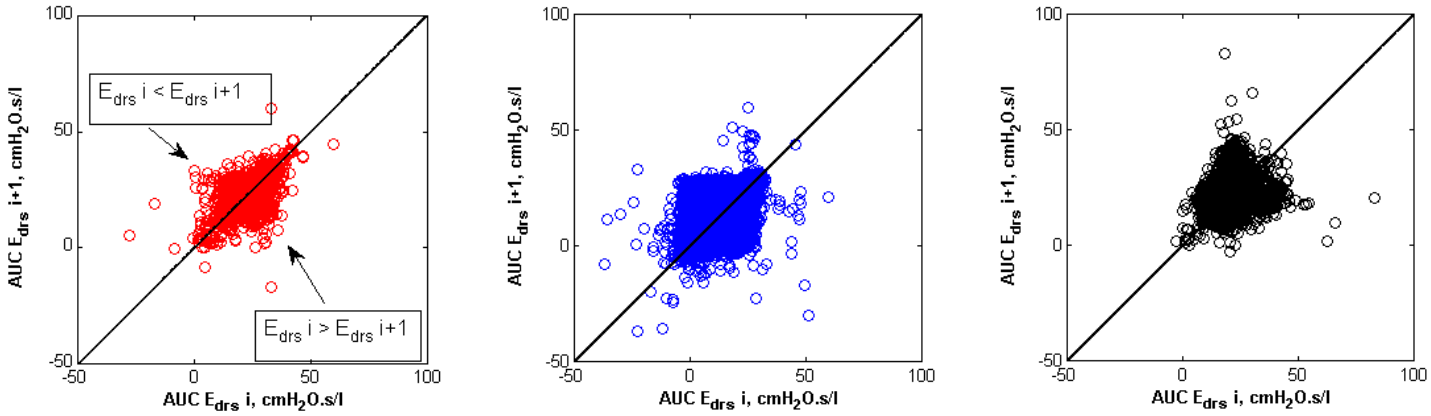

Figure 6.8 Poincare´ breath to breath plot of AUC E_{drs} for Patient 1 by (*Left*) Day 1 (*Middle*) Day 2 (*Right*) Day 3.

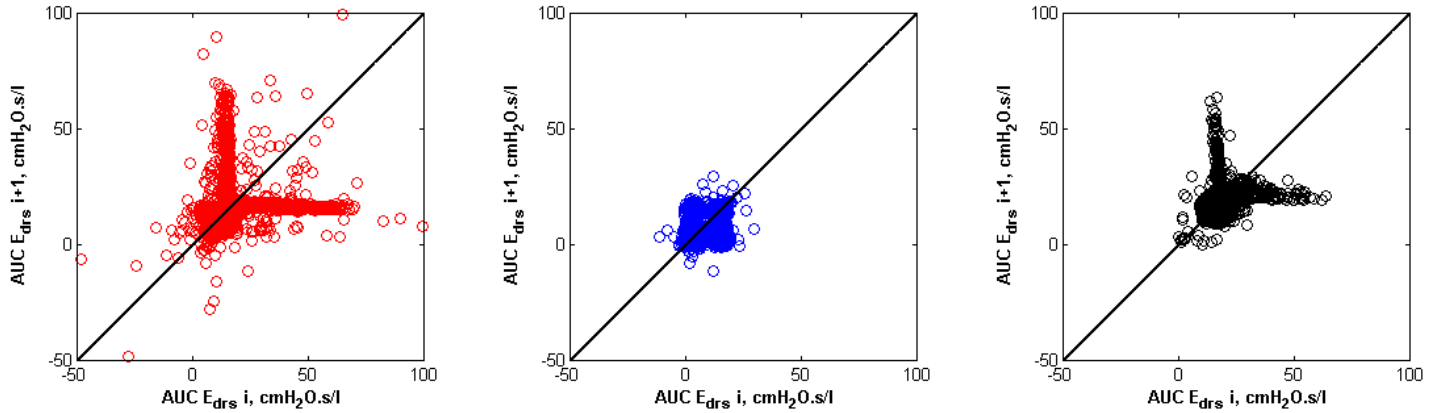

Figure 6.9: Poincare´ breath to breath plot of AUC E_{drs} for Patient 3 by (*Left*) Day 1 (*Middle*) Day 2 (*Right*) Day 3.

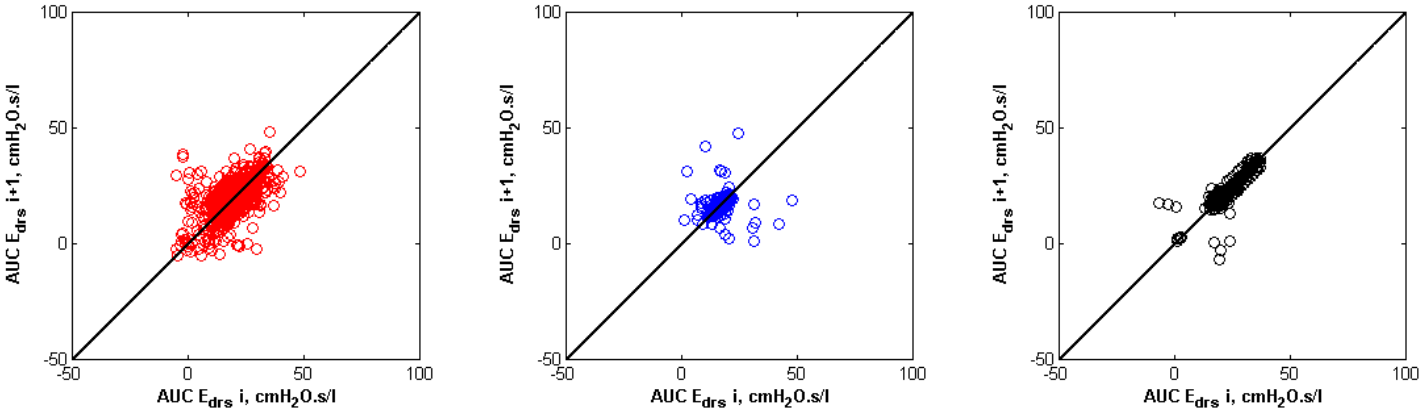

Figure 6.10: Poincare´ breath to breath plot of AUC E_{drs} for Patient 4 by (*Left*) Day 1 (*Middle*) Day 2 (*Right*) Day 3.

6.4 Discussions

6.4.1 Variability by ventilation days and PEEP levels

Tables 6.2 and 6.3 and the corresponding Figures 6.1 to 6.2 show the variability of AUC E_{drs} elastance with respect to mechanical ventilation days and PEEP. It can be clearly seen that the AUC E_{drs} varies at each day and PEEP level. Specifically, Patients 1 and 3 have higher RCV values of 1.04 and 1.41 on day 2 of ventilation, respectively. In contrast, Patient 4 has the least variability for all 3 days of ventilation with RCV ranges from 0.02 to 0.14.

Furthermore, the AUC E_{drs} varies at PEEP level for each patient. Specifically, for Patient 1, the highest variability of elastance was observed at PEEP = 16 cmH_2O with RCV value of 0.85. Patient 2 also has a highest variability of elastance of RCV = 0.76 at PEEP = 15 cmH_2O whereas Patient 3 has the highest RCV value of 1.02 at PEEP = 19 cmH_2O**.**

These variability changes were observed in ventilation days, as expected, due to recovery or worsening of the patient's condition, and would likely be observed over clinically relevant,

but shorter time frame. However, not all patients exhibit similar behaviour compared to fully controlled ventilation modes with little patient-induced spontaneous breathing effort. Equally, the per-patient variability was equally wide in Figure 6.6-6.7

6.4.2 Variability by patients

Patients included in this study are all ventilated using SIMV volume control mode. During controlled ventilation, these patients exhibits variability in lung elastance, as shown in Figures 6.1 and 6.2. For example, Patients 1 and 3 have significantly higher variability due to the asynchronies that existed during synchronized intermittent mandatory ventilation (SIMV) mode, as shown in Figure 6.3 and 6.4, respectively. Asynchrony happens when the patient's breathing effort is not synchronised with mechanical ventilation's breathing support. However, it happens more frequently during non-invasive ventilation or partially assisted modes, where the patient is breathing spontaneously and the ventilator support is triggered by patient respiratory effort (Epstein 2011; Tobin et al. 2001; Vignaux et al. 2009). Hence, the choice of SIMV ventilated patients in this specific study.

Asynchrony events can be regards as a significant mismatch between airway pressure and flow. Thus, this mismatch also affects the estimation of respiratory system mechanics, where the respiratory elastance can be under or overestimated compared to synchronised breathing cycles. In some cases, the estimated elastance can overshoot to a very high value as compared to normal airway pressure (Poole et al. 2014), as depicted in Figure 6.4 in Patient 3. This overshoot can be seen as the model capturing the external force generated from patient-specific and breath-specific spontaneous breathing efforts. Similarly, Patient 1 exhibits a SB effort although the patient was in fully sedated condition. This resulting with a constantly

asynchrony airway pressure as shown in Figure 6.3, that reduced the value of the elastance, limiting the calculation of accurate values of the lung elastance.

Occasional AUC E_{drs} spikes that were observed in Patients 1 and 3 in Figures 6.3 and 6.4 indicate that asynchronous events occur at any time throughout the ventilation period. This asynchrony events resulting with a variability in the respiratory elastance. Due to the asynchrony, the range of variability in AUC E_{drs} measurement in Patient 1 and 3 is higher with the RCV of 0.44 and 0.35, respectively. Thus, these results show that there is spontaneous variability and underlying variability. Due to the breath to breath variability in SB efforts, there is large variability due to the resulting negative component of the respiratory elastance in Equation 6.2 (Chiew et al. 2015). This negative component of elastance will be further discussed in Chapter 7.

In contrast, a smooth and transient AUC E_{drs} is observed in Patient 2 (Figure 6.5). Specifically, there is no pressure mismatch and thus no asynchrony events. Thus, these results clearly validate the idea that asynchrony events play a significant role in the observed, model-based variability in breath-specific elastance in each patient.

6.4.3 Distribution and variability of median AUC E_{drs} all patients at all PEEP

From the CDF of all patients in Figure 6.6, it can be concluded the variability of AUC E_{drs} increases per patient. It can also be seen that Patient 1 is significantly different in median from all other patients ($p<0.005$) and significantly different in variability compared to all patients ($p< 0.005$). Examining the median and IQR of Patient 1, it shows that Patient 1 has higher ranger of AUC E_{drs} with 18.25 [9.98 - 23.57] $cmH_2O.s/l$ across all PEEP levels. For

example, the 95% confidence interval (5^{th} and 95^{th} percentile) value is significantly larger in Patient 1 than Patient 4 ($p < 0.005$) as in Figure 6.7, although both patients have almost similar median value of 18.25 $cmH_2O.s/l$ and 18.40 $cmH_2O.s/l$ respectively. In contrast, Patient 4 has a comparatively smaller range in the 5^{th} to 95^{th} range of AUC E_{drs}. This result is as expected, as Patient 1 exhibits a significant asynchrony compared to Patient 4. These results show that the central tendency of AUC E_{drs} is the same, but that the shape of the distribution can vary differently, patient-to-patient, clearly capturing patient-specific differences in condition and response to MV.

6.4.4 Breath to breath variability

Furthermore, Figures 6.8-6.10 show a Poincare´ plot for breath to breath analysis in Patients 1, 3, and 4 for the 3 ventilation days. The patients are chosen based on the RCV value with Patients 1 and 3 having a higher variability, whereas, in contrast, Patient 4 has a much lower variability. In the Poincare´ plot, the first AUC E_{drs} (AUC $E_{drs\,i}$) for the first breath (Poincare´ plot) is represented on the x-axis, and the AUC E_{drs} of the following breath (AUC $E_{drs\,i+1}$) is plotted on the y-axis. The Poincare´ plot also demonstrates that if the AUC $E_{drs\,i+1}$ is less than AUC $E_{drs\,i}$, this then indicates that the elastance is decreasing for the next breath. A consistent decreasing trend would indicate improving patient condition, shown in such figures as a bias around the 1:1 line.

It can be seen from Figure 6.10 that the variation or Poincare´ plots for Patient 4 for all 3 days is almost a straight line, especially on Day 3 with RCV = 0.02. Although a few points exist outside the linear line, the majority of the points are within a 90% range that has much less

variability in elastance for Patient 4, which agrees with a small RCV value of 0.10, and indicates the clear per-patient differences that may be seen.

In contrasts, the Poincare´ plots for Patient 3 in Figure 6.9 demonstrate that the distribution of data are scattered away from the linear line. This elucidates the breath to breath variability of elastance in Patient 3 is higher with a RCV value of 0.35. Similarly, the same results apply to Patient 1, with breath to breath variability of data points are scattered away from the liner line. The much higher variability in AUC E_{drs} in Patients 1 and 3 is expected, due to the much more frequent, stronger and more variable SB effort produced by both patients. This outcome can be seen from Figures 6.8 and 6.9, where there exists data points of AUC E_{drs} in the negative regions, which further validates the idea the negative values of elastance that decrease the overall values of E_{drs} and, in this case, results in negative values of $E_{drs}(t)$ and far greater variability in overall respiratory elastance. The investigation of the negative elastance SB effort will be discussed in detail in Chapter 7.

Specifically, for Patient 1, on day 2, some of the AUC E_{drs} data points lie above the linear line as shown in Figure 6.8. This implies that AUC $E_{drs\ i}$ is greater than AUC $E_{drs\ i+1}$ which elucidates that the lung condition is getting worse for every consequence breaths. However, on day 3, some of the AUC E_{drs} points lie under the linear line which show that the AUC $E_{drs\ i}$ is lesser than AUC $E_{drs\ i+1}$. Thus, this result indicates that the lung condition of Patient 1 has improved.

6.5 Summary

In this chapter, this research quantified the variability identified and estimated respiratory mechanics properties used to potentially guide ventilation care in sedated patients. With this information, it could guide ventilation in PEEP titration to the optimal elastance which could protect the lung from over-distension condition. Clinically, results on the variability of elastance have shown significant implications for managing PEEP titration for MV patients. However, due to patient-specific breathing effort, it produced a negative elastance, resulting with a variability in elastance. The asynchrony is also known as another factor that contributes to the variability in elastance. Thus, Chapter 8 will then introduce a model-based that could re-construct the pressure that has been reduced due to the asynchrony problem, and improving the estimation of the accurate value of the lung elastance.

CHAPTER 7

Lung Elastance Monitoring for Spontaneously Breathing Patient

7.1 Introduction

Most of the lung models that have been developed are only effective for fully sedated patients (Brochard et al. 2012; Hickling 1998a; Sundaresan et al. 2009). They cannot be applied directly to the spontaneously breathing (SB) patients due to the different lung mechanisms between fully sedated and SB patient. In particular, they add input energy in the form of negative pressure due to their muscles opening the chest cavity and allowing air to enter. This SB input cannot be accurately modelled at this time and cannot be predicted accurately. However, because there are a significant number of patients on mechanical ventilation (MV) who have some level of SB effort, it will be valuable to develop and integrate a metric that allows analysis of the true respiratory mechanics in SB patients (Kallet & Branson 2007).

SB patients have individual breathing efforts aside from the ventilator support (Grinnan & Truwit 2005). These efforts modify the measurable airway pressure and/or flow waveforms, which can significantly alter the identified lung mechanics. The main obstacle is to be able to find a metric that able to detect the presence of the SB effort and to then identify or estimate the level of SB effort exerted by the patient. A suitable method might thus quantify the effort from sudden or unnatural changes in the pressure or flow waveforms, or may require direct measurement of the SB patient's muscular movement, as seen in invasive measurements in the NAVA system (Chiew et al. 2013).

There are some techniques that have been applied to directly measure or attempt to monitor the breathing effort made by SB patients. One of the most well-known methods is the balloon-catheter technique used to measure the oesophageal pressure, which is the surrogate of the pleural pressure (P_{pl}) (Khirani et al. 2010; Talmor et al. 2008). However, this technique is not suitable for clinical practise as it requires the balloon to be inserted into the patient and used to interrupt breathing. It is thus a very intrusive measurement and not feasible for regular clinical use despite its potential to accurately measure SB effort and thus potentially optimise and guide MV for SB patients with ARDS (Guérin & Richard 2012).

Another approach to measure the SB effort is by monitoring the electrical activity of the diaphragm (E_{adi}) of the ventilated patient. This measurement captures muscle activity as a surrogate for this SB input. It can thus provide a better monitoring of patient-ventilator synchrony in SB patients (Moorhead et al. 2013; Piquilloud et al. 2011). However, there is a potential of tidal volume leak in this, also invasive, measurement that can affect the measurement of the SB effort (Moorhead et al. 2013). In addition, this measurement requires an additional expensive sensor that must be very accurately positioned.

In Chapter 6, it was mentioned that one of the reasons of the variability is due to the negative elastance effectively caused by un-modelled the SB effort. This negative elastance is hypothesised to be due to a positive lung volume intake through the SB effort induced negative pressure in the lung compartment (Chiew et al. 2015). Thus, in this chapter, a non-invasive model-based method, based on time varying respiratory system elastance, is implemented to review the distribution of negative elastance in SB patients to quantify its potential level and impact.

7.2 Methodology

7.2.1 Patient Data

In this study, this model is assessed using clinical data from Clinical Utilisation of Respiratory Elastance (CURE) study patients. The associated protocols have been described in detail in Chapter 6, along with demographics and ethics approval details, so they are not covered here.

7.2.2 Spontaneously Breathing Respiratory Model

The model is based on the time varying elastance model described in details in Chapter 4, and repeated here for clarity as:

$$P_{aw}(t) = R_{rs} \times Q(t) + E_{drs} \times V(t) \quad (7.1)$$

$$E_{drs}(t) = E_{cage} + E_{demand} + E_{lung} \quad (7.2)$$

During inspiration, Q is positive leading to an increasing integrated volume (V). In SB patients, E_{demand} represents the change in elastance due to patient-specific SB effort. Thus, this elastance, E_{demand}, has a negative value due to the diaphragm contracting and the intercostal muscles that move the rib cage upwards, which both increase the volume of the chest compartment. This increase, creates a negative pressure gradient that draws air into the lungs and is the sole mechanics of breathing in healthy individuals. As patient demand aids the breathing effort, the effective overall pressure based on Equation 7.1, is therefore reduced, leading to a reduced identified value of elastance.

7.3 Data analysis

In this study, the area under the curve (AUC) for the time-varying elastance, E_{drs}, is estimated for each SB patient. The results are reported as median and interquartile range (IQR) for continuous data with CURE collecting a total of 82 hours.

7.4 Results

Figures 7.1-7.3 present the distribution of positive and negative AUC E_{drs} for all 5 patients. For the same patients, the 5th, 25th, 59th, 75th, and 95th percentiles of the negative and positive AUC E_{drs} data are also tabulated in Table 7.1. Separating the positive and negative values into two plots allows easier quantification at these elastance values. A negative AUC indicates the entire elastance E_{drs} profile was less than 0. This behaviour occurs when as seen in Figure 7.4. The vast majority have AUC $E_{drs} > 0$ as expected.

Table 7.1: Negative and positive AUC E_{drs} (5th, 25th, 59th, 75th, 95th percentile) for all 5 patients.

Patient	**Negative AUC E_{drs}**					**Positive AUC E_{drs}**				
	5th	**25th**	**50th**	**75th**	**95th**	**5th**	**25th**	**50th**	**75th**	**95th**
1	-7.76	-3.03	-1.65	-0.70	-0.18	2.51	12.15	18.94	23.85	31.63
2	-16.81	-3.89	-2.08	-0.92	-0.23	2.91	3.73	4.67	6.85	16.70
3	-11.52	-1.76	-0.66	-0.19	-0.03	2.40	10.85	14.99	17.90	21.15
4	-6.08	-3.22	-2.27	-0.69	-0.16	14.87	17.20	18.36	20.34	21.43
5	-6.02	-2.27	-0.98	-0.47	-0.19	14.50	17.47	19.73	21.16	24.57

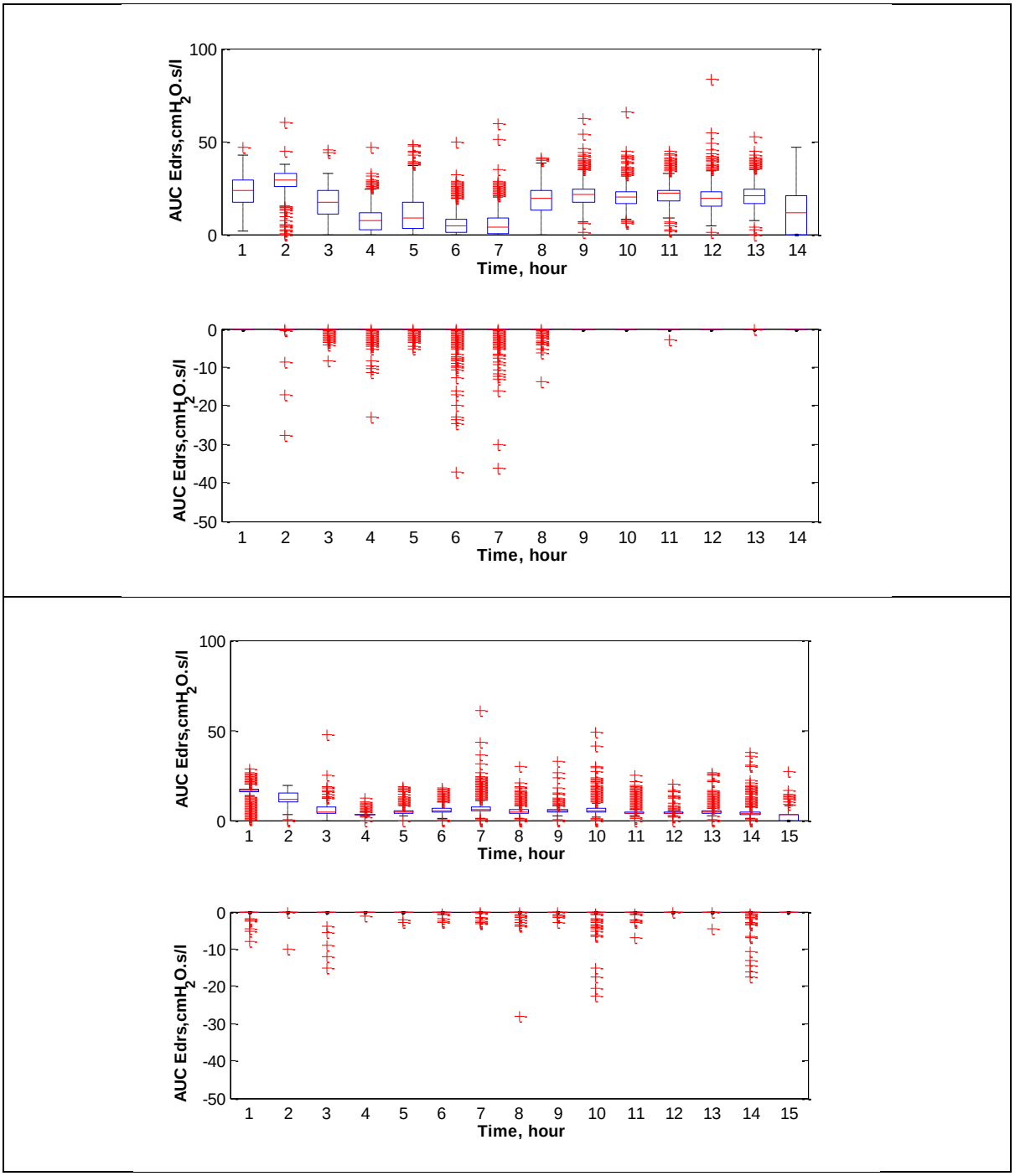

Figure 7.1: The distribution of positive (upper) and negative (lower) values of AUC E_{drs} by hour for (*Top*) Patient 1 and (*Bottom*) Patient 2. The positive and negative values are combined for the entire distribution.

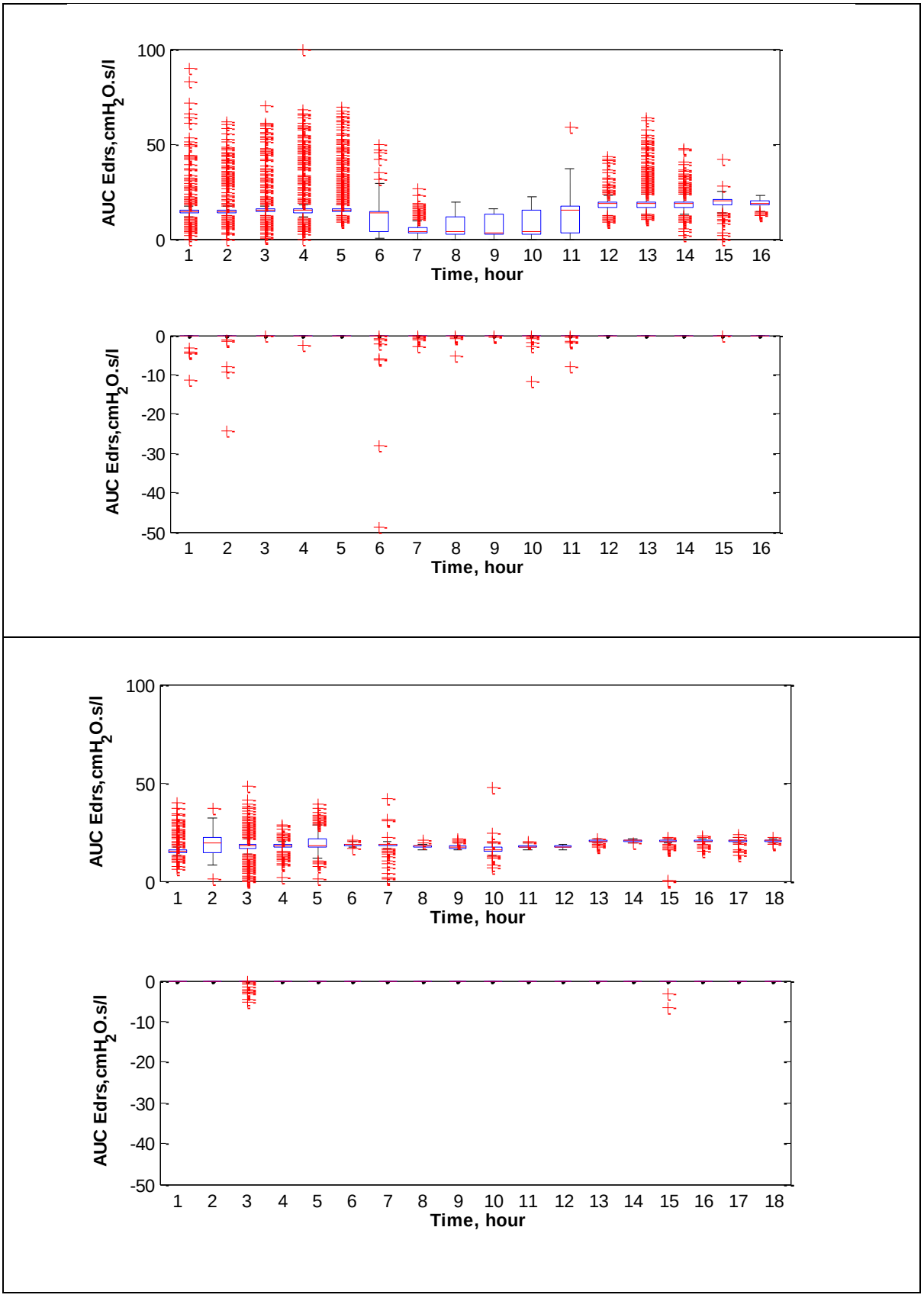

Figure 7.2: The distribution of positive (upper) and negative (lower) values of AUC E_{drs} by hour for (*Top*) Patient 3 and (*Bottom*) Patient 4. The positive and negative values are combined for the entire distribution.

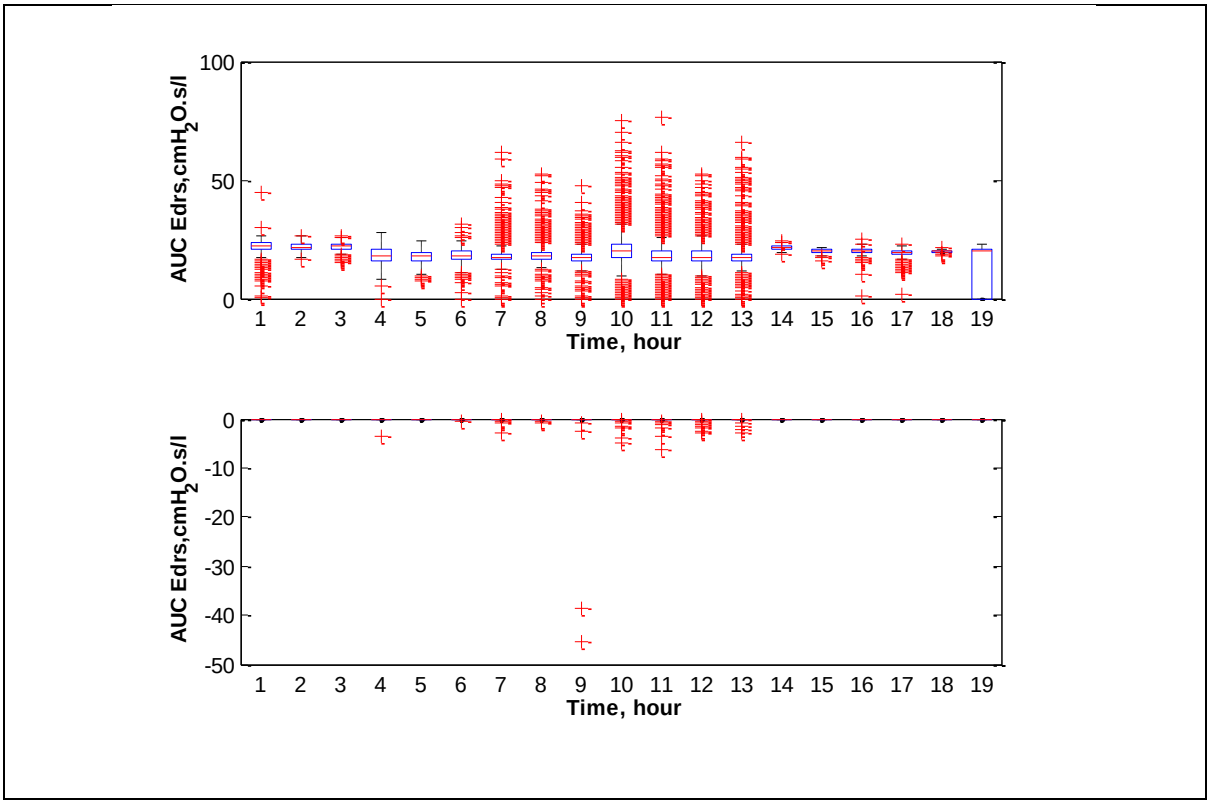

Figure 7.3: The distribution of positive (*upper*) and negative (*lower*) values of AUC E_{drs} by hour for Patient 5. The positive and negative values are combined for the entire distribution.

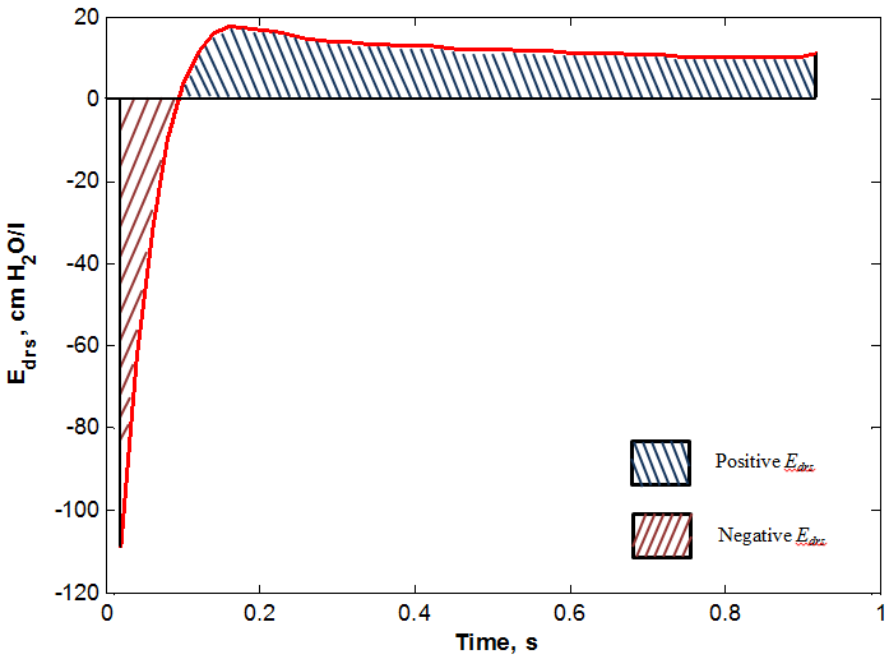

Figure 7.4: The E_{drs} for a single breath for Patient 3 that shows the negative and positive values of E_{drs}.

7.5 Discussion

In this study, it was observed that all 5 patients had some negative AUC E_{drs}, as shown in Figures 7.1-7.3. Negative elastance occurs when negative pressure is generated in the patient's pleural space causing air volume to enter the lung. As pleural pressure decreases due to patient's inspiratory demand, the airway pressure or flow changes. More specifically, E_{drs} will be less than zero when patient breathing demand is high at the beginning of inspiration, and will gradually decrease in magnitude as patient demand decreases during the breath. A negative AUC of E_{drs} occurs when this negative area outweighs the positive area when $E_{drs} < 0$, as seen in Figure 7.4.

Table 7.1 shows the negative and positive data of the AUC E_{drs}. It can be seen that that the 95^{th} percentile of the positive AUC E_{drs} was above 25 $cmH_2O.s/l$ for Patient 1, although this patient exhibits a negative elastance due to SB efforts. ARDS patients have been shown to have higher respiratory elastance with $E_{drs} > 25$ cmH_2O/l (The ARDS Definition Task Force 2012). These results show that, the proposed AUC E_{drs} metric is able to capture mechanics similar to those observed in ARDS patients when fully sedated in MV, giving confidence of the clinical relevance of the AUC E_{drs} value used here. For the other patients, the 95^{th} percentile of AUC E_{drs} were below than 25 cmH_2O/l, which suggests that the patients in this SB study were more compliant than that of fully sedated ARDS patients lungs, as might be expected for SB patients with less intrusive ventilation (Chiew et al. 2014).

The AUC E_{drs} for SB patient is dependent on the initial pleural pressure or the magnitude of negative $E_{demand.}$ Thus, a lower AUC E_{drs} may indicate that a patient has comparatively higher individual breathing effort than others, and obviously more than a sedated patient. Thus, the

AUC E_{drs} metric is able to uniquely capture the information of SB patients without the use of invasive protocols.

Specifically, for Patient 4, the negative AUC E_{drs} occurred only at 3 and 15 hours. The existence of the negative elastance might be due to the ventilator setting of the patient during this time when the ventilation mode was switched to an assisted spontaneous breathing (ASB) mode. As expected, Patients 1 and 3 have the largest distribution of negative AUC E_{drs} values due to the larger number of asynchrony events they experienced, which were discussed previously in Chapter 6.

This model can thus be generalised over the SB and sedated MV patients based on the E_{drs} value, where negative E_{drs} relates to SB effort and reduced AUC E_{drs} can also indicate SB efforts. Thus, the E_{drs} value and trajectory can be used as a simple, real-time indicator to assess patient-specific disease state and response to MV specifically for SB patients monitoring.

7.6 Summary

This proposed spontaneous breathing model monitoring is able to capture unique dynamic respiratory mechanics specifically for spontaneously breathing patient without additional measuring equipment or interruption of care. Thus, with this metric, it is able to guide clinicians in setting the optimal mode of the ventilation that meet the patient's demand.

CHAPTER 8

Processing of Pressure Waves for Respiratory Mechanics Estimation by Spontaneously Breathing Efforts

8.1 Introduction

Estimation of respiratory mechanics can enable individualised mechanical ventilation (MV) therapy (Lauzon & Bates 1991; Lucangelo et al. 2007). However, most of the mathematical lung models developed are only suitable for fully sedated patients (Brochard et al. 2012; Sundaresan et al. 2011a; Talmor et al. 2008; Talmor et al. 2006). Others are also too complex for use as a bedside application (Donovan 2011; Kitaoka et al. 2007; Tawhai & Bates 2011; Tawhai et al. 2004).

Current bedside respiratory models are limited and cannot be applied directly to spontaneously breathing (SB) patients. These patients exhibit modified airway pressure and flow profiles due to their own variable inspiratory effort (Grinnan & Truwit 2005). These modified airway pressure and flow are variable and heterogeneous in level and appearance, rendering the underlying pulmonary mechanics of SB patients difficult to identify correctly from measured airway pressure and flow data alone. However, due to the significant number of patients on MV who demonstrate intermittent SB effort, as seen in Chapter 6 and 7, it is essential to have a mathematical model that can be applied to analyse respiratory system mechanics in SB patients.

In particular, this specific problem arises when a patient exhibits SB effort on top of a ventilator supported breathing cycle. This phenomenon is known as reverse triggering (Akoumianaki et al. 2013), which results in a consistent occurrence of 'entrainment' in observed airway pressure waveforms. This 'entrainment' can be denoted as an M-wave due to its shape, as shown in Figure 8.1. This M-wave pressure curve creates a significant problem in identifying accurate values for respiratory system elastance and airway resistance (Chiew et al. 2011). Hence, it is important to have a method to overcome the impact of these M-waves and provide a more consistent estimation of the underlying and SB unaffected respiratory system mechanics for clinical monitoring.

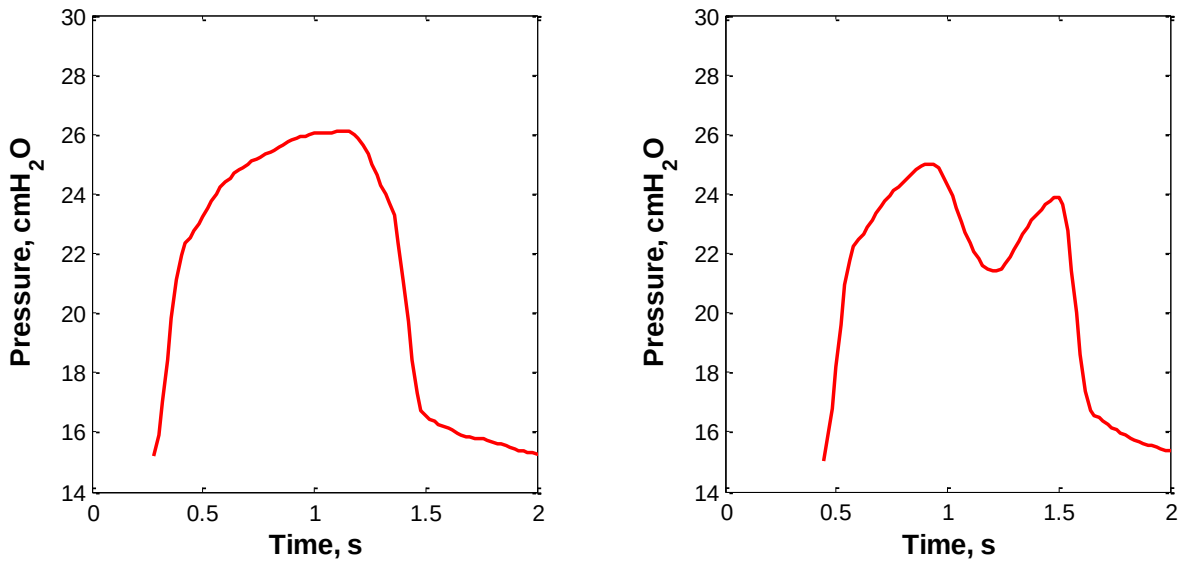

Figure 8.1: *Left*: Normal airway pressure *Right*: M-wave airway pressure.

During volume controlled ventilation, if the patient breaths on top of a ventilation support, the patient's breath-specific inspiratory effort induces a reduction in airway pressure that the model sees as reduced respiratory elastance due to the same volume being delivered for less pressure (Alencar et al. 2002; Chiew et al. 2015). This M-wave pressure curve creates a significant problem in identifying accurate values for the true, underlying respiratory system

elastance and airway resistance as this input is not known or modelled (Schranz et al. 2012b). Hence, it is important to have a method to overcome the impact of these M-waves and provide a more consistent estimation of the underlying respiratory system mechanics for clinical monitoring especially for SB patients.

In addition to reducing the impact of M-waves, it is essential to have a metric that detects the presence of these M-waves and quantifies how much breathing effort is exerted by the patient during reverse triggering. Currently, there are no metrics that quantify SB effort during MV without using highly invasive oesophageal pressure catheters (Benditt 2005; Khirani et al. 2010; Talmor et al. 2006).

Clinically, these SB efforts need to be assessed to determine if the MV mode needs to be adjusted or adapted to patient breathing effort for better patient-ventilator interaction (Piquilloud et al. 2011). Thus, a metric that can act as a surrogate of SB effort and its contribution in altering the airway pressure waveform is required, clinically, as well as for model-based methods. An automated, model-based approach would also offer first ever quantification of the incidence and severity of SB efforts and asynchrony.

In this chapter, a model-based method is used to reconstruct the M-wave affected airway pressure curve. This method hypothesizes that the true, underlying respiratory mechanics do not change significantly breath to breath at a given pressure level, as is already evident in sedated patients without SB efforts. This method aims to provide a more consistent respiratory mechanics monitoring through reconstruction of the ‘actual’ airway pressure. Using the reconstructed pressure and the M-wave affect pressure, metric to identify breath

and patient-specific effort is developed. This information is capable of providing new clinical insight to patient condition and response to treatment.

8.2 Methodology

8.2.1 Clinical data

Data recorded from a clinical trial carried out in the intensive care unit (ICU) of Christchurch, New Zealand were used in this study, with the data acquisition process detailed in Chapter 6 (Szlavecz et al. 2014).

Table 8.1: Characteristics of the patients.

Patient No.	Gender	Age	Clinical Diagnostic
1	Female	53	Faecal peritonitis
2	Male	71	Cardiac surgery and contracted hospital acquired pneumonia
3	Male	60	Pneumonia
4	Male	36	Pneumonia
5	Male	61	Pneumonia

8.2.2 Time Varying Respiratory Elastance Model

Model-based time-varying elastance is identified breath-to-breath using a single compartment lung model which has been described in detail in Chapter 4 in Equations 4.1 and 4.2 (Chiew et al. 2015; Lauzon & Bates 1991). These two equations are

$$P_{aw}(t) = R_{rs}Q(t) + E_{rs}(t)V(t) + P_0 \quad (8.1)$$

$$\int P_{aw}(t)dt = R_{rs}\int Q(t)dt + E_{rs}(t)\int V(t)\,dt + \int P_0\,dt \quad (8.2)$$

Then, an average lung resistance (R_{ave}) is calculated based on the value of R_{rs} for every PEEP level and it is substituted into Equation 7.3 where the dynamic elastance, E_{drs} is defined as a time-varying lung elastance and identified using (van Drunen et al. 2014):

$$E_{drs}(t) = \frac{P_{aw}(t) - P_0 - (R_{ave}Q(t))}{V(t)} \quad (8.3)$$

For each breathing cycle, the area under the curve of E_{drs} (AUC E_{drs}) is then calculated as a surrogate of respiratory elastance (Chiew et al. 2015).

8.2.3 Pressure Reconstruction Method

Patients with the ability to breathe spontaneously, even if sedated, create abnormal airway pressure waveforms shaped like an "M" (Akoumianaki et al. 2013), as shown in Figure 8.2. The lower pressures and M-wave curves result in a significantly lower identified elastance since pressure is reduced by patient-specific induced inspiratory effort for the same volume delivered. In Figure 8.2, the respiratory system elastance and airway resistance for the normal airway pressure (left) are 25.85 cmH_2O/l and 10.22 $cmH_2O{\cdot}s/l$, respectively. In contrast, direct application of Equation 8.1 using the M-wave airway pressure results in an elastance of 13.70 cmH_2O/l and a resistance of 12.91 $cmH_2O.s/l$. Thus, to provide a more consistent clinically useful result, to identify the true, underlying mechanics, unaffected by patient-specific inspiratory effort, a simple pressure wave reconstruction method to remove or reduce the impact of SB efforts or measured airway pressure waveforms is necessary.

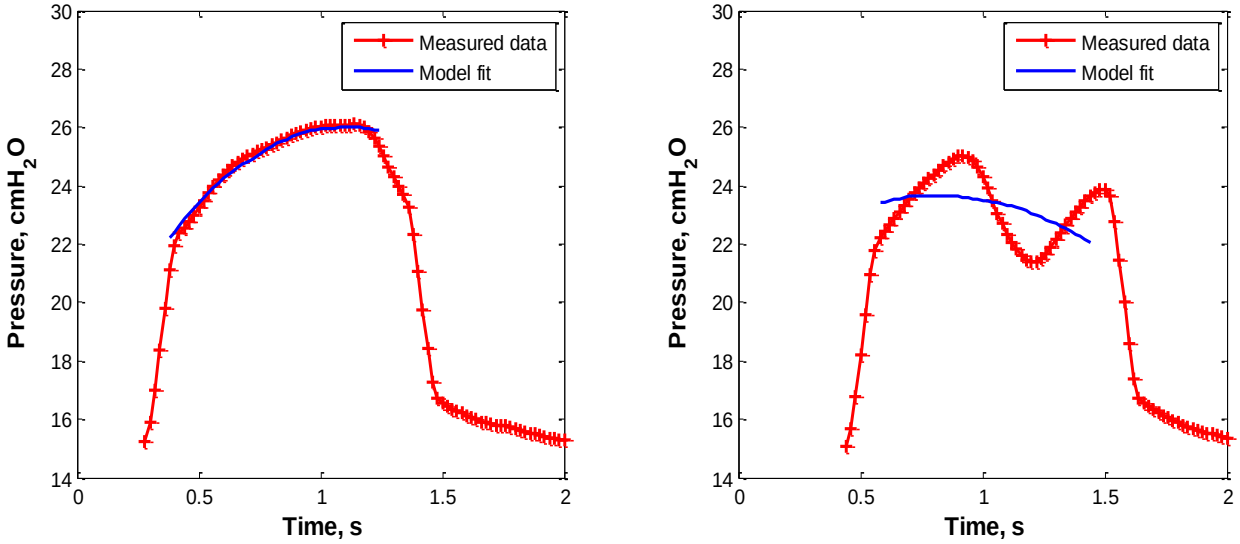

Figure 8.2: *Left*: Normal airway pressure provides well-fit model. *Right*: M-wave causing poor model fit.

The proposed pressure reconstruction method identifies and compares both the maximum peaks of the inspiration pressure waveform (Figure 8.3). Point b_1 is defined as five data points after the end of inspiration, while a_1 is defined as five data points after point b_1. These two points will be used as a reference point to determine the gradient of the airway pressure during expiration (Figure 8.3b). A line that connects a_1 and point b_1 is extrapolated to point c_1, which has the same pressure value as the maximum pressure for the breath (c_2 on Figure 8.3c). Point c_1 and the maximum peak c_2 are connected by a line that connects the peak and end inspiratory gradient. Figure 8.3 shows the sequence of how the airway pressure reconstruction is performed. This method is also applicable when the peak pressure occurs after the asynchrony event, and is the second peak. In that case, the process is reversed.

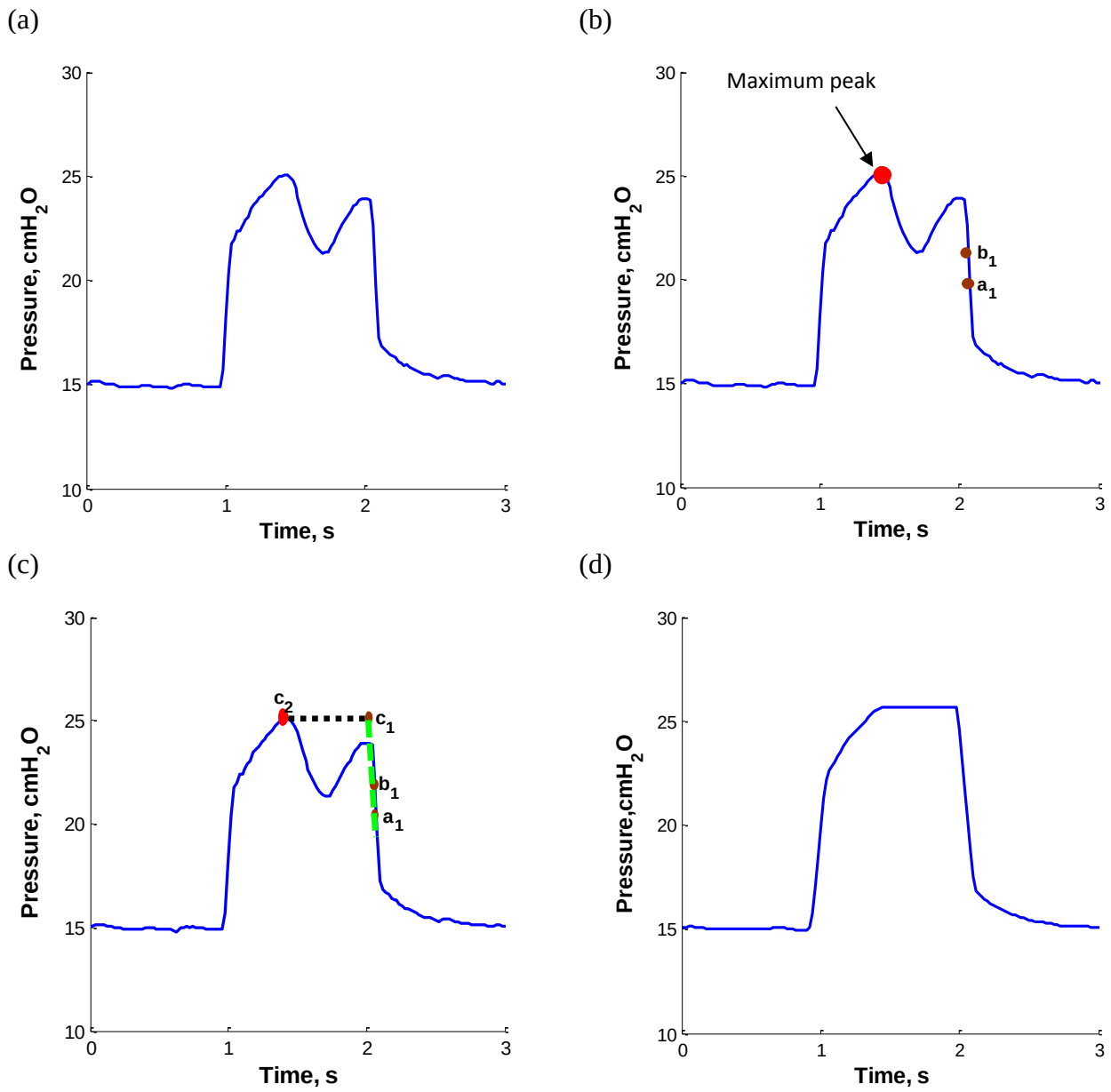

Figure 8.3: The steps on the reconstruction process (a) The M-wave airway pressure. (b) The maximum peak, point a_1 and point b_1 are identified. (c) The slope of point a_1 and point b_1 is extrapolated until point c_1, which has the same pressure value as the maximum peak. (d) The estimated final result of the reconstruction airway pressure.

8.2.4 Assessing Spontaneous Breathing Effort

The overall goal of the reconstruction method is to reduce the pressure drop created by the patient-specific inspiratory effort that reduces the measured airway pressure. The enclosed

area, shown in Figure 8.4 (A_2), is hypothesized to be a surrogate of patient-specific inspiratory effort that could be used to assess the strength of SB efforts.

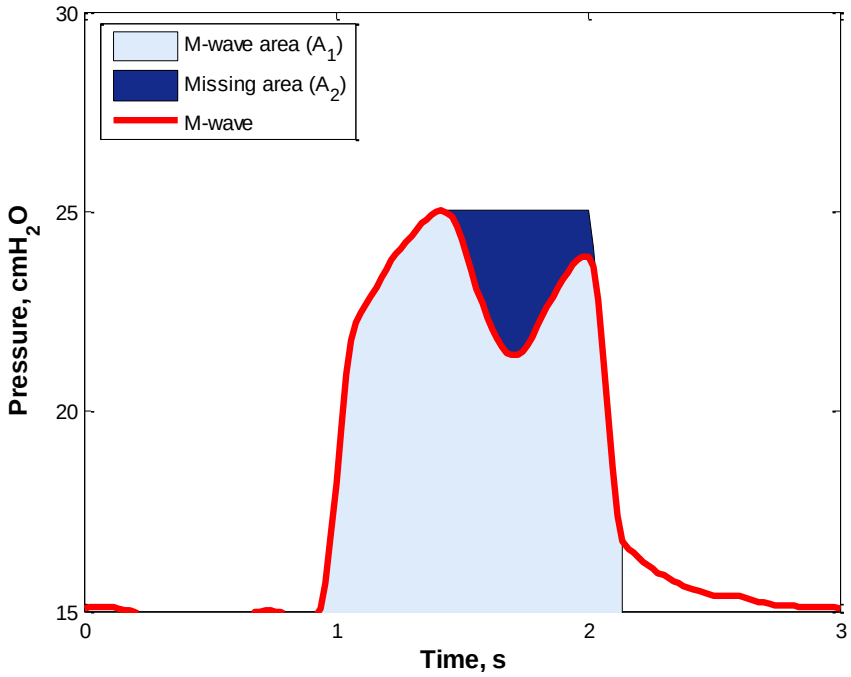

Figure 8.4: The area of the missing pressure, A_2 is shaded with dark colour.

The area of the M-wave over PEEP pressure is identified as A_1 and it has reduced pressure compared to the reconstructed curve, resulting in a lower overall time varying elastance (AUC E_{drs}). However, by adding the area of a missing pressure (A_2), the effect of the patient-specific breathing effort is reduced, leading to a higher value of identified elastance. Thus, the percentage of spontaneous breathing effort can be defined:

$$\text{SB effort} = \frac{A_2}{A_1 + A_2} \times 100\% \tag{8.4}$$

where it is important to note that A_1 and A_2 are independent of the PEEP level, which is 15cmH_2O in Figure 8.4.

Furthermore, from Equation 8.3, an accurate value of E_{drs} can be estimated and defined:

$$\frac{P_{A_1} + P_{A_2} - R_{ave}Q(t)}{V(t)} = E_{drs\_real} \tag{8.5}$$

Where P_{A_1} is the unreconstructed pressure, P_{A_2} is the pressure of the missing A_2, and E_{drs_real} is the accurate value of the respiratory elastance after the reconstruction process. If the resistance is constant and the volume controlled ventilation mode is set to have a fixed flow pattern to deliver set tidal volume, then $R_{ave}Q(t)$ can be assumed constant. Due to the SB breathing effort, E_{drs} is lower compared to normal breathing pressure, as only the P_{A_1} component of pressure is present, yielding:

$$\frac{P_{A_1}}{V(t)} - \frac{R_{ave}Q(t)}{V(t)} = E_{drs\_low} \tag{8.6}$$

E_{drs} is expected to be lower when there is additional unmodelled and unmeasurable energy input from the patient due to their SB effort, to add air volume. Therefore, it takes less pressure from the ventilator to achieve the target volume. Accounting for this difference using P_{A_2} yields:

$$\left(\frac{P_{A_1}}{V(t)} + \frac{P_{A_2}}{V(t)}\right) - \frac{R_{ave}Q(t)}{V(t)} = E_{drs\_low} + E_{drs\_SB} \tag{8.7}$$

If the term $R_{ave}Q(t)$ is assumed to be constant, E_{drs} relies heavily on the change of pressure. Hence, the elastance difference due to the SB effort can be defined:

$$E_{drs\_SB} = \frac{P_{A_2}}{V(t)} \tag{8.8}$$

Given that *V(t)* is the same in both cases, it can be said that:

$$P_{A_2} \propto E_{drs\_SB} \tag{8.9}$$

Therefore, $E_{drs_SB}$is a good surrogate of SB effort specific to a particular breath and patient. This approach thus creates a unique, new and non-invasive estimate of SB effort with no additional measurement or intervention required.

Finally, the work done by breathing can be determined using:

$$WOB = \int_{\Delta V} P_{A_1}(V)dV \tag{8.10}$$

Equation 8.10 can then be modified to utilise the lines shown in Figure 8.5, yielding:

$$\%\ of\ WOB_{SB} = \int_{\Delta V} \frac{P_{A_2}}{P_{A_1} + P_{A_2}}(V)dV \times 100\% \tag{8.11}$$

8.2.5 Data analysis

In this study, the E_{drs} for every breathing cycle of each patient is normalised and the AUC E_{drs} is calculated both with and without pressure reconstruction, to prove the concept for different PEEP levels in 5 patients for all 275 breathing cycles recorded. It is hypothesized that the true underlying mechanics change little, if at all, from breath-to-breath at a given PEEP level, matching results from sedated patients with no SB effort (Chiew et al. 2011; Chiew et al. 2015). Intermittent and variable SB efforts thus add variability to identified elastance and mechanics. The variability in AUC E_{drs} for the reconstruction method was also determined and compared with the AUC E_{drs} for the unreconstructed pressure by using the robust coefficient of variation (RCV = median absolute deviation/median), to compare the resulting variability in each metric over several breaths.

8.3 Results

Figure 8.6 shows the reconstructed airway pressure and the calculated AUC E_{drs} values for Patient 1 at PEEP of 15 cmH_2O. Figure 8.6 shows that many observed airway pressure waves were the typical airway pressure waveform expected from fully sedated patients. However, there are some breaths that exhibit M-wave characteristics. The highest AUC E_{drs} values were associated with the least effected pressure waves. E_{rs} and R_{ave} were calculated to determine the AUC E_{drs} using Equation 8.3. The E_{drs} curves are shown in Figure 8.7 for two of these breaths, one M-wave and one normal, and the difference in area under the E_{drs} curve between the normal wave and M-wave can be observed.

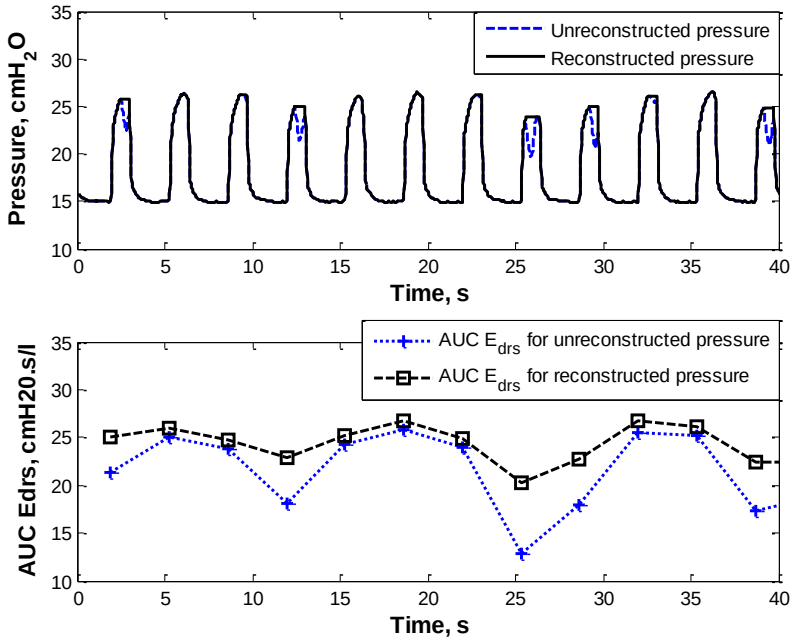

Figure 8.5: *Top:* The unreconstructed with M-wave airway pressure and reconstructed airway pressure for Patient 1 PEEP = 15 cmH_2O. *Bottom*: The AUC E_{drs} for both airway pressures at PEEP = 15 cmH_2O for Patient 1.

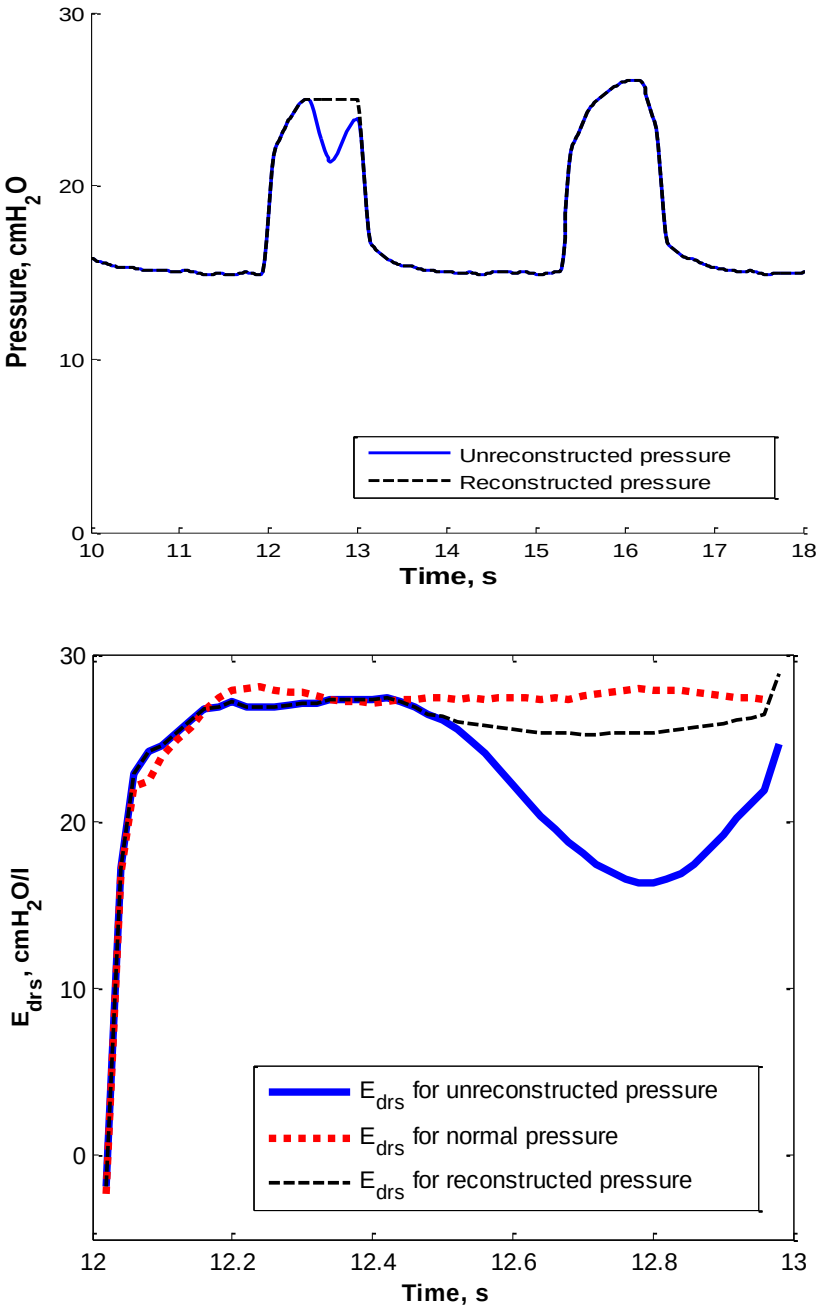

Figure 8.6: Example of airway pressure curve and E_{drs} curves for Patient 1 *Top*: The M-wave and normal pressure curve at PEEP = 15 cmH_2O. *Bottom* The E_{drs} curves for the M-wave and reconstructed M-wave and normal wave breaths normalized to the same inspiratory time at PEEP = 15 cmH_2O. Reconstruction improves estimate towards unaffected breath.

Figure 8.7 illustrates the reconstructed pressure volume (PV) curves for Patient 1 at a PEEP of 15 cmH_2O that captures the behaviour exhibited in the breath that was free from SB efforts. Figures 8.8 and 8.9 show unreconstructed airway pressure, reconstructed airway pressure, and the comparison of AUC E_{drs} for each PEEP level for Patients 1 and 4.

Reconstruction inevitably leads to higher modelled pressure and higher elastance, and thus, in this case, less variability in the calculated AUC E_{drs}. Figures 8.8 and 8.9 also show the surrogate inspiratory breathing effort based on Equation 8.4.

Table 8.2 summarises the calculated AUC E_{drs} and breathing effort for all 275 breathing cycles. A total of 81 cycles (~30%) were affected with the M-waves across all patients. The results between unreconstructed pressure and reconstructed pressure were compared. The RCV is calculated and compared for each PEEP level per patient and tabulated in Table 8.2. Figure 8.10 depicts the distribution plot for % of WOB against % of SB effort across all patients at all PEEP levels.

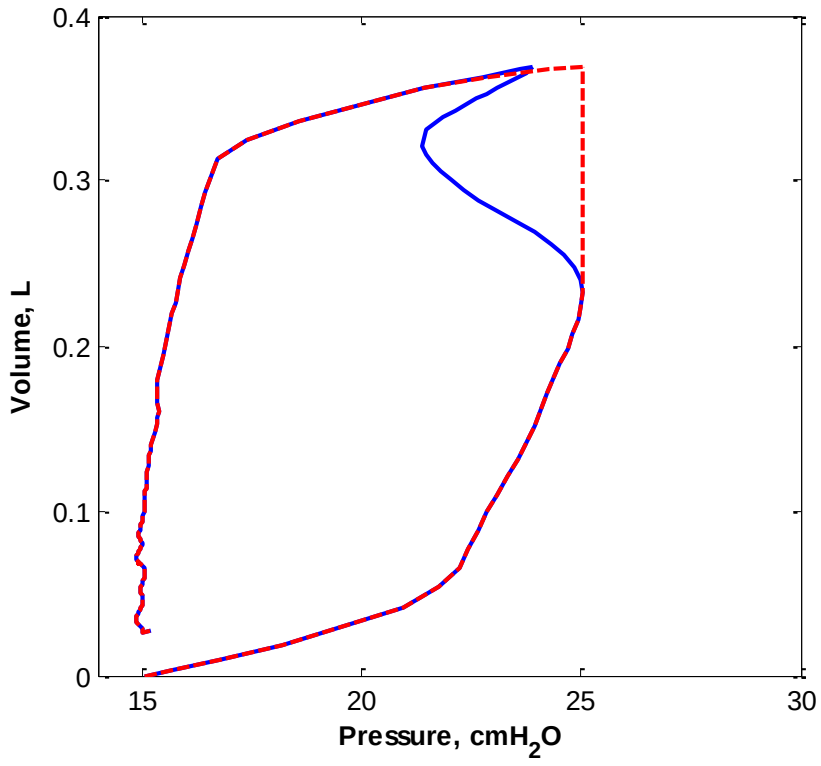

Figure 8.7: The PV curve of Patient 1 at PEEP 15 cmH_2O for M-wave (blue line) and reconstructed curves (red line).

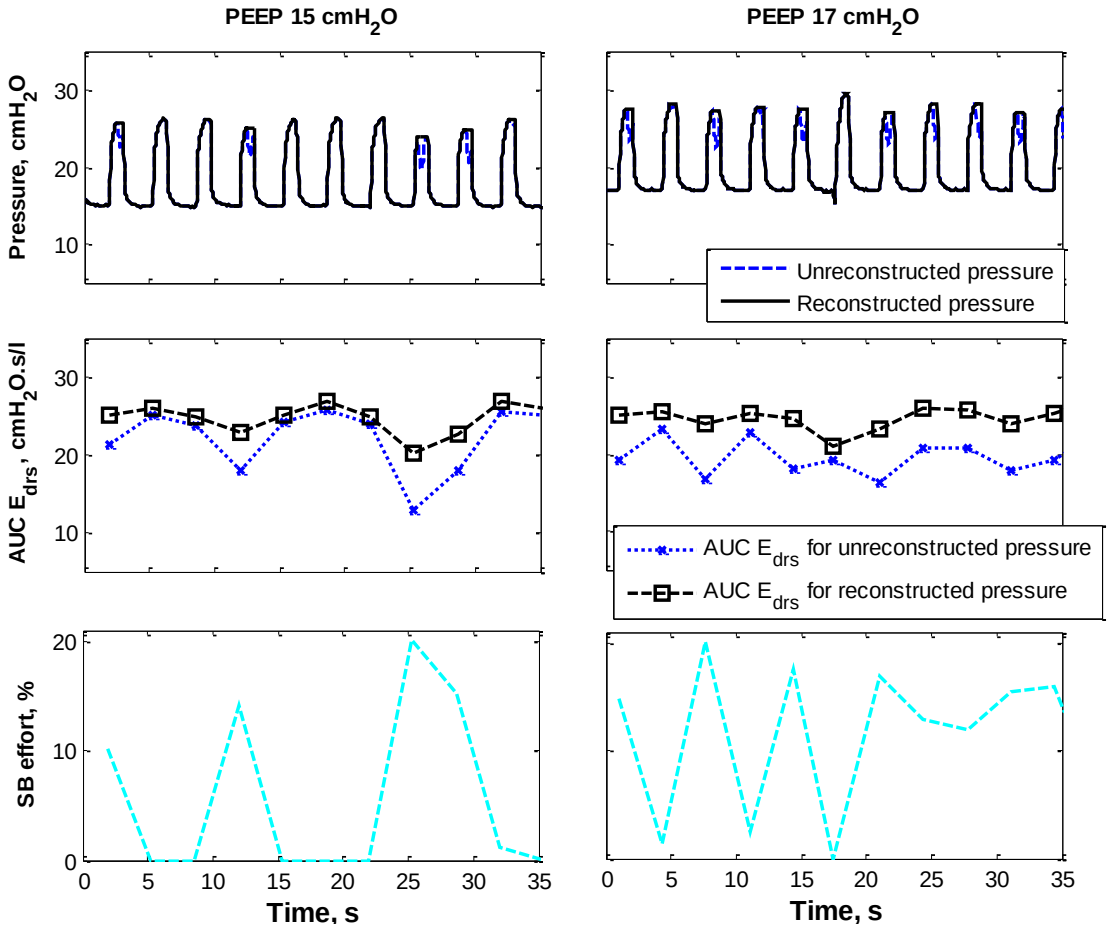

Figure 8.8: The AUC E_{drs} and for M-wave and reconstructed airway pressure and the surrogate inspiratory effort that added by the Patient 1 using reconstruction method for *Left*: PEEP = 15 cmH_2O and *Right*: PEEP = 17 cmH_2O.

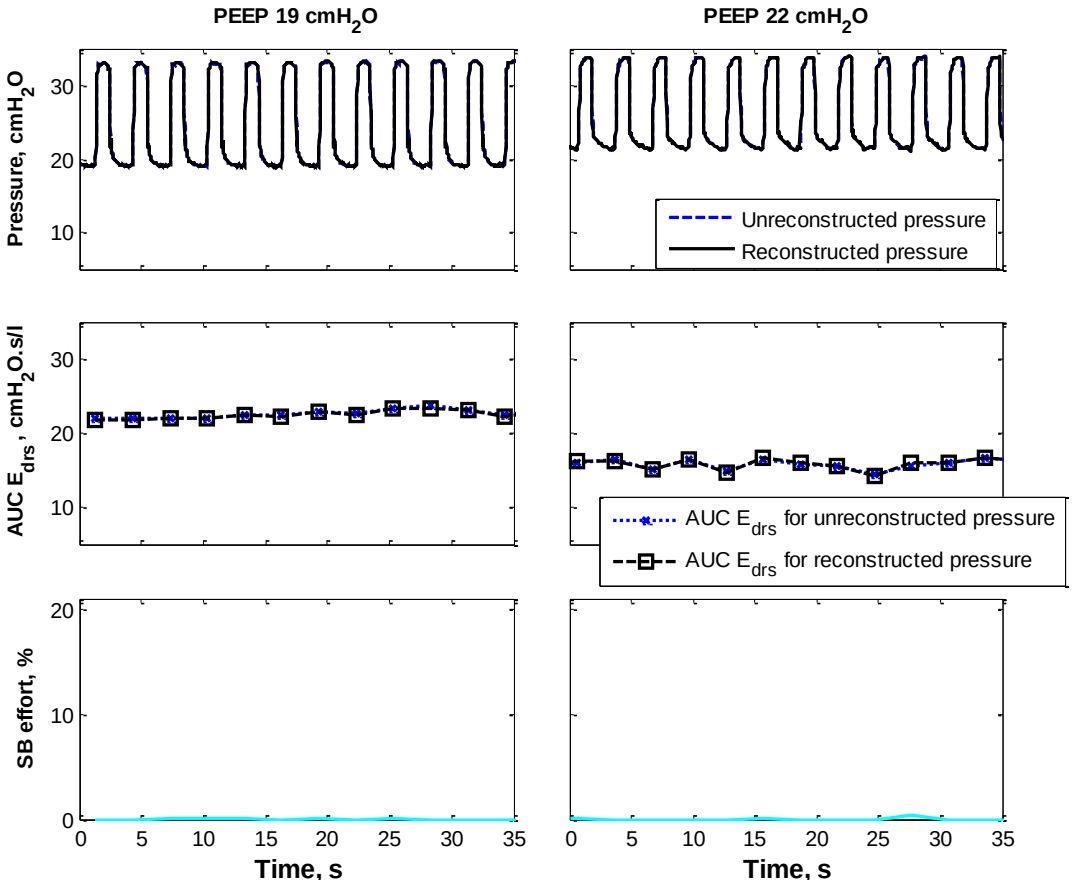

Figure 8.9: The AUC E_{drs} and for unreconstructed and reconstructed airway pressure, and the surrogate inspiratory effort that added by the Patient 4 using reconstruction method for *Left*: PEEP = 19 cmH_2O and *Right*: PEEP = 22 cmH_2O.

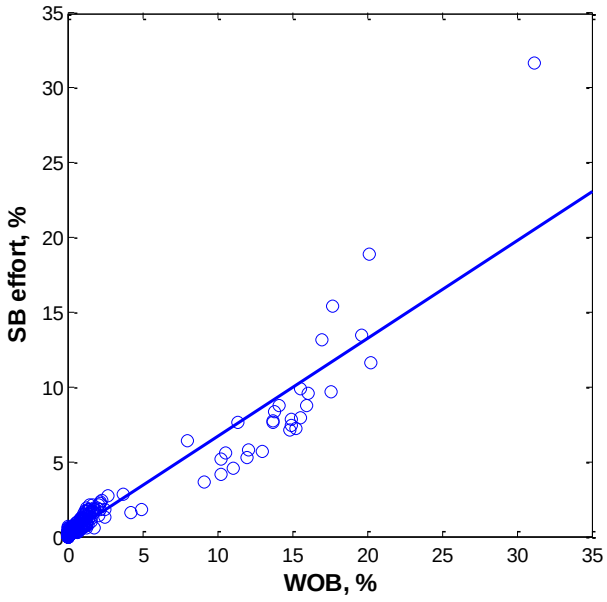

Figure 8.10: Plot of % of WOB against % SB effort across all patient breaths at all PEEP levels.

Table 8.2: The AUC E_{drs} and RCV for unreconstructed M-wave and reconstructed M-wave, and the percentage of SB surrogate for 5 patients at different PEEP levels

Patient	PEEP (cmH_2O)	Breathing cycle	M-wave cycle	Unreconstructed AUC E_{drs}(cmH_2O·s/l)	Reconstructed method AUC E_{drs} (cmH_2O·s/l)	SB Effort (%)	WOB (%)	RCV for AUC E_{drs} (M-wave)	RCV for AUC E_{drs} (Reconstructed)
1	15	29	15	21.99 [18.37-24.06]	22.95 [21.38-24.09]	0.00 [0.00-11.38]	0.06 [0.00-6.60]	0.14	0.08
	17	33	19	20.69 [19.10-24.28]	23.95 [22.71-24.99]	10.95 [0.00-14.79]	4.56 [0.01-7.74]	0.14	0.05
2	15	30	7	16.73 [16.38-17.06]	16.95 [16.69-17.24]	1.13 [0.98-1.43]	1.53 [0.75-1.78]	0.02	0.01
	17	18	8	22.01 [21.08-23.49]]	22.48 [20.84-23.70]	0.76 [0.00-1.22]	0.75 [0.10-1.09]	0.07	0.07
3	13	32	5	18.88 [18.05-19.59]	19.16 [18.36-19.92]	0.62 [0.22-0.92]	0.43 [0.25-0.62]	0.05	0.04
	14	31	5	15.24 [15.00-15.57]	15.56 [15.28-15.82]	0.00 [0.00-0.24]	0.33 [0.10-0.56]	0.03	0.03
4	19	29	4	22.80 [22.57-23.11]	22.80 [22.61-23.12]	0.00 [0.00-0.14]	0.33 [0.19-0.41]	0.03	0.02
	22	31	6	15.56 [14.77-16.20]	15.89 [15.02-16.24]	0.00 [0.00-0.12]	0.22 [0.08-0.39]	0.04	0.04
5	17	21	8	19.98 [18.98-20.31]	20.22 [19.22-20.61]	0.66 [0.41-0.77]	0.76 [0.53-1.12]	0.05	0.05
	21	21	4	22.18 [22.02 – 22.82]	22.77 [22.51-23.25]	1.15 [0.91-1.75]	1.31 [1.00-1.71]	0.03	0.03
Median [IQR]				**19.21 [16.30-22.47]**	**20.41 [16.68-22.81]**	**0.45 [0.00-1.15]**	**0.54 [0.18-1.21]**	**0.05 [0.03-0.07]**	**0.04 [0.03-0.05]**

8.4 Discussion

SB efforts by MV patients during volume controlled ventilation will alter airway pressures and affect identified respiratory mechanics. In this study, it was observed that all patients exhibit different levels of rate and severity of SB affected breaths, despite being sedated and ventilated in a fully controlled ventilation mode. When M-waves occur, the AUC E_{drs} is reduced since the same volume is delivered for apparently less input air pressure, thus reducing observed, but not physiological, pulmonary elastance (Figure 8.5). AUC E_{drs} rises to a consistent value reflecting the true, underlying passive respiratory mechanics when fully-sedated airway pressure waveforms resume.

These results suggested that the variance in AUC E_{drs} can be used to determine the presence of SB efforts. Since it is not clinically desirable to use additional invasive measuring tools or induce further sedation to suppress patient muscle activity (Kress et al. 2000; Ostermann et al. 2000), a method is required to re-construct the M-wave airway pressure to approximate a normal breath. In this proof of concept analysis, a reconstruction method is introduced and compared with the unreconstructed pressure, as in Figures 8.6-8.9. The goal is to estimate the true underlying mechanical properties, which might be expected to be relatively constant over a short period or at a set PEEP level, as seen in sedated patients (Chiew et al. 2011; Chiew et al. 2015).

Figure 8.6 shows a specific example of two breaths, where one would expect the underlying respiratory mechanics to be very similar. However, directly solving Equation 8.3 yielded very different results for E_{drs}, despite the lack of change assumed in the patient's pulmonary physiology. Using the reconstruction method, the E_{drs} curve for the M-wave breaths have

almost the same shape as the normal wave, and thus the AUC E_{drs} for the reconstructed and SB-free pressure wave have almost the same area. These results show how a very simple reconstruction method can be used to accurately estimate the underlying lung mechanics, despite SB efforts.

M-wave affected airway pressure was observed in more than 50% of the total breathing cycles for both PEEP levels in Patient 1 (34/62, Table 8.2). It can be seen that most reconstructed airway pressure waveforms have approximately the same height and area, resulting in a more consistent estimation of the AUC E_{drs}, and thus the underlying respiratory mechanics, as seen in Figure 8.8. The RCV of AUC E_{drs} for Patient 1 is higher for unreconstructed waveforms with RCV= 0.14 at both PEEP 15 cmH_2O and PEEP 17 cmH_2O, compared to the reconstruction method with RCV = 0.08 at PEEP = 15 cmH_2O and RCV = 0.05 at PEEP = 17 cmH_2O. Thus, the reconstruction method yields the expected, more constant value of AUC E_{drs} due to greater reconstruction or restoration of the pressure "lost" to SB efforts as compared to unreconstructed cases.

Using the reconstructed airway pressure, the area of missing pressure (A_2) due to patient induced SB effort can be calculated. In particular, it carries breath-specific SB effort that cannot be quantified without the use of invasive oesophageal pressure measurements (Benditt 2005; Khirani et al. 2010; Talmor et al. 2006). Overall, as A_2 increases, it indicates increased SB effort, as A_2 is directly proportional to SB effort as shown in Equation 8.9. Hence, A_2 can be used as a surrogate of the magnitude of SB.

This value also has potential clinical benefit as it could be used to guide clinicians in real time to improve patient-ventilator interaction. A second use would be deciding whether to

extubate or re-sedate the patient. These decisions are otherwise clinically difficult and variable, and thus much more subjective decisions in clinical practise, which can lead to greater variability in care.

Patients 2-5 exhibit relatively minor SB efforts compared to Patient 1 (Table 8.2). This lower incidence of SB effort results in a lower missing area (A_2) in those patients. Patients 2-5 have more consistent breathing, more consistent pressure waveforms, and a lower rate of M-waves compared to Patient 1 for the sections of data used. Thus, the AUC E_{drs} of reconstructed airway is almost equal to AUC E_{drs} of the unreconstructed airway. For example, this outcome can be seen in Table 8.2 with the RCV values of unreconstructed pressure for Patient 5 is similar to the RCV values of reconstructed pressure across all PEEP levels. Hence, these results show that the reconstruction method is robust when there is a relative lack of SB effort.

These results also show how reverse triggering occurs randomly and not all patients exhibit similar rates or levels. The reconstruction method does not negatively affect the outcomes for patients that do not have significant SB efforts. Hence, the process could be safely embedded within algorithms that track pulmonary elastance without the need for a secondary algorithm to diagnose SB effort prior to implementation. Moreover, pressure reconstruction inevitably leads to higher pressure for the affected M-wave, as seen in Figure 8.7. The reconstruction ultimately leads to a PV curve that provides a better fit to PV curves for breaths that are unaffected by SB efforts. This result shows how this simple pressure reconstruction is able to provide a reasonable estimate of the pressure wave that could be expected in the absence of SB effort.

Figure 8.10 shows the distribution data of % of SB effort against the % of WOB_{SB} which leads to a highly correlated value with R = 0.94 across all patients. This result elucidates a trend between the % SB effort and % WOB_{SB}. The trend indicates that by implementing the pressure reconstruction method, SB effort and the WOB_{SB} of MV patient can be determined without having to use invasive sensors or procedures, and without having to interrupt care.

8.5 Limitations

Although the reconstructed airway pressure can estimate the elastance for a spontaneously breathing patient, there are limitations to its predictive capability. In particular, SB can occur at any time during MV, and the variation of M-waves may differ depending on the ventilation mode. This proof of concept study is thus, a first step to explore the possibility of this type of very simple reconstruction method, which could be expanded to other ventilation modes as desired. Thus, more patient data are required to show the full robustness of the reconstruction method. However, this small data set of patients approach was sensible to test the method and exhibit the potential benefit in M-wave analysis in SB patients.

Conversely, the latter results imply the importance of measuring SB effort to potentially provide clinicians with an indicator to fine tune ventilator for better patient-ventilator interaction or weaning process. The weaning process is a critical phase in respiratory therapy and a difficult clinical decision (Boles et al. 2007; Esteban et al. 1994). Recent studies have shown that MV patients who have the ability to breath by themselves have a higher chance of recovery and higher success rate in weaning (Kogler 2009; Marini 2011; Putensen et al. 1999). Thus, this simple reconstructed airway pressure and proof of concept analysis could

open up new options in deciding the optimal, or at very least, consistent, patient condition to extubate or re-sedate the patient, which is crucial in MV therapy.

8.5 Summary

This proof of concept study presents a novel, computationally simple method to reconstruct airway pressure to better estimate respiratory mechanics and quantify the level of patient-specific SB effort at every breath. This simple reconstruction method is easy to implement without requiring additional sedation or intense clinical protocols, and is computationally simple enough for real-time implementation. This method reduces variability in estimated mechanical properties that arise from patient-specific SB efforts, and do not represent variability in the underlying lung mechanics. Clinically, this method could have impact in guiding MV and provide unique information that can potentially be used for clinicians in deciding the optimal ventilator settings and improve patient's condition.

CHAPTER 9

Conclusion

This thesis developed and validated model-based and patient-specific methods for assessing lung mechanics that provide further insight into lung mechanics of mechanically ventilated (MV) Acute Respiratory Distress Syndrome (ARDS) patients. Four unique models are developed based on physiologically relevant and mechanically accurate components using clinical data that are able to describe patient-specific conditions and could be used to guide MV therapy. These models and validation provides a foundation on which model-based MV can be created and clinically implemented.

In Chapter 2, a well-known model-based method, the dynostatic algorithm (DSA), is applied to estimate the alveolar pressure of the lung based on the dynostatic curve by using the retrospective clinical data. The estimated alveoli pressure is based on assumption that airway resistance is always the same during inspiration and expiration at isovolume. The estimation of alveolar pressure allows insight into the lung condition and prevents the lung from over-stretched due to the higher PEEP that applied during MV therapy.

Chapter 3 presents a novel model based method patient-specific airway branching model (ABMps) based on individual physiological measurement by using a classical simple Poiseuille flow and minor loss equations. The ABMps was applied to retrospective clinical data and showed how to estimate the airway pressure drop at each bronchial generation using patient-specific physiological measurement. This model can be generated from data measured at the bedside with the extension to a patient-specific airway dimension, α. The α value relates to the patient condition, where, for example, it was found in Chronic Obstructive

Pulmonary Disease (COPD) patients that α ranges from 0.45 – 0.62, which relates to the smaller effective diameter of the airways that result mathematically from the lung blockage that occurs in COPD. In this chapter, the results of ABMps are compared with the well-accepted DSA by using the same retrospective clinical data. Results show that it is able to capture similar alveolar pressure as the DSA while providing significant further insight into patient-specific airway dimensions and patient condition. Hence, the ABMps offers significant potential to guide clinicians in setting an optimal MV, is non-invasive, and can be personalized.

Chapter 5 extends the investigation on the relation of the parameter *K* in the expiratory time constant model with respiratory system elastance by using data from the expiration breathing cycle of ARDS patients. The model used retrospective clinical data from two different cohorts to identify the variation of respiratory elastance and parameter *K* in response to different PEEP levels. It was found that significant variation in lung resistance leads to a poor correlation between *K* and respiratory system elastance. However, *K* has delivered a good indicator for COPD patients. Thus, *K* has potential in tracking the changes in disease state for MV patients in real-time, and could be directly used with COPD patients now.

Chapter 6 focused on quantifying the variability of dynamic respiratory (E_{drs}) elastance in ARDS patients using a time-varying elastance model. To investigate the variability of respiratory elastance, clinical data from ARDS patients who underwent a specific clinical protocol were used. The area under the curve of E_{drs} (AUC E_{drs}) is estimated and analysed based on ventilation days, PEEP levels and breath to breath variability. It was found that due to patient-specific breathing effort, it produced a negative elastance resulting in increased variability in E_{drs}. Equally, monitoring the variability of E_{drs} can highlight for clinicians the

presence of moderate and smaller spontaneous breathing (SB) efforts in MV patients leading to adjustments in care. Furthermore, with the information on elastance variability, it could guide clinicians in managing PEEP titration for MV patients.

Due to the SB efforts that occurred in MV patients, it is essential to develop a non-invasive model that is able to monitor the respiratory mechanics of SB patients. These SB patients modify their airway pressure and flow due to their own, variable, inspiratory effort. As mentioned in Chapter 6, the variability of lung elastance happened due to the negative elastance that causes by the SB effort. Thus, Chapter 7 reviews the distribution of negative elastance of SB patients by using a non-invasive time-varying elastance model. The resulting metrics of negative elastance due to SB effort provides an indicator, capable of providing unique information to guide MV for spontaneously breathing patients, who make up an increasing number of MV patients.

Finally, Chapter 8 presents an airway pressure reconstruction method that is able to reconstruct the missing pressure that was due to the SB effort. The missing area of the measured airway pressure is hypothesized to be a surrogate of the patient-specific and breath-specific inspiratory effort, which can be used to assess the strength of SB efforts. By using the clinical data from ARDS patients, this simple pressure reconstruction method has demonstrated that it is able to deliver with a quality clinical metric that able to measure the respiratory system properties of a SB patient and measure the surrogate of the SB effort, that latter can be useful for clinicians in deciding whether to extubate or re-sedate the patient.

Overall, the patient-specific models and metrics presented in this thesis provide unique capability in providing new clinical insight into patient-specific and even breath-specific lung

condition and patient-specific response to MV settings. The models have been tested using clinical data from different cohorts and have shown promising results that will be useful in guiding MV decision making in an ICU for both fully sedated and SB patients. Thus, the modelling approach discussed in this thesis shows great potential to be used as the foundation for clinical decision support tool for managing and optimizing patient-specific MV setting.

CHAPTER 10

Future Work

The models and metrics presented in this thesis have created a good platform to deliver optimized ventilation therapy for ARDS patients. However, further optimization and extensive clinical study can, and should, be implemented to fully validate the ability of these models and the robustness of the system.

10.1 Additional Monitoring Tools for Model Validation

In this thesis, the models and metrics developed have presented clinical potential to guide optimal MV setting. However, validation of the clinical relevance and physiological insight of a model-based approach is currently limited. Specifically, the ABMps model could capture patient-specific airway pressure changes and unique patient-specific clinical information (Damanhuri et al. 2014). However, the current findings warrant further investigation. Thus, it would be a significant advantage to have additional lung imaging methods such as Computed Tomography (CT) scans, to provide better information and physiological insight on the airway branching and bifurcations on each patient. With these measurements, the models can be further and better validated, and this level of validation would more strongly encourage and support the model's clinical application to guide MV.

Furthermore, additional monitoring tools, such as in-vivo microscopy, Electrical Impedance Tomography (EIT) (Denai et al. 2010; Zhao et al. 2010b) and lung ultrasound (Bouhemad et al. 2007; Peris et al. 2010), allows the recruitment of collapsed of lung units to be directly

observed in real-time. Hence, with the results from the models and methods developed will have their predictive capability and clinical potential directly validated by clinically well-accepted, more direct, but invasive measurements.

10.2 Clinical Protocol and Data Collection

Further investigation and validation could also be applied to the expiratory time constant model using the CURE clinical data. Previously, van Drunen et al. (van Drunen et al. 2013) studied the model based on animal data only. Based on results in Chapter 5, the model using human data showed different results for the correlation between the expiratory time constant, (K) and lung elastance, (E_{rs}) for two different cohorts. Thus, by using a standard clinical protocol, the larger clinical cohort may provide more consistency in results between K and E_{rs} and settle this discrepancy. To investigate the expiratory time constant model further, a clinical protocol could be designed where the tidal volume (V_t) is varied between low and higher values at a constant PEEP.

In addition, recruiting more ARDS patients for clinical trials remains the main focus for model-based studies. A non-invasive clinical protocol that is suitable for data collection has been put forward in Chapter 6. This protocol has several unique features that are designed for this purpose.

In particular, this thesis has discussed that SB effort can occur at any time during MV, which has been explained in Chapter 8. The airway pressure reconstruction is able to estimate the respiratory mechanics of SB patients. However, the variation application of SB efforts may differ depending on clinical protocol and ventilation mode. Thus, a standard protocol that

specifically designed to monitor SB effort would be of significant utility. With more SB patient data, it can show the full robustness of the airway reconstruction method.

Protocol standardisation will not only improve data sample size, the significant data samples can indirectly lead to a development of a virtual patient database. This database will lead to more comprehensive study in model-based MV. It may also provide further clinical or physiological insight via machine learning or other modelling and/or analytics.

10.3 COPD patients

The patient-specific ABM model (ABMps) (Damanhuri et al. 2014) has shown its capability for assessing airway pressure drops in ARDS patients with the specific airway dimension, α that relates to patients disease state. The results presented in this thesis found that patients suffering from COPD had smaller effective diameter for these physiological measurements compared to other ARDS patients, as discussed in Chapter 3. Furthermore, it also showed in Chapter 5 that COPD patients have higher airway resistance due the smaller effective diameter of the lung branches because the airway blockages in COPD increase airway pressure drop in the lung. Thus, larger cohorts consisting of COPD patients may provide more significant results that are potentially useful in diagnosing and providing further insight into lung condition in COPD patients.

References

Akoumianaki, E, Lyazidi, A, Rey, N, Matamis, D, Perez-Martinez, N, Giraud, R, Mancebo, J, Brochard, L & Richard, J-CM 2013, 'Mechanical Ventilation-Induced Reverse-Triggered BreathsReverse TriggeringA Frequently Unrecognized Form of Neuromechanical Coupling', *CHEST Journal,* vol. 143, no. 4, pp. 927-38.

Al-Rawas, N, Banner, MJ, Euliano, NR, Tams, CG, Brown, J, Martin, AD & Gabrielli, A 2013, 'Expiratory time constant for determinations of plateau pressure, respiratory system compliance, and total resistance', *Crit Care,* vol. 17, no. 1, p. R23.

Albaiceta, G, Garcia, E & Taboada, F 2007, 'Comparative study of four sigmoid models of pressure-volume curve in acute lung injury', *Biomedical Engineering OnLine,* vol. 6, no. 1, p. 7.

Albaiceta, GM, Blanch, L & Lucangelo, U 2008, 'Static pressure-volume curves of the respiratory system: were they just a passing fad?', *Current Opinion in Critical Care,* vol. 14, no. 1, pp. 80-6 10.1097/MCC.0b013e3282f2b8f4.

Albaiceta, GM, Piacentini, E, VillagrÃ¡, A, Lopez-Aguilar, J, Taboada, F & Blanch, L 2003, 'Application of continuous positive airway pressure to trace static pressure-volume curves of the respiratory system', *Crit Care Med,* vol. 31, no. 10, pp. 2514-9.

Alencar, AM, Arold, SP, Buldyrev, SV, Majumdar, A, Stamenović, D, Stanley, HE & Suki, B 2002, 'Physiology: Dynamic instabilities in the inflating lung', *Nature,* vol. 417, no. 6891, pp. 809-11.

Amato, MBP, Barbas, CSV, Medeiros, DM, Magaldi, RB, Schettino, GP, Lorenzi-Filho, G, Kairalla, RA, Deheinzelin, D, Munoz, C, Oliveira, R, Takagaki, TY & Carvalho, CRR 1998, 'Effect of a Protective-Ventilation Strategy on Mortality in the Acute Respiratory Distress Syndrome', *N Engl J Med,* vol. 338, no. 6, pp. 347-54.

Andreassen, S, Steimle, KL, Mogensen, ML, Bernardino de la Serna, J, Rees, S & Karbing, DS 2010, 'The effect of tissue elastic properties and surfactant on alveolar stability', *J Appl Physiol,* vol. 109, no. 5, pp. 1369-77.

Anzueto, A, Peters, JI, Tobin, MJ, De Los Santos, R, Seidenfeld, JJ, Moore, G, Cox, WJ & Coalson, JJ 1997, 'Effects of prolonged controlled mechanical ventilation on diaphragmatic function in healthy adult baboons', *Critical Care Medicine,* vol. 25, no. 7, pp. 1187-90.

Ashbaugh, DG, Bigelow, DB, Petty, TL & Levine, BE 1967, 'Acute respiratory distress in adults', *Lancet,* vol. 2, no. 7511, pp. 319-23.

Avanzolini, G & Barbini, P 1984, 'A versatile identification method applied to analysis of respiratory mechanics', *IEEE Trans Biomed Eng,* vol. 31, no. 7, pp. 520-6.

Barber, D & Brown, B 1984, 'Applied potential tomography', *Journal of physics. E. Scientific instruments,* vol. 17, no. 9, pp. 723-33.

Bates, JH & Irvin, CG 2002, 'Time dependence of recruitment and derecruitment in the lung: a theoretical model', *Journal of Applied Physiology,* vol. 93, no. 2, pp. 705-13.

Bates, JHT 2009, *Lung mechanics an inverse modelling approach*, Cambridge University Press, United States of America.

Ben-Tal, A 2006, 'Simplified models for gas exchange in the human lungs', *J Theor Biol,* vol. 238, pp. 474 - 95.

Benditt, JO 2005, 'Esophageal and gastric pressure measurements', *Respiratory care,* vol. 50, no. 1, pp. 68-77.

Bernard, GR 2005, 'Acute respiratory distress syndrome: a historical perspective', *Am J Respir Crit Care Med,* vol. 172, pp. 798 - 806.

Bernard, GR, Artigas, A, Brigham, KL, Carlet, J, Falke, K, Hudson, L, Lamy, M, Legall, JR, Morris, A & Spragg, R 1994a, 'The American-European Consensus Conference on ARDS. Definitions, mechanisms, relevant outcomes, and clinical trial coordination', *Am J Respir Crit Care Med,* vol. 149, pp. 818 - 24.

Bernard, GR, Artigas, A, Brigham, KL, Carlet, J, Falke, K, Hudson, L, Lamy, M, LeGall, JR, Morris, A & Spragg, R 1994b, 'Report of the American-European consensus conference on ARDS: Definitions, mechanisms, relevant outcomes and clinical trial coordination', *Intensive Care Med,* vol. 20, no. 3, pp. 225-32.

Bersten, AD 1998, 'Measurement of overinflation by multiple linear regression analysis in patients with acute lung injury', *Eur Respir J,* vol. 12, no. 3, pp. 526-32.

Boles, J-M, Bion, J, Connors, A, Herridge, M, Marsh, B, Melot, C, Pearl, R, Silverman, H, Stanchina, M & Vieillard-Baron, A 2007, 'Weaning from mechanical ventilation', *European Respiratory Journal,* vol. 29, no. 5, pp. 1033-56.

Bouhemad, B, Zhang, M, Lu, Q & Rouby, J-J 2007, 'Clinical review: Bedside lung ultrasound in critical care practice', *Critical Care,* vol. 11, no. 1, p. 205.

Brenner, DJ & Hall, EJ 2007, 'Computed Tomography -- An Increasing Source of Radiation Exposure', *N Engl J Med,* vol. 357, no. 22, pp. 2277-84.

Briel, M, Meade, M, Mercat, A, Brower, RG, Talmor, D, Walter, SD, Slutsky, AS, Pullenayegum, E, Zhou, Q, Cook, D, Brochard, L, Richard, JC, Lamontagne, F, Bhatnagar, N, Stewart, TE & Guyatt, G 2010, 'Higher vs lower positive end-expiratory pressure in patients with acute lung injury and acute respiratory distress syndrome: systematic review and meta-analysis', *JAMA,* vol. 303, no. 9, pp. 865-73.

Brochard, L, Martin, GS, Blanch, L, Pelosi, P, Belda, FJ, Jubran, A, Gattinoni, L, Mancebo, J, Ranieri, VM & Richard, J 2012, 'Clinical review: Respiratory monitoring in the ICU-a consensus of 16', *Crit Care,* vol. 16, no. 2, p. 219.

Brochard, L, Roudot-Thoraval, F, Roupie, E, Delclaux, C, Chastre, J, Fernandex-Mondejar, E, Clementi, E, Mancebo, J, Factor, P, Matamis, D, Ranieri, M, Blanch, L, Rodi, G, Mentec, H, Dreyfuss, D, Ferrer, M, Brun-Buisson, C, Tobin, M & Lemaire, F 1998, 'Tidal Volume Reduction for Prevention of Ventilator-induced Lung Injury in Acute Respiratory Distress Syndrome', *Am J Respir Crit Care Med,* vol. 158, no. 6, pp. 1831-8.

Brower, RG, Lanken, PN, MacIntyre, N, Matthay, MA, Morris, A, Ancukiewicz, M, Schoenfeld, D & Thompson, BT 2004, 'Higher versus Lower Positive End-Expiratory Pressures in Patients with the Acute Respiratory Distress Syndrome', *N Engl J Med,* vol. 351, no. 4, pp. 327-36.

Bruhn, A, Bugedo, D, Riquelme, F, Varas, J, Retamal, J, Besa, C, Cabrera, C & Bugedo, G 2011, 'Tidal volume is a major determinant of cyclic recruitment-derecruitment in acute respiratory distress syndrome', *Minerva Anestesiol,* vol. 77, no. 4, pp. 418-26.

Burleson, BS & Maki, ED 2005, 'Acute Respiratory Distress Syndrome', *Journal of Pharmacy Practice,* vol. 18, no. 2, pp. 118-31.

Burrowes, KS, Clark, AR, Marcinkowski, A, Wilsher, ML, Milne, DG & Tawhai, MH 2011, 'Pulmonary embolism: predicting disease severity', *Philos Transact A Math Phys Eng Sci,* vol. 369, no. 1954, pp. 4255-77.

Burrowes, KS, Hunter, PJ & Tawhai, MH 2005, 'Anatomically based finite element models of the human pulmonary arterial and venous trees including supernumerary vessels', *J Appl Physiol,* vol. 99, no. 2, pp. 731-8.

Caironi, P, Cressoni, M, Chiumello, D, Ranieri, M, Quintel, M, Russo, SG, Cornejo, R, Bugedo, G, Carlesso, E, Russo, R, Caspani, L & Gattinoni, L 2010, 'Lung opening and closing during ventilation of acute respiratory distress syndrome', *Am J Respir Crit Care Med,* vol. 181, no. 6, pp. 578-86.

Caramez, MP, Kacmarek, RM, Helmy, M, Miyoshi, E, Malhotra, A, Amato, MB & Harris, RS 2009, 'A comparison of methods to identify open-lung PEEP', *Intensive Care Medicine,* vol. 35, no. 4, pp. 740-7.

Carley, DW & Shannon, DC 1988, 'A minimal mathematical model of human periodic breathing', *J Appl Physiol,* vol. 65, no. 3, pp. 1400-9.

Carney, DE, Bredenberg, CE, Schiller, HJ, Picone, AL, McCANN, UG, Gatto, LA, Bailey, G, Fillinger, M & Nieman, GF 1999, 'The mechanism of lung volume change during mechanical ventilation', *American Journal of Respiratory and Critical Care Medicine,* vol. 160, no. 5, pp. 1697-702.

Carvalho, A, Jandre, F, Pino, A, Bozza, F, Salluh, J, Rodrigues, R, Ascoli, F & Giannella-Neto, A 2007, 'Positive end-expiratory pressure at minimal respiratory elastance represents the best compromise between mechanical stress and lung aeration in oleic acid induced lung injury', *Critical Care,* vol. 11, no. 4, p. R86.

Carvalho, A, Jandre, F, Pino, A, Bozza, F, Salluh, J, Rodrigues, R, Soares, J & Giannella-Neto, A 2006, 'Effects of descending positive end-expiratory pressure on lung mechanics and aeration in healthy anaesthetized piglets', *Critical Care,* vol. 10, no. 4, p. R122.

Carvalho, A, Spieth, P, Pelosi, P, Vidal Melo, M, Koch, T, Jandre, F, Giannella-Neto, A & de Abreu, M 2008, 'Ability of dynamic airway pressure curve profile and elastance for positive end-expiratory pressure titration', *Intensive Care Medicine,* vol. 34, no. 12, pp. 2291-9.

Carvalho, AR, Bergamini, BC, Carvalho, NS, Cagido, VR, Neto, AC, Jandre, FC, Zin, WA & Giannella-Neto, A 2013, 'Volume-independent elastance: A useful parameter for open-lung positive end-expiratory pressure adjustment', *Anesthesia & Analgesia,* vol. 116, no. 3, pp. 627-33.

Chao, DC & Scheinhorn, DJ 1996, 'Barotrauma vs volutrauma', *CHEST Journal,* vol. 109, no. 4, pp. 1127-8.

Chase, JG, Hann, CE, Jackson, M, Lin, J, Lotz, T, Wong, X-W & Shaw, GM 2006a, 'Integral-based filtering of continuous glucose sensor measurements for glycaemic control in critical care', *Computer Methods and Programs in Biomedicine,* vol. 82, no. 3, pp. 238-47.

Chase, JG, Yuta, T, Mulligan, K, Shaw, G & Horn, B 2006b, 'A novel mechanical lung model of pulmonary diseases to assist with teaching and training', *BMC Pulmonary Medicine,* vol. 6, no. 1, p. 21.

Cheng, W, DeLong, DS, Franz, GN, Petsonk, EL & Frazer, DG 1995, 'Contribution of opening and closing of lung units to lung hysteresis', *Respir Physiol,* vol. 102, no. 2-3, pp. 205-15.

Chiew, Y, Chase, J, Shaw, G & Desaive, T 2012, 'Respiratory system elastance monitoring during PEEP titration', *Critical Care,* vol. 16, pp. 1-189.

Chiew, YS 2013, *Model-based Mechanical Ventilation for the Critically Ill: A Thesis Submitted for the Degree of Doctor of Philosophy in Mechanical Engineering at the University of Canterbury, Christchurch, New Zealand* University of Canterbury,

Chiew, YS, Chase, JG, Lambermont, B, Roeseler, J, Pretty, C, Bialais, E, Sottiaux, T & Desaive, T 2013, 'Effects of Neurally Adjusted Ventilatory Assist (NAVA) levels in non-invasive ventilated patients: titrating NAVA levels with electric diaphragmatic activity and tidal volume matching', *BioMedical Engineering OnLine,* vol. 12, no. 1, pp. 1-11.

Chiew, YS, Chase, JG, Shaw, G, Sundaresan, A & Desaive, T 2011, 'Model-based PEEP Optimisation in Mechanical Ventilation', *Biomedical Engineering OnLine,* vol. 10, no. 1, p. 111.

Chiew, YS, Poole, SF, Redmond, DP, van Drunen, EJ, Damanhuri, NS, Pretty, C, Docherty, PD, Lambermont, B, Shaw, GM & Desaive, T 2014, 'Time-Varying Respiratory Elastance for Spontaneously Breathing Patients', *19th World Congress of the International Federation of Automatic Control*, Cape Town, South Africa, pp. 5659-64

Chiew, YS, Pretty, C, Docherty, PD, Lambermont, B, Shaw, GM, Desaive, T & Chase, JG 2015, 'Time-Varying Respiratory System Elastance: A Physiological Model for Patients Who Are Spontaneously Breathing', *PloS one,* vol. 10, no. 1

Chiumello, D, Carlesso, E, Cadringher, P, Caironi, P, Valenza, F, Polli, F, Tallarini, F, Cozzi, P, Cressoni, M, Colombo, A, Marini, JJ & Gattinoni, L 2008, 'Lung Stress and Strain during Mechanical Ventilation for Acute Respiratory Distress Syndrome', *Am J Respir Crit Care Med,* vol. 178, no. 4, pp. 346-55.

Costa, EL & Amato, MB 2013, 'The new definition for acute lung injury and acute respiratory distress syndrome: is there room for improvement?', *Current Opinion in Critical Care,* vol. 19, no. 1, pp. 16-23.

Crotti, S, Mascheroni, D, Caironi, P, Pelosi, P, Ronzoni, G, Mondino, M, Marini, JJ & Gattinoni, L 2001, 'Recruitment and Derecruitment during Acute Respiratory Failure . A Clinical Study', *Am J Respir Crit Care Med,* vol. 164, no. 1, pp. 131-40.

Damanhuri, N, Chiew, Y, Othman, N, Docherty, P, Shaw, G & Chase, J 2015, 'Pressure reconstruction method for spontaneous breathing effort monitoring', *Critical Care,* vol. 19, no. Suppl 1, p. P259.

Damanhuri, NS, Chiew, YS, Docherty, P, Geoghegan, P & Chase, G 2012, 'Respiratory airway resistance monitoring in mechanically ventilated patients', *2012 IEEE EMBS Conference on Biomedical Engineering and Sciences (IECBES 2012)*, IEEE, Langkawi, Malaysia, pp. 311-5

Damanhuri, NS, Docherty, PD, Chiew, YS, van Drunen, EJ, Desaive, T & Chase, JG 2014, 'A Patient-Specific Airway Branching Model for Mechanically Ventilated Patients', *Computational and Mathematical Methods in Medicine,* vol. 2014

Dasta, JF, McLaughlin, TP, Mody, SH & Piech, CT 2005, 'Daily cost of an intensive care unit day: The contribution of mechanical ventilation', *Crit Care Med,* vol. 33, no. 6, pp. 1266-71.

Davidson, SM, Redmond, DP, Laing, H, White, R, Radzi, F, Chiew, YS, Poole, SF, Damanhuri, NS, Desaive, T & Shaw, GM 2014, 'Clinical Utilisation of Respiratory Elastance (CURE): Pilot Trials for the Optimisation of Mechanical Ventilation Settings for the Critically Ill', *World Congress*, pp. 8403-8

de Ryk, J, Thiesse, J, Namati, E & McLennan, G 2007, 'Stress distribution in a three dimensional, geometric alveolar sac under normal and emphysematous conditions', *International Journal of Chronic Obstructive Pulmonary Disease,* vol. 2(1), pp. 81-91.

Denai, MA, Mahfouf, M, Mohamad-Samuri, S, Panoutsos, G, Brown, BH & Mills, GH 2010, 'Absolute Electrical Impedance Tomography (aEIT) Guided Ventilation Therapy in Critical Care Patients: Simulations and Future Trends', *Information Technology in Biomedicine, IEEE Transactions on,* vol. 14, no. 3, pp. 641-9.

DiCarlo, SE 2008, 'Teaching alveolar ventilation with simple, inexpensive models', *Adv Physiol Educ,* vol. 32, no. 3, pp. 185-91.

DiRocco, JD, Pavone, LA, Carney, DE, Lutz, CJ, Gatto, LA, Landas, SK & Nieman, GF 2006, 'Dynamic alveolar mechanics in four models of lung injury', *Intensive Care Med,* vol. 32, no. 1, pp. 140-8.

Donovan, GM 2011, 'Multiscale mathematical models of airway constriction and disease', *Pulm Pharmacol Ther,* vol. 24, no. 5, pp. 533-9.

Dreyfuss, D & Saumon, G 1992, 'Barotrauma is volutrauma, but which volume is the one responsible?', *Intensive Care Medicine,* vol. 18, no. 3, pp. 139-41.

Dreyfuss, D & Saumon, G 1998, 'Ventilator-induced lung injury: lessons from experimental studies', *Am J Resp Crit Care Med,* vol. 157, pp. 294 - 323.

Eichacker, PQ, Gerstenberger, EP, Banks, SM, Cui, X & Natanson, C 2002, 'Meta-analysis of acute lung injury and acute respiratory distress syndrome trials testing low tidal volumes', *American Journal of Respiratory and Critical Care Medicine,* vol. 166, no. 11, pp. 1510-4.

Epstein, SK 2011, 'How often does patient-ventilator asynchrony occur and what are the consequences?', *Respiratory care,* vol. 56, no. 1, pp. 25-38.

Esteban, A, Alia, I, Ibañez, J, Benito, S & Tobin, MJ 1994, 'Modes of Mechanical Ventilation and Weaning A National Survey of Spanish Hospitals', *CHEST Journal,* vol. 106, no. 4, pp. 1188-93.

Fanelli, V, Vlachou, A, Ghannadian, S, Simonetti, U, Slutsky, AS & Zhang, H 2013, 'Acute respiratory distress syndrome: new definition, current and future therapeutic options', *J Thorac Dis,* vol. 5, no. 3, pp. 326-34.

Ferguson, ND, Frutos-Vivar, F, Esteban, A, Anzueto, A, Alia, I, Brower, RG, Stewart, TE, Apezteguia, C, Gonzalez, M, Soto, L, Abroug, F & Brochard, L 2005, 'Airway pressures, tidal volumes, and mortality in patients with acute respiratory distress syndrome', *Crit Care Med,* vol. 33, no. 1, pp. 21-30.

Forel, J-M, Voillet, F, Pulina, D, Gacouin, A, Perrin, G, Barrau, K, Jaber, S, Arnal, J-M, Fathallah, M & Auquier, P 2012, 'Ventilator-associated pneumonia and ICU mortality in severe ARDS patients ventilated according to a lung-protective strategy', *Crit Care,* vol. 16, no. 2, p. R65.

Gattinoni, L, Caironi, P, Pelosi, P & Goodman, LR 2001, 'What has computed tomography taught us about the acute respiratory distress syndrome?', *Am J Respir Crit Care Med,* vol. 164, no. 9, pp. 1701-11.

Gattinoni, L, Caironi, P, Valenza, F & Carlesso, E 2006, 'The role of CT-scan studies for the diagnosis and therapy of acute respiratory distress syndrome', *Clin Chest Med,* vol. 27, pp. 559 - 70.

Gattinoni, L & Pesenti, A 2005, 'The concept of "baby lung"', *Intensive Care Medicine,* vol. 31, no. 6, pp. 776 - 84.

Grasso, S, Stripoli, T, De Michele, M, Bruno, F, Moschetta, M, Angelelli, G, Munno, I, Ruggiero, V, Anaclerio, R, Cafarelli, A, Driessen, B & Fiore, T 2007, 'ARDSnet Ventilatory Protocol and Alveolar Hyperinflation: Role of Positive End-Expiratory Pressure', *Am J Respir Crit Care Med,* vol. 176, no. 8, pp. 761-7.

Grinnan, DC & Truwit, JD 2005, 'Clinical review: respiratory mechanics in spontaneous and assisted ventilation', *Critical Care,* vol. 9, no. 5, p. 472.

Grodins, FS, Buell, J & Bart, AJ 1967, 'Mathematical analysis and digital simulation of the respiratory control system', *J Appl Physiol,* vol. 22, no. 2, pp. 260-76.

Guérin, C & Richard, J-C 2012, 'Comparison of 2 correction methods for absolute values of esophageal pressure in subjects with acute hypoxemic respiratory failure, mechanically ventilated in the ICU', *Respiratory care,* vol. 57, no. 12, pp. 2045-51.

Guttmann, J, Eberhard, L, Fabry, B, Zappe, D, Bernhard, H, Lichtwarck-Aschoff, M, Adolph, M & Wolff, G 1994, 'Determination of volume-dependent respiratory system mechanics in

mechanically ventilated patients using the new SLICE method', *Technol Health Care,* vol. 2, pp. 175 - 91.

Halter, JM, Steinberg, JM, Gatto, LA, DiRocco, JD, Pavone, LA, Schiller, HJ, Albert, S, Lee, HM, Carney, D & Nieman, GF 2007, 'Effect of positive end-expiratory pressure and tidal volume on lung injury induced by alveolar instability', *Crit Care,* vol. 11, no. 1, p. R20.

Halter, JM, Steinberg, JM, Schiller, HJ, DaSilva, M, Gatto, LA, Landas, S & Nieman, GF 2003, 'Positive End-Expiratory Pressure after a Recruitment Maneuver Prevents Both Alveolar Collapse and Recruitment/Derecruitment', *Am J Respir Crit Care Med,* vol. 167, no. 12, pp. 1620-6.

Hann, CE, Chase, JG, Lin, J, Lotz, T, Doran, CV & Shaw, GM 2005, 'Integral-based parameter identification for long-term dynamic verification of a glucose-insulin system model', *Computer Methods and Programs in Biomedicine,* vol. 77, no. 3, pp. 259-70.

Harris, RS 2005, 'Pressure-volume curves of the respiratory system', *Respir Care,* vol. 50, no. 1, pp. 78-98.

Henderson, WR & Sheel, AW 2012, 'Pulmonary mechanics during mechanical ventilation', *Respiratory Physiology & Neurobiology,* vol. 180, no. 2, pp. 162-72.

Henzler, D, Orfao, S, Rossaint, R & Kuhlen, R 2003, 'Modification of a sigmoidal equation for the pulmonary pressure-volume curve for asymmetric data', *J Appl Physiol,* vol. 95, pp. 2183 - 4.

Hickling, Keith G 1998a, 'The Pressure-Volume Curve Is Greatly Modified by Recruitment . A Mathematical Model of ARDS Lungs', *Am. J. Respir. Crit. Care Med.,* vol. 158, no. 1, pp. 194-202.

Hickling, KG 1998b, 'The pressure-volume curve is greatly modified by recruitment. A mathematical model of ARDS lungs', *Am J Respir Crit Care Med,* vol. 158, no. 1, pp. 194-202.

Hickling, KG 2002, 'Reinterpreting the pressure-volume curve in patients with acute respiratory distress syndrome', *Curr Opin Crit Care,* vol. 8, pp. 32 - 8.

Hodgson, C, Tuxen, D, Davies, A, Bailey, M, Higgins, A, Holland, A, Keating, J, Pilcher, D, Westbrook, A, Cooper, D & Nichol, A 2011, 'A randomised controlled trial of an open lung strategy with staircase recruitment, titrated PEEP and targeted low airway pressures in patients with acute respiratory distress syndrome', *Critical Care,* vol. 15, no. 3, p. R133.

Horsfield, K, Dart, G, Olson, DE, Filley, GF & Cumming, G 1971, 'Models of the human bronchial tree', *Journal of Applied Physiology,* vol. 31, no. 2, pp. 207-17.

Horsfield, K & Woldenberg, MJ 1989, 'Diameters and cross-sectional areas of branches in the human pulmonary arterial tree', *The Anatomical Record,* vol. 223, no. 3, pp. 245-51.

Imai, Y, Nakagawa, S, Ito, Y, Kawano, T, Slutsky, AS & Miyasaka, K 2001, 'Comparison of lung protection strategies using conventional and high-frequency oscillatory ventilation', *Journal of Applied Physiology,* vol. 91, no. 4, pp. 1836-44.

Jaswal, DS, Leung, JM, Sun, J, Cui, X, Li, Y, Kern, S, Welsh, J, Natanson, C & Eichacker, PQ 2014, 'Tidal Volume and Plateau Pressure Use for Acute Lung Injury From 2000 to Present: A Systematic Literature Review*', *Critical Care Medicine,* vol. 42, no. 10, pp. 2278-89.

Jonson, B, Richard, JC, Straus, C, Mancebo, J, Lemaire, F & Brochard, L 1999, 'Pressure-Volume Curves and Compliance in Acute Lung Injury . Evidence of Recruitment Above the Lower Inflection Point', *Am J Respir Crit Care Med,* vol. 159, no. 4, pp. 1172-8.

Kallet, R & Branson, R 2007, 'Respiratory controversies in the critical care setting. Do the NIH ARDS Clinical Trials Network PEEP/FIO2 tables provide the best evidence-based guide to balancing PEEP and FIO2 settings in adults?', *Respiratory care,* vol. 52, no. 4, p. 461.

Kárason, S, Søndergaard, S, Lundin, S & Stenqvist, O 2001, 'Continuous on-line measurements of respiratory system, lung and chest wall mechanics during mechanic ventilation', *Intensive Care Medicine,* vol. 27, no. 8, pp. 1328-39.

Karason, S, Sondergaard, S, Lundin, S, Wiklund, J & Stenqvist, O 2000, 'A new method for non-invasive, manoeuvre-free determination of "static" pressure-volume curves during dynamic/therapeutic mechanical ventilation', *Acta Anaesthesiologica Scandinavica,* vol. 44, no. 5, pp. 578-85.

Karason, S, Sondergaard, S, Lundin, S, Wiklund, J & Stenqvist, O 2001, 'Direct tracheal airway pressure measurements are essential for safe and accurate dynamic monitoring of respiratory mechanics. A laboratory study', *Acta Anaesthesiol Scand,* vol. 45, no. 2, pp. 173-9.

Kattwinkel, J, Robinson, M, Bloom, BT, Delmore, P & Ferguson, JE 2004, 'Technique for intrapartum administration of surfactant without requirement for an endotracheal tube', *J Perinatol,* vol. 24, pp. 360-5.

Katz, IM, Martin, AR, Muller, PA, Terzibachi, K, Feng, CH, Caillibotte, G, Sandeau, J & Texereau, J 2011, 'The ventilation distribution of helium-oxygen mixtures and the role of inertial losses in the presence of heterogeneous airway obstructions', *J Biomech,* vol. 44, no. 6, pp. 1137-43.

Katz, IM, Martin, A.R., Feng, C.H., Majoral, C., Caillibotte, G., Marx, T., Bazin, J.E., Daviet, 2012, 'Airway pressure distribution during xenon anesthesia: The insufflation phase at constant flow (volume controlled mode)', *Applied Cardiopulmonary Pathophysiology,* vol. 16, pp. 5-16.

Khirani, S, Polese, G, Aliverti, A, Appendini, L, Nucci, G, Pedotti, A, Colledan, M, Lucianetti, A, Baconnier, P & Rossi, A 2010, 'On-line monitoring of lung mechanics during spontaneous breathing: a physiological study', *Respiratory medicine,* vol. 104, no. 3, pp. 463-71.

Kitaoka, H, Nieman, GF, Fujino, Y, Carney, D, DiRocco, J & Kawase, I 2007, 'A 4-Dimensional Model of the Alveolar Structure', *The Journal of Physiological Sciences,* vol. 57, no. 3, pp. 175-85.

Kogler, VM 2009, 'Advantage of spontaneous breathing in patients with respiratory failure', *SIGNA VITAE,* vol. 4, no. 1

Kollef, MH & Schuster, DP 1995, 'The Acute Respiratory Distress Syndrome', *New England Journal of Medicine,* vol. 332, no. 1, pp. 27-37.

Kress, JP, Pohlman, AS, O'Connor, MF & Hall, JB 2000, 'Daily Interruption of Sedative Infusions in Critically Ill Patients Undergoing Mechanical Ventilation', *New England Journal of Medicine,* vol. 342, no. 20, pp. 1471-7.

Kuebler, WM, Mertens, M & Pries, AR 2007, 'A two-component simulation model to teach respiratory mechanics', *Advances in Physiology Education,* vol. 31, no. 2, pp. 218-22.

Lambermont, B, Ghuysen, A, Janssen, N, Morimont, P, Hartstein, G, Gerard, P & D'Orio, V 2008, 'Comparison of functional residual capacity and static compliance of the respiratory system during a positive end-expiratory pressure (PEEP) ramp procedure in an experimental model of acute respiratory distress syndrome', *Critical Care,* vol. 12, no. 4, p. R91.

Lauzon, A & Bates, J 1991, 'Estimation of time-varying respiratory mechanical parameters by recursive least squares', *J Appl Physiol,* vol. 71, no. 3, pp. 1159-65.

Levy, MM 2004, 'PEEP in ARDS-how much is enough?', *NEW ENGLAND JOURNAL OF MEDICINE.,* vol. 351, pp. 389-90.

Lichtwarck-Aschoff, M, Kessler, V, Sjostrand, UH, Hedlund, A, Mols, G, Rubertsson, S, Markstrom, AM & Guttmann, J 2000, 'Static versus dynamic respiratory mechanics for setting the ventilator', *Br J Anaesth,* vol. 85, no. 4, pp. 577-86.

Lipes, J, Bojmehrani, A & Lellouche, F 2012, 'Low Tidal Volume Ventilation in Patients without Acute Respiratory Distress Syndrome: A Paradigm Shift in Mechanical Ventilation', *Critical Care Research and Practice,* vol. 2012

Lourens, MS, van den Berg, B, Aerts, JG, Verbraak, AF, Hoogsteden, HC & Bogaard, JM 2000, 'Expiratory time constants in mechanically ventilated patients with and without COPD', *Intensive Care Med,* vol. 26, no. 11, pp. 1612-8.

Lu, Q, Malbouisson, LM, Mourgeon, E, Goldstein, I, Coriat, P & Rouby, JJ 2001, 'Assessment of PEEP-induced reopening of collapsed lung regions in acute lung injury: are one or three CT sections representative of the entire lung?', *Intensive Care Med,* vol. 27, no. 9, pp. 1504-10.

Lu, Q & Rouby, J-J 2000, 'Measurement of pressure-volume curves in patients on mechanical ventilation: methods and significance', *Critical Care,* vol. 4, no. 2, pp. 91 - 100.

Lucangelo, U, Bernabe, F & Blanch, L 2007, 'Lung mechanics at the bedside: make it simple', *Current Opinion in Critical Care,* vol. 13, no. 1, pp. 64-72.

Luhr, OR, Antonsen, K, Karlsson, M, Aardal, S, Thorsteinsson, A, Frostell, CG & Bonde, J 1999, 'Incidence and mortality after acute respiratory failure and acute respiratory distress syndrome in Sweden, Denmark, and Iceland. The ARF Study Group', *Am J Respir Crit Care Med,* vol. 159, no. 6, pp. 1849-61.

Ma, B & Bates, J 2010, 'Modeling the Complex Dynamics of Derecruitment in the Lung', *Annals of Biomedical Engineering,* vol. 38, no. 11, pp. 3466-77.

Maggiore, SM, Richard, JC & Brochard, L 2003, 'What has been learnt from P/V curves in patients with acute lung injury/acute respiratory distress syndrome', *Eur Respir J,* vol. 22, no. 42_suppl, pp. 22s-6.

Manzano, F, Yuste, E, Colmenero, M, Aranda, A, Garcia-Horcajadas, A, Rivera, R & Fernandez-Mondejar, E 2005, 'Incidence of acute respiratory distress syndrome and its relation to age', *J Crit Care,* vol. 20, no. 3, pp. 274-80.

Marini, JJ 2011, 'Spontaneously regulated vs. controlled ventilation of acute lung injury/acute respiratory distress syndrome', *Current Opinion in Critical Care,* vol. 17, no. 1, pp. 24-9 10.1097/MCC.0b013e328342726e.

Marini, JJ, Capps, JS & Culver, BH 1985, 'The inspiratory work of breathing during assisted mechanical ventilation', *Chest,* vol. 87, no. 5, pp. 612-8.

McCann, UG, Schiller, HJ, Carney, DE, Gatto, LA, Steinberg, JM & Nieman, GF 2001, 'Visual validation of the mechanical stabilizing effects of positive end-expiratory pressure at the alveolar level.', *J Surg Res,* vol. 99, no. 2, pp. 335-42.

Mead, J, Takishima, T & Leith, D 1970, 'Stress distribution in lungs: a model of pulmonary elasticity', *Journal of Applied Physiology,* vol. 28, no. 5, pp. 596-608.

Mead, J & Whittenberger, JL 1953, 'Physical properties of human lungs measured during spontaneous respiration', *Journal of Applied Physiology,* vol. 5, no. 12, pp. 779-96.

Meade, MO, Cook, DJ, Guyatt, GH, Slutsky, AS, Arabi, YM, Cooper, DJ, Davies, AR, Hand, LE, Zhou, Q, Thabane, L, Austin, P, Lapinsky, S, Baxter, A, Russell, J, Skrobik, Y, Ronco, JJ, Stewart, TE & for the Lung Open Ventilation Study, I 2008, 'Ventilation Strategy Using Low Tidal Volumes, Recruitment Maneuvers, and High Positive End-Expiratory Pressure for Acute Lung Injury and Acute Respiratory Distress Syndrome: A Randomized Controlled Trial', *JAMA,* vol. 299, no. 6, pp. 637-45.

Mercat, A, Richard, J-CM, Vielle, B, Jaber, S, Osman, D, Diehl, J-L, Lefrant, J-Y, Prat, G, Richecoeur, J, Nieszkowska, A, Gervais, C, Baudot, J, Bouadma, L, Brochard, L & for the Expiratory Pressure Study, G 2008, 'Positive End-Expiratory Pressure Setting in Adults With Acute Lung Injury and Acute Respiratory Distress Syndrome: A Randomized Controlled Trial', *JAMA,* vol. 299, no. 6, pp. 646-55.

Möller, K, Zhao, Z, Stahl, C & Guttmann, J 2010, 'On the analysis of dynamic lung mechanics separately in ins-and expiration', *XII Mediterranean Conference on Medical and Biological Engineering and Computing 2010*, Springer, pp. 164-7

Mols, G, Kessler, V, Benzing, A, Lichtwarck-Aschoff, M, Geiger, K & Guttmann, J 2001, 'Is pulmonary resistance constant, within the range of tidal volume ventilation, in patients with ARDS?', *British Journal of Anaesthesia,* vol. 86, no. 2, pp. 176-82.

Mols, G, Priebe, HJ & Guttmann, J 2006, 'Alveolar recruitment in acute lung injury', *Br J Anaesth,* vol. 96, no. 2, pp. 156-66.

Moorhead, KT, Piquilloud, L, Lambermont, B, Roeseler, J, Chiew, YS, Chase, JG, Revelly, J-P, Bialais, E, Tassaux, D & Laterre, P-F 2013, 'NAVA enhances tidal volume and diaphragmatic electro-

myographic activity matching: a Range90 analysis of supply and demand', *Journal of Clinical Monitoring and Computing,* vol. 27, no. 1, pp. 61-70.

Morris, J, Ingenito, E, Mark, L, Kamm, R & Johnson, M 2001, 'Dynamic behavior of lung surfactant', *Journal of biomechanical engineering,* vol. 123, no. 1, pp. 106-13.

Munson, BR, Young, DF & Okiishi, TH 1990, *Fundamentals of fluid mechanics*, New York.

Oostveen, E, MacLeod, D, Lorino, H, Farre, R, Hantos, Z, Desager, K & Marchal, F 2003, 'The forced oscillation technique in clinical practice: methodology, recommendations and future developments', *European Respiratory Journal,* vol. 22, no. 6, pp. 1026-41.

Ostermann, ME, Keenan, SP, Seiferling, RA & Sibbald, WJ 2000, 'Sedation in the intensive care unit: a systematic review', *JAMA,* vol. 283, no. 11, pp. 1451-9.

Otis, AB, Fenn, WO & Rahn, H 1950, 'Mechanics of Breathing in Man', *Journal of Applied Physiology,* vol. 2, no. 11, pp. 592-607.

Parsons, PE, Eisner, MD, Thompson, BT, Matthay, MA, Ancukiewicz, M, Bernard, GR, Wheeler, AP & Network, tNARDSCT 2005, 'Lower tidal volume ventilation and plasma cytokine markers of inflammation in patients with acute lung injury', *Crit Care Med,* vol. 33, no. 1, pp. 1-6.

Pavone, L, Albert, S, DiRocco, J, Gatto, L & Nieman, G 2007, 'Alveolar instability caused by mechanical ventilation initially damages the nondependent normal lung', *Critical Care,* vol. 11, no. 5, p. R104.

Pedley, TJ, Schroter, RC & Sudlow, MF 1970, 'The prediction of pressure drop and variation of resistance within the human bronchial airways', *Respir Physiol,* vol. 9, no. 3, pp. 387-405.

Pelosi, P, Goldner, M, McKibben, A, Adams, A, Eccher, G, Caironi, P, Losappio, S, Gattinoni, L & Marini, JJ 2001, 'Recruitment and derecruitment during acute respiratory failure: an experimental study', *Am J Respir Crit Care Med,* vol. 164, pp. 122 - 30.

Peris, A, Zagli, G, Barbani, F, Tutino, L, Biondi, S, Di Valvasone, S, Batacchi, S, Bonizzoli, M, Spina, R, Miniati, M, Pappagallo, S, Giovannini, V & Gensini, GF 2010, 'The value of lung ultrasound monitoring in H1N1 acute respiratory distress syndrome', *Anaesthesia,* vol. 65, no. 3, pp. 294-7.

Pesenti, A, Tagliabue, P, Patroniti, N & Fumagalli, R 2001, 'Computerised tomography scan imaging in acute respiratory distress syndrome', *Intensive Care Med,* vol. 27, pp. 631 - 9.

Petersen, GW, Baier, H. 1983, 'Incidence of pulmonary barotrauma in a medical ICU.', *Crit Care Med,* vol. 11, pp. 67-9.

Phua, J, Badia, JR, Adhikari, NKJ, Friedrich, JO, Fowler, RA, Singh, JM, Scales, DC, Stather, DR, Li, A, Jones, A, Gattas, DJ, Hallett, D, Tomlinson, G, Stewart, TE & Ferguson, ND 2009, 'Has Mortality from Acute Respiratory Distress Syndrome Decreased over Time?: A Systematic Review', *Am J Respir Crit Care Med,* vol. 179, no. 3, pp. 220-7.

Piquilloud, L, Vignaux, L, Bialais, E, Roeseler, J, Sottiaux, T, Laterre, P-F, Jolliet, P & Tassaux, D 2011, 'Neurally adjusted ventilatory assist improves patient–ventilator interaction', *Intensive Care Medicine,* vol. 37, no. 2, pp. 263-71.

Poole, SF, Chiew, YS, Redmond, DP, Davidson, SM, Damanhuri, NS, Pretty, C, Docherty, PD, Desaive, T, Shaw, GM & Chase, JG 2014, 'Real-Time Breath-to-Breath Asynchrony Event Detection using Time-Varying Respiratory Elastance Model'

Putensen, C, Mutz, Norbert J, Putensen-Himmer, G & Zinserling, J 1999, 'Spontaneous Breathing During Ventilatory Support Improves Ventilation-Perfusion Distributions in Patients with Acute Respiratory Distress Syndrome', *Am. J. Respir. Crit. Care Med.,* vol. 159, no. 4, pp. 1241-8.

Puybasset, L, Gusman, P, Muller, JC, Cluzel, P, Coriat, P & Rouby, JJ 2000, 'Regional distribution of gas and tissue in acute respiratory distress syndrome. III. Consequences for the effects of positive end-expiratory pressure. CT Scan ARDS Study Group. Adult Respiratory Distress Syndrome', *Intensive Care Med,* vol. 26, pp. 1215 - 27.

Ranieri, VM, Zhang, H, Mascia, L, Aubin, M, Lin, C-Y, Mullen, JB, Grasso, S, Binnie, M, Volgyesi, GA, Eng, P & Slutsky, AS 2000, 'Pressure–Time Curve Predicts Minimally Injurious Ventilatory Strategy in an Isolated Rat Lung Model', *Anesthesiology,* vol. 93, no. 5, pp. 1320-8.

Reddy, PI, Al-Jumaily, AM & Bold, GT 2011, 'Dynamic surface tension of natural surfactant extract under superimposed oscillations', *J Biomech,* vol. 44, no. 1, pp. 156-63.

Reynolds, HN, McCunn, M, Borg, U, Habashi, N, Cottingham, C & Bar-Lavi, Y 1998, 'Acute respiratory distress syndrome: estimated incidence and mortality rate in a 5 million-person population base', *Critical Care,* vol. 2, no. 29, pp. 29–34.

Ricard, JD, Dreyfuss, D & Saumon, G 2003, 'Ventilator-induced lung injury', *Eur Respir J,* vol. 22, no. 42_suppl, pp. 2s-9.

Rouby, J-J, Arbelot, C, Brisson, H, Lu, Q & Bouhemad, B 2013, 'Measurement of alveolar recruitment at the bedside: the beginning of a new era in respiratory monitoring?', *Respiratory care,* vol. 58, no. 3, pp. 539-42.

Rouby, JJ, Contantin, JM, Girardi, C, Zhang, M & Qin, L 2004, 'Mechanical Ventilation in patients with acute respiratory distress syndrome', *Anesthesiology,* vol. 101, pp. 228 - 34.

Rubenfeld, GD, Caldwell, E, Peabody, E, Weaver, J, Martin, DP, Neff, M, Stern, EJ & Hudson, LD 2005, 'Incidence and outcomes of acute lung injury', *N Engl J Med,* vol. 353, no. 16, pp. 1685-93.

Schiller, HJ, McCann, UG, 2nd, Carney, DE, Gatto, LA, Steinberg, JM & Nieman, GF 2001, 'Altered alveolar mechanics in the acutely injured lung', *Crit Care Med,* vol. 29, no. 5, pp. 1049-55.

Schiller, HJ, Steinberg, J, Halter, J, McCann, U, DaSilva, M, Gatto, LA, Carney, D & Nieman, G 2003, 'Alveolar inflation during generation of a quasi-static pressure/volume curve in the acutely injured lung', *Critical Care Medicine,* vol. 31, no. 4, pp. 1126-33.

Schirrmann, K, Mertens, M, Kertzscher, U, Kuebler, WM & Affeld, K 2010, 'Theoretical modeling of the interaction between alveoli during inflation and deflation in normal and diseased lungs', *J Biomech,* vol. 43, no. 6, pp. 1202-7.

Schranz, C, Docherty, PD, Chiew, YS, Chase, JG & Moller, K 2012a, 'Structural identifiability and practical applicability of an alveolar recruitment model for ARDS patients', *IEEE Trans Biomed Eng,* vol. 59, no. 12, pp. 3396-404.

Schranz, C, Docherty, PD, Chiew, YS, Moller, K & Chase, JG 2012b, 'Iterative integral parameter identification of a respiratory mechanics model', *Biomed Eng Online,* vol. 11, p. 38.

Schranz, C, Kno, x, bel, C, Kretschmer, J, Zhao, Z, Mo & ller, K 2011, 'Hierarchical Parameter Identification in Models of Respiratory Mechanics', *Biomedical Engineering, IEEE Transactions on,* vol. 58, no. 11, pp. 3234-41.

Schuessler, TF, Gottfried, SB & Bates, JHT 1997, 'A model of the spontaneously breathing patient: applications to intrinsic PEEP and work of breathing', *J Appl Physiol,* vol. 82, no. 5, pp. 1694-703.

Servillo, G, Svantesson, C, Beydon, L, Roupie, E, Brochard, L, Lemaire, F & Jonson, B 1997, 'Pressure-volume curves in acute respiratory failure: automated low flow inflation versus occlusion', *American Journal of Respiratory and Critical Care Medicine,* vol. 155, no. 5, pp. 1629-36.

Sigurdsson, M, Sigvaldason, K, Gunnarsson, T, Moller, A & Sigurdsson, G 2013, 'Acute respiratory distress syndrome: nationwide changes in incidence, treatment and mortality over 23 years', *Acta Anaesthesiologica Scandinavica,* vol. 57, no. 1, pp. 37-45.

Slutsky, AS 1999, 'Lung injury caused by mechanical ventilation', *Chest,* vol. 116, no. 1 Suppl, pp. 9S-15S.

Sondergaard, S, Kárason, S, Hanson, A, Nilsson, K, Wiklund, J, Lundin, S & Stenqvist, O 2003a, 'The dynostatic algorithm accurately calculates alveolar pressure on-line during ventilator treatment in children', *Pediatric Anesthesia,* vol. 13, no. 4, pp. 294-303.

Sondergaard, S, Kárason, S, Wiklund, J, Lundin, S & Stenqvist, O 2003b, 'Alveolar pressure monitoring: an evaluation in a lung model and in patients with acute lung injury', *Intensive Care Medicine,* vol. 29, no. 6, pp. 955-62.

Soong, T, Nicolaides, P, Yu, C & Soong, S 1979, 'A statistical description of the human tracheobronchial tree geometry', *Respiration Physiology,* vol. 37, no. 2, pp. 161-72.

Stahl, CA, Moller, K, Schumann, S, Kuhlen, R, Sydow, M, Putensen, C & Guttmann, J 2006, 'Dynamic versus static respiratory mechanics in acute lung injury and acute respiratory distress syndrome', *Crit Care Med,* vol. 34, pp. 2090 - 8.

Stenqvist, O 2003, 'Practical assessment of respiratory mechanics', *British Journal of Anaesthesia,* vol. 91, no. 1, pp. 92-105.

Straus, C, Louis, B, Isabey, D, Lemaire, F, Harf, A & Brochard, L 1998, 'Contribution of the Endotracheal Tube and the Upper Airway to Breathing Workload', *Am. J. Respir. Crit. Care Med.,* vol. 157, no. 1, pp. 23-30.

Suarez-Sipmann, F, Bohm, S, Tusman, G, Pesch, T, Thamm, O, Reissmann, H, Reske, A, Magnusson, A & Hedenstierna, G 2007, 'Use of dynamic compliance for open lung positive end-expiratory pressure titration in an experimental study', *Crit Care Med,* vol. 35, pp. 214 - 21.

Suh, GY, Yoon, JW, Park, SJ, Ham, HS, Kang, SJ, Koh, WJ, Chung, MP, Kim, HJ & Kwon, OJ 2003, 'A practical protocol for titrating "optimal" PEEP in acute lung injury: Recruitment maneuver and PEEP decrement', *Journal of Korean Medical Science,* vol. 18, no. 3, pp. 349-54.

Sundaresan, A 2010, *Applications of Model-Based Lung Mechanics in the Intensive Care Unit*, Ph.D Thesis Thesis, University of Canterbury, New Zealand,

Sundaresan, A, Chase, J, Shaw, G, Chiew, YS & Desaive, T 2011a, 'Model-based optimal PEEP in mechanically ventilated ARDS patients in the Intensive Care Unit', *Biomedical Engineering OnLine,* vol. 10, no. 1, p. 64.

Sundaresan, A & Chase, JG 2012, 'Positive end expiratory pressure in patients with acute respiratory distress syndrome – The past, present and future', *Biomedical Signal Processing and Control,* vol. 7, no. 2, pp. 93-103.

Sundaresan, A, Chase, JG, Hann, CE & Shaw, GM 2010, 'Model-based PEEP selection in mechanically ventilated patients – First clinical trial results', in *UKACC International Conference on Control*, Coventry, UK, 7 - 10 September, 2010.

Sundaresan, A, Chase, JG, Shaw, GM, Chiew, YS & Desaive, T 2011b, 'Model-based optimal PEEP in mechanically ventilated ARDS patients in the intensive care unit', *Biomed Eng Online,* vol. 10, p. 64.

Sundaresan, A, Geoffrey Chase, J, Hann, CE & Shaw, GM 2011c, 'Dynamic functional residual capacity can be estimated using a stress-strain approach', *Comput Methods Programs Biomed,* vol. 101, no. 2, pp. 135-43.

Sundaresan, A, Yuta, T, Hann, CE, Geoffrey Chase, J & Shaw, GM 2009, 'A minimal model of lung mechanics and model-based markers for optimizing ventilator treatment in ARDS patients', *Computer Methods and Programs in Biomedicine,* vol. 95, no. 2, pp. 166-80.

Suter, PM, Fairley, HB & Isenberg, MD 1975, 'Optimum end-expiratory airway pressure in patients with acute pulmonary failure', *N Engl J Med,* vol. 292, pp. 284 - 9.

Suter, PM, Fairley, HB & Isenberg, MD 1978, 'Effect of tidal volume and positive end-expiratory pressure on compliance during mechanical ventilation', *Chest,* vol. 73, pp. 158 - 62.

Szlavecz, A, Chiew, YS, Redmond, D, Beatson, A, Glassenbury, D, Corbett, S, Major, V, Pretty, C, Shaw, GM & Benyo, B 2014, 'The Clinical Utilisation of Respiratory Elastance Software (CURE Soft): a bedside software for real-time respiratory mechanics monitoring and mechanical ventilation management', *BioMedical Engineering OnLine,* vol. 13, no. 1, p. 140.

Talmor, D, Sarge, T, Malhotra, A, O'Donnell, CR, Ritz, R, Lisbon, A, Novack, V & Loring, SH 2008, 'Mechanical Ventilation Guided by Esophageal Pressure in Acute Lung Injury', *New England Journal of Medicine,* vol. 359, no. 20, pp. 2095-104.

Talmor, D, Sarge, T, O'Donnell, CR, Ritz, R, Malhotra, A, Lisbon, A & Loring, SH 2006, 'Esophageal and transpulmonary pressures in acute respiratory failure', *Critical Care Medicine,* vol. 34, no. 5, p. 1389.

Tawhai, M, Clark, A, Donovan, G & Burrowes, K 2011, 'Computational Modeling of Airway and Pulmonary Vascular Structure and Function: Development of a', *Critical Reviews™ in Biomedical Engineering,* vol. 39, no. 4

Tawhai, MH & Bates, JH 2011, 'Multi-scale lung modeling', *J Appl Physiol,* vol. 110, no. 5, pp. 1466-72.

Tawhai, MH, Hunter, P, Tschirren, J, Reinhardt, J, McLennan, G & Hoffman, EA 2004, 'CT-based geometry analysis and finite element models of the human and ovine bronchial tree', *J Appl Physiol,* vol. 97, no. 6, pp. 2310-21.

The Acute Respiratory Distress Syndrome Network 2000, 'Ventilation with Lower Tidal Volumes as Compared with Traditional Tidal Volumes for Acute Lung Injury and the Acute Respiratory Distress Syndrome', *N Engl J Med,* vol. 342, no. 18, pp. 1301-8.

The ARDS Definition Task Force 2012, 'Acute respiratory distress syndrome', *JAMA,* vol. 307, no. 23, pp. 2526-33.

Tobin, MJ, Jubran, A & Laghi, F 2001, 'Patient-Ventilator Interaction', *Am. J. Respir. Crit. Care Med.,* vol. 163, no. 5, pp. 1059-63.

Tremblay, LN & Slutsky, AS 1997, 'Ventilator-induced injury: from barotrauma to biotrauma', *Proceedings of the Association of American Physicians,* vol. 110, no. 6, pp. 482-8.

Trueb, TJ, Cherniack, NS, D'Souza, AF & Fishman, AP 1971, 'A mathematical model of the controlled plant of the respiratory system', *Biophys J,* vol. 11, no. 10, pp. 810-34.

Tubiana, M, Nagataki, S, Feinendegen, LE, Dimitroyannis, DA, Frush, DP, Goske, MJ, Hernanz-Schulman, M, Soyer, P, Varnholt, H, Brenner, DJ & Hall, EJ 2008, 'Computed Tomography and Radiation Exposure', *N Engl J Med,* vol. 358, no. 8, pp. 850-3.

van Drunen, EJ, Chiew, YS, Chase, JG, Shaw, GM, Lambermont, B, Janssen, N, Damanhuri, NS & Desaive, T 2013, 'Expiratory model-based method to monitor ARDS disease state', *Biomed Eng Online,* vol. 12, p. 57.

van Drunen, EJ, Chiew, YS, Pretty, C, Shaw, GM, Lambermont, B, Janssen, N, Chase, JG & Desaive, T 2014, 'Visualisation of time-varying respiratory system elastance in experimental ARDS animal models', *BMC Pulm Med,* vol. 14, no. 1, p. 33.

Venegas, JG, Harris, RS & Simon, BA 1998, 'A comprehensive equation for the pulmonary pressure-volume curve', *J Appl Physiol,* vol. 84, pp. 389 - 95.

Vieira, SR, Puybasset, L, Richecoeur, J, Lu, Q, Cluzel, P, Gusman, PB, Coriat, P & Rouby, JJ 1998, 'A lung computed tomographic assessment of positive end-expiratory pressure-induced lung overdistension', *Am J Respir Crit Care Med,* vol. 158, no. 5 Pt 1, pp. 1571-7.

Vignaux, L, Vargas, F, Roeseler, J, Tassaux, D, Thille, AW, Kossowsky, MP, Brochard, L & Jolliet, P 2009, 'Patient–ventilator asynchrony during non-invasive ventilation for acute respiratory failure: a multicenter study', *Intensive Care Medicine,* vol. 35, no. 5, pp. 840-6.

Villar, J, Kacmarek, RM, Pérez-Méndez, L & Aguirre-Jaime, A 2006, 'A high positive end-expiratory pressure, low tidal volume ventilatory strategy improves outcome in persistent acute respiratory distress syndrome: A randomized, controlled trial', *Crit Care Med,* vol. 34, no. 5, pp. 1311-8.

Ward, NS, Lin, DY, Nelson, DL, Houtchens, J, Schwartz, WA, Klinger, JR, Hill, NS & Levy, MM 2002, 'Successful determination of lower inflection point and maximal compliance in a population of patients with acute respiratory distress syndrome', *Crit Care Med,* vol. 30, pp. 963 - 8.

Ware, LB & Matthay, MA 2000, 'The Acute Respiratory Distress Syndrome', *N Engl J Med,* vol. 342, no. 18, pp. 1334-49.

Weibel, ER 1963a, 'Morphometry of the human lung'

Weibel, ER 1963b, 'Principles and methods for the morphometric study of the lung and other organs', *Lab Invest,* vol. 12, pp. 131-55.

West, JB 2012, *Respiratory physiology: the essentials*, Lippincott Williams & Wilkins.

Wysocki, M, Cracco, C, Teixeira, A, Mercat, A, Diehl, J-L, Lefort, Y, Derenne, J-P & Similowski, T 2006, 'Reduced breathing variability as a predictor of unsuccessful patient separation from mechanical ventilation *', *Crit Care Med,* vol. 34, no. 8, pp. 2076-83 10.1097/01.CCM.0000227175.83575.E9.

Yuta, T, Chase, JG, Shaw, GM & Hann, C 2004, 'Dynamic models of ARDS lung mechanics for optimal patient ventilation', *Proceedings of the 26th International Conf of IEEE Engineering in Med and Biology Society (EMBC 2004)*, San Francisco, CA, pp. 861-4

Zhao, Y, Rees, SE, Kjaergaard, S & Andreassen, S 2006, 'Simulation of Pulmonary Pathophysiology During Spontaneous Breathing', *Engineering in Medicine and Biology Society, 2005. IEEE-EMBS 2005. 27th Annual International Conference of the*, IEEE, pp. 6128-31

Zhao, Z, Guttmann, J & Moller, K 2012a, 'Adaptive Slice Method: A new method to determine volume dependent dynamic respiratory system mechanics', *Physiol Meas.,* vol. 33, no. 1, pp. 51-64.

Zhao, Z, Josef, G & Knut, M 2012b, 'Assessment of a volume-dependent dynamic respiratory system compliance in ALI/ARDS by pooling breathing cycles', *Physiological Measurement,* vol. 33, no. 8, p. N61.

Zhao, Z, Steinmann, D, Frerichs, I, Guttmann, J & Moller, K 2010a, 'PEEP titration guided by ventilation homogeneity: a feasibility study using electrical impedance tomography', *Crit Care,* vol. 14, no. 1, p. R8.

Zhao, Z, Steinmann, D, Muller-Zivkovic, D, Martin, J, Frerichs, I, Guttmann, J & Moller, K 2010b, 'A lung area estimation method for analysis of ventilation inhomogeneity based on electrical impedance tomography', *J Xray Sci Technol,* vol. 18, no. 2, pp. 171-82.